Sjoerd van Kuijk

On the creation of aquatic inspired adhesive products with polyketones

Master thesis of Chemical Engineering in the area of chemical product design, supervised by Dr. Raquel Costa and Prof. Hermínio Sousa, defended at the Department of Chemical Engineering of the Faculty of Science and Technology of the University of Coimbra

September 2011

· U C ·

UNIVERSIDADE DE COIMBRA

University of Groningen
The Netherlands

University of Cambridge
United Kingdom

University of Coimbra
Portugal

Master Thesis

On the creation of aquatic-inspired adhesive products with polyketones

Fitting chemical product engineering with technology push research

File
Thesis SRvK 3.docx

Version
3

Date
12 September 2011

Author
Sjoerd Reindert van Kuijk BSc

Student Number
1535552

Study
Chemical Engineering (Ma)

Instructors
Prof. dr. A.A. Broekhuis
Dr. G.D. Moggridge
Prof. Dr. H. Sousa
Dr. R. Costa

Preface

This thesis is an account of work carried out in the Department of Chemical Engineering, University of Groningen, during the months of September 2010, January 2011, July 2011 and August 2011; the Department of Chemical Engineering and Biotechnology, University of Cambridge, between October 2010 and January 2010; and the Department of Chemical Engineering, University of Coimbra, between February 2011 and July 2011.

I declare that this thesis is the results of my own work and includes nothing which is the outcome of work done in collaboration with others, except where specifically indicated in the text. No part of it has been, or is being, submitted for a degree, diploma, or other qualification at these or any other University.

In addition, I declare that I have written this thesis completely by myself, and that I have used no other sources or resources than those mentioned. I have indicated all quotes and citations that were literally taken from publications, or that were in close accordance with the meaning of those publications, as such.

In case of proof that this work has not been constructed in accordance with this declaration, it is considered as negligence or as a deliberate act that has been aimed at making correct judgment of the candidate's expertise, insights and skills impossible. In case of plagiarism the examiner has the right to declare the study results obtained in the course as null and void, to exclude the author from any further participation in the particular assignment, and to exclude the author from further participation in the programme.

S.R. van Kuijk BSc

Abstract

This thesis describes the research project aimed at mimicking the underwater adhesion biochemistry of aquatic organisms by modifying synthetic polyketone polymers to contain similar chemical functionalities. A general introduction to the fields of chemical product engineering research, adhesives, biomimetics and polyketones is followed by detailed literature reviews regarding the state-of-the-art knowledge on both aquatic adhesion and synthetic aquatic-inspired adhesives. The results of the practical work on the creation of novel dopamine-modified polyketones for use as water-resistant adhesives is discussed thereafter, followed by detailed recommendations for future work. In short, the present work demonstrates that existing research at the University of Groningen on functionalizing a specific type of low molecular weight alternating aliphatic polyketones through Paal-Knorr reactions with amines could be expanded successfully to include the molecules dopamine and tyramine. These novel modified polymers were obtained in a relatively facile way without the use of a protective atmosphere or synthetic protection-deprotection strategies. The polymeric material could be cured through use of oxidative chemistry to yield significant adhesion bond strengths up to 3 MPa on aluminium under dry conditions. Continuation of the project in the near future will be directed towards enlarging the adhesive bond strength dataset and increasing the adhesive wettability of the aluminium adherends underwater.

Resumo

Esta tese descreve a modificação de policetonas para conterem funcionalidades químicas semelhantes às de organismos aquáticos com o objectivo de imitar a adesão destes a materiais submersos em água. É feita uma introdução genérica às áreas de investigação em engenharia de produto, adesivos, biomimética e policetonas, seguida de uma revisão detalhada da literatura sobre o estado-da-arte de adesivos aquáticos naturais e sintéticos. É discutida a síntese em laboratório de policetonas modificadas com grupos dopamina para uso como adesivos resistentes à água, e posteriormente são apresentadas recomendações para trabalho futuro. Em suma, o presente trabalho demonstra que a investigação levada a cabo pela Universidade de Groningen na funcionalização de determinadas policetonas de baixo peso molecular pode ser alargada com sucesso à inclusão de grupos dopamina e tiramina recorrendo a reacções de Paal-Knorr. Estes novos polímeros modificados foram obtidos em condições reaccionais menos restritivas do que as que se encontram descritas na literatura, evitando o uso de uma atmosfera protectora ou estratégias de síntese de protecção-desprotecção. O material polimérico foi reticulado por oxidação, tendo-se obtido forças de adesão até 3 MPa numa placa de alumínio na ausência de humidade. A continuação do projecto num futuro próximo vai ser direccionado para o aumento da força e capacidade molhante do adesivo no alumínio submerso em água.

Table of contents

1 General introduction

This chapter discusses the general context of the research project described by this thesis by introducing the four existing research fields involved: (i) chemical product engineering, (ii) (bio)adhesives, (iii) biomimetics and (iv) polyketones. It is concluded by the specific motivation for the project and the outline of the document.

1.1 Chemical product engineering

The World Chemical Engineering Council (WCEC) was formally launched at the closing ceremony of the Sixth World Congress of Chemical Engineering on 27 of September 2001 in Melbourne, Australia [1][1]. Although a main driver for the foundation of the WCEC was the recognition of the global scale at which many of the economic and ecological challenges of the 21st century have to be met, its core activity since that moment has been to monitor how the education of chemical engineers meets the requirements of employment [2][2]. The apparent importance of this occupation mirrors the predictive words of Professor Danckwerts on chemical engineering science in his presidential address delivered to the Institution of Chemical Engineers in 1966 [3][3] (and recalled by many [4-7] [4,5,6,7] thereafter):

"It would be a great mistake to think of the content of chemical engineering science as permanently fixed. It is likely to alter greatly over the years, in response to the changing requirements of industry and to new scientific discoveries and ideas for their application."

From the industrial point of view, a remarkable shift has indeed been observed in the employment of chemical engineering graduates over the three decades that followed. For instance, the share of graduates from Cambridge and Minnesota Universities hired by petrochemical and commodity chemical companies has dropped from three quarters in 1975 to less than a quarter in 2000, whilst the share for more 'product-oriented' companies has risen from less than a quarter to more than half in the same period [6,8,9][8,9]. Similar observations have been made at other universities [10-12][10,11,12]. Although the recent AIChE Centennial report states contrastingly that the share of B.S. graduates hired by the petrochemical industry actually increased from 40% in 1981 to 50% in 2001 (based on AIChE Initial Placement Surveys), its main conclusion on the future role for chemical engineers is similar; they will work for a wider array of companies than in the past, and the nature of their work will differ from that in the traditional companies like chemicals and petroleum refining [13][13].

One school of thought that has attempted to rationalize and translate this development into a new framework (or paradigm) in the field of chemical engineering for both education and research has come to be known as 'chemical product engineering' (CPE) over the past decade. Also referred to as 'formulation engineering' [14][14], 'product engineering' [15][15] or 'product technology' [16][16] in its early stages, it has been defined as the science and art of developing and producing performance products to meet the demands and requirements of society, achieved by adding value to materials by improving

existing or designing new products [16]. A more recent review defined CPE as the whole science and art of creating chemical products, in which chemical product design (CPD) is seen as the core activity [7]. CPD is defined in turn as a systematic procedure or framework of methodologies and tools whose aim it is to provide a more efficient and faster design of chemical products able to meet market demands [6,7]. These definitions reflect the main drivers for the creation of this new field through its stated contents: (i) the whole design procedure of creating chemical products is emphasized, not just the manufacturing process, (ii) needs from society and consumers play a key role, (iii) efficiency and speed of design are critical, and (iv) the art in designing (complex) chemical products is relevant.

Naturally, the goals and drivers of CPE originate from more than just the observed shift in graduate employment. Major changes in the product portfolios, R&D targets and management styles of chemical industries [5,8, 10, 11, 12, 17, 18][17,18] combined with existing contemplations on the future challenges in chemical engineering research [19-22][19,20,21,22] lay at the root of its emergence. Significant work on the actual content of the framework has been done through case studies and theoretical considerations in the years that followed, illustrated by the appearance of several text books [23-30][23,24,25,26,27,28,29,30]. With such progress in the body of knowledge it seems justified to select CPE as a starting framework in research projects when dealing with the task of discovering new chemical compounds and assessing their usefulness for possible applications as or in a chemical product. However, controversy still exists to what extent it can prove to be useful as a commonality, hindering widespread identification and/or acceptance in the chemical engineering community [31][31]. The limited 'hard' evidence for backing-up many of its aspirations regarding integrated product and process design [32][32] and the expanded variety of models and procedures for applying CPE successfully [6-8,11,33-39][33,34,35,36,37,38,39] also indicate that a critical review of existing frameworks is commendable prior to usage.

1.2 The world of adhesives

An example of a multi-billion dollar global chemical industry featuring a wide variety of chemical products tuned for specific applications is the adhesives industry [40,41][40,41]. Defined in general as materials used to join two or more other materials (often called adherends) through surface attachment to form a final assembly [41], adhesives are utilised on many scales throughout the world, with a large range of characteristics, by both nature and man. Global Industry Analysts Inc. mentions more specifically current widespread usage in the sectors of packaging, automotive, electronics, footwear, construction repair and remodeling, textiles, consumer goods and shipbuilding [42][42]. Figure 1.1 provides a graphical illustration of the adhesive consumption by end use in 2009. The scope and liveliness of this world can be illustrated further by recent examples from the academic literature. Adhesives have for instance been used for (i) recovery of DNA from crime scene items [43][43], (ii) assembly of load-carrying parts made of lightweight composites by the aerospace industry [44][44], and (iii) wound closure, fracture fixation and microscale vascular surgery [45][45].

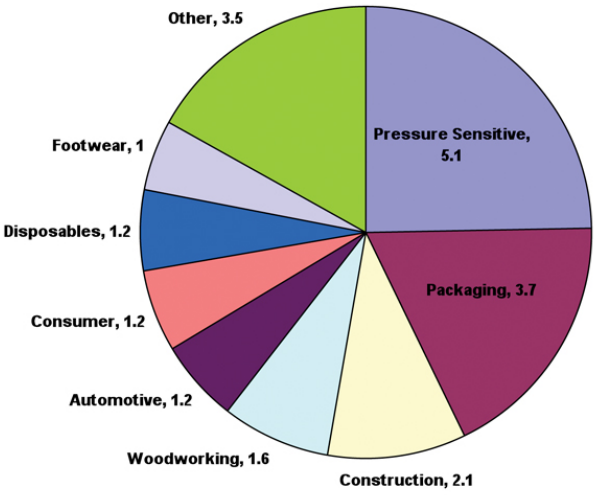

Figure 1.1: Adhesive consumption by end use in dollars for 2009 ($20,6 billion total) [46][46]

The widespread and varied usage of adhesives, combined with the diversity in the utilized chemistry, application methods and sources of the components, has resulted in multiple methods of classification. One common classification is loosely by strength of the created joints [40,41]. This method makes a distinction between three main types: (i) pressure-sensitive adhesives, which possess a very limited adhesive strength; (ii) semi-structural adhesives (divided into hot-melt and solvent-based groups), capable of supporting a small load (0.3 – 3 MPa) for a long time; (iii) structural adhesives, able to bear a significant load (> 7 MPa) for a long time. However, driven by strongly fluctuating price and the availability of products derived from petroleum [41] and increased general concerns on the impact of industrialized societies on the environment and public health, adhesive producers are also confronted with the challenge of becoming more sustainable [47][47]. The additional classification of natural product-based (or bio-based) adhesives, contrasted to fossil fuel-based, is therefore important to mention [41], as are the corresponding general features of environmentally benign production, recyclability and biodegradability.

The concerns and features highlighted here are treated specifically by a recent market analysis on the global adhesives and sealants industry (based on 386 companies) [48][48]. This analysis projects the global market for adhesives to exceed 25.4 billion pounds in 2015 after reversing the negative sales trend in 2010 [42]. This growth in the medium to long-term period is deemed to stem in particular from the rising tide of research activity in the field of volatile organic compound (VOC) compliant adhesives and environmentally friendly technologies [42]. In this regard, regulatory measures (e.g. REACH in Europe) focused on (i) solvent reduction in adhesive processing (and use) and (ii) more carefully selected raw materials by adhesive formulators and end-users affect the market economics significantly [41]. Any business operation in the field should therefore be aware of these macroscale developments.

1.3 A natural influence: bioadhesives and biomimetics

As mentioned briefly in the previous section, not only mankind has designed and used a wide variety of adhesives: nature provides many examples of sophisticated adhesive systems developed by organisms over time for their own benefit [49][49]. These materials can be utilized directly as (ingredients for) adhesive formulations [41], as well as providing inspiration for research initiatives [50][50]. Both topics are introduced in this section.

The first influence of nature on adhesive development is through direct use of its materials. Adhesives of natural origin, or so called bioadhesives, have in fact been used by man since ancient times [40]. The earliest adhesives originated from flora (e.g. tree resins and vegetable oils), fauna (e.g. casein, blood, and collagen), or a combination of these from prehistoric times (such as bitumen and tar) [40]. It must be noted though that the definition of a bioadhesive has been used not strictly for adhesives of natural origin used by man (bio-based adhesives; type I) [40] or unmodified adhesive formulations as found in nature (type II) [50]. It has also been used more loosely for synthetic adhesives developed from biological monomers (type III) [51][51] and for a (partially) synthetic material designed to adhere to biological tissue (type IV) [52][52]. The distinction between these four types is not derived from general consensus, but devised here for increased clarity as response to the different uses of the term encountered in the literature. For example, it has been summarized that bioadhesives (of type II) may consist of proteins, polysaccharides, polyphenols, lipids or a combination of these compounds [53][53]. A short overview of the occurrence of these molecules is presented in Table 1.1 and Table 1.2. However, bioadhesives of type IV are not restricted to these compounds. This type also includes poly(acrylic acid), maleic anhydride co-polymers, poly(ethylene oxide), poly(vinyl alcohol) and poly(vinyl-pyrrolidone), as these bioadhesive polymers are all used for various pharmaceutical and medical purposes [52].

The second influence of nature on adhesive development belongs to the field of biomimetics. This field has been defined in general as a research initiative that seeks to identify and replicate adaptive biological attributes with potential technological applications [54][54]. Classic examples of biomimetic materials developed in the field of interfacial technology have utilised (i) lotus leaf inspired superhydrophobic and microstructured self-cleaning surfaces [54,56][55,56], (ii) shark-skin inspired fluid drag reduced surfaces [56,57][57], (iii) burdock fruits inspired reversible attachment surfaces (Velcro) [56], and (iv) gecko feet inspired reversible adhesive and self-cleaning surfaces [55]. For adhesives in particular, another popular inspiration originates from aquatic organisms (both freshwater and marine), which have evolved a multitude of workable solutions for adhesive bonding of dissimilar materials underwater [58][58]. For example, the single most alluring aspect about mussel adhesion is that bonding to metal and mineral surfaces takes place rapidly in a turbulent, wet and saline environment at ambient temperature: an amazing feature synthetic adhesives cannot (yet) replicate [53,54].

Table 1.1: Main components of bioadhesive materials encountered in several organisms (based on [49])

Organisms/material	*Main organic component**
Abalone shell	P
Algal attachment	PC, C
Barnacle cement	P
Blackfly larval glue	P
Bumblebee mating plug	F
Frog exudate	P
Fungal hydrophobins	P
Microbial EPS**	C
Mussel plaque	P
Polychaete cement	P
Salamander extrudate	P
Sea star footprint	P
Silkworm sericin	P
Spiderweb glue	P
Spumalin/egg glues	C

Table 1.2: Some biomolecules with adhesive properties (based on [50,53])

Biomolecule	*Type**	*Source*
Cellulose	C	Cell walls of plants
Chitin	C	Cell walls of fungi and exoskeletons of arthropods
Collagen	P	Skin, tendons and bone
Elastin	P	Connective tissue
Fibrin (incl. fibronectin, fibrinogen)	P	Blood
Keratin	P	Horns, hoofs, feathers, skin, hair and nails
Laminin	P	Extracellular structure scaffolding in tissues
Mucin	P	Mucous secretions
Silk fibroins	P	Spiders and butterfly larvae

*: P = protein, C = carbohydrate or F = lipid or fatty acid. Two letters denote two components in comparable amounts.
**: Extracellular Polymeric Substance

Two important observations regarding the field of bioadhesives (including all types) can be made at this point. Firstly, the growth of the field is fuelled not only by the general concerns and sustainability drivers for the adhesives industry as mentioned earlier. It is also driven by the increasing understanding of the complex adhesive systems found in nature and correlated advances in biomimetic research for finding systems with yet unachievable characteristics in man-made adhesives. Secondly, the field as a whole appears to be relatively young: only in the past five years have two dedicated text books [59,60][59,60] and an encyclopaedia including articles on the subject [49,52] appeared. Exiting opportunities for bioadhesives can thus be expected to lie ahead.

1.4 Polyketones in adhesives

An example of a synthetic polymer which has emerged in recent years as a promising backbone material for chemical modifications and use in adhesives is polyketone [61,62][61,62]. This research is preceded by an interesting history of the polymeric component itself. The pioneering synthesis of the random aliphatic form of this polymer by copolymerization of carbon monoxide and olefins took place around 1940 [63,64][63,64], followed by the first synthesis of the alternating aliphatic form (Figure 1.2) reported in 1951 [65][65]. Decennia of intense work in both industry and academia followed upon these discoveries to improve product characteristics and processing efficiency, in addition to finding

suitable applications for the polymeric compound. These developments have been reviewed by many, including [66-69][66],[67],[68],[69].

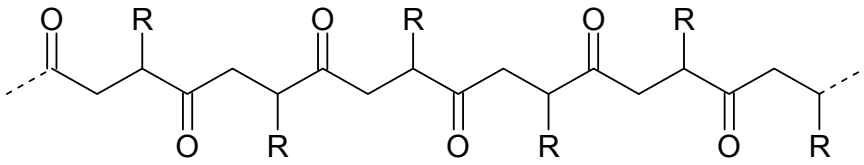

Figure 1.2: Scheme of perfectly alternating (1-olefin)-CO copolymer (R = H, alkyl, aryl, etc.)

Four drivers for the enduring research in this field are often mentioned:

1. The monomers carbon monoxide and olefins are particularly plentiful and inexpensive [70][70];
2. The presence of the carbonyl chromophore in the backbone makes the copolymers more photo- and biodegradable than their polyolefin analogues [71,72][71], [72];
3. Properties such as average molecular weight, polarity, crystallinity, mechanical and surface properties of the polymer can be easily adjusted to meet specific requirement, for example by varying the olefin monomer and catalytic system for the polymerization [73,74][73],[74];
4. Polyketones serve as excellent starting materials for other classes of functionalized polymers because of the ease with which the carbonyl group can be chemically modified [70,72].

With regards to the modification driver, alternating polyketones have attracted special interest in research for two main reasons. Firstly, alternating olefin-carbon monoxide copolymers made through metal-catalyzed polymerizations have the highest possible concentration of the reactive carbonyl groups (olefin:CO = 1), since carbon monoxide does not homopolymerize and random ethylenecarbon monoxide copolymer made through radical-initiated polymerization have higher monomer ratios (C_2H_4:CO>1) [70]. Secondly, the 1,4-arrangement of the carbonyl groups in the alternating form provides additional functionalization pathways [75][75]. The latter has proved that possible modifications not only include obtaining polymers with methylenes, alcohols, amines, amides, oximes, thiols, cyanohydrins, hemiacetals, acetals, and α-hydroxy-phosphonic acids, but also include obtaining poly(furans), poly(pyrroles) and poly(thiophenes) [69]. These modifications are illustrated in Figure 1.3.

As indicated by the four main research drivers, polyketones have several general advantages over other polymers. These have resulted in a range of industrial applications from objects to fibers, film coatings, membranes, photoresists, packaging materials and adhesives [68]. The chemically unmodified use of polyketones in various types of adhesive has been patented [76-79],[76],[77],[78],[79], as well as the use of relatively low molecular weight (1000 – 4000 g mol^{-1}) polyketones in wood adhesives, in which the polymers are cured with amines [80,81],[80],[81]. The latter systems allow fast curing thermoset applications and make use of terpolymers of CO, ethylene, and propylene [82][82]. These polymers show a reduced melting temperature (T_m) compared to the more crystalline copolymers of ethylene/CO, which is caused by the incorporation of a certain amount of propylene/CO segments

into the polymer backbone [82]. Depending on the ratio between propene and ethene incorporated in the polymer backbone, the product consistency ranges from viscous flowing at room temperature for the ethene-free types, to waxy or melting solids at an ethene content of about 80 wt% (on total olefin content) [83][83].

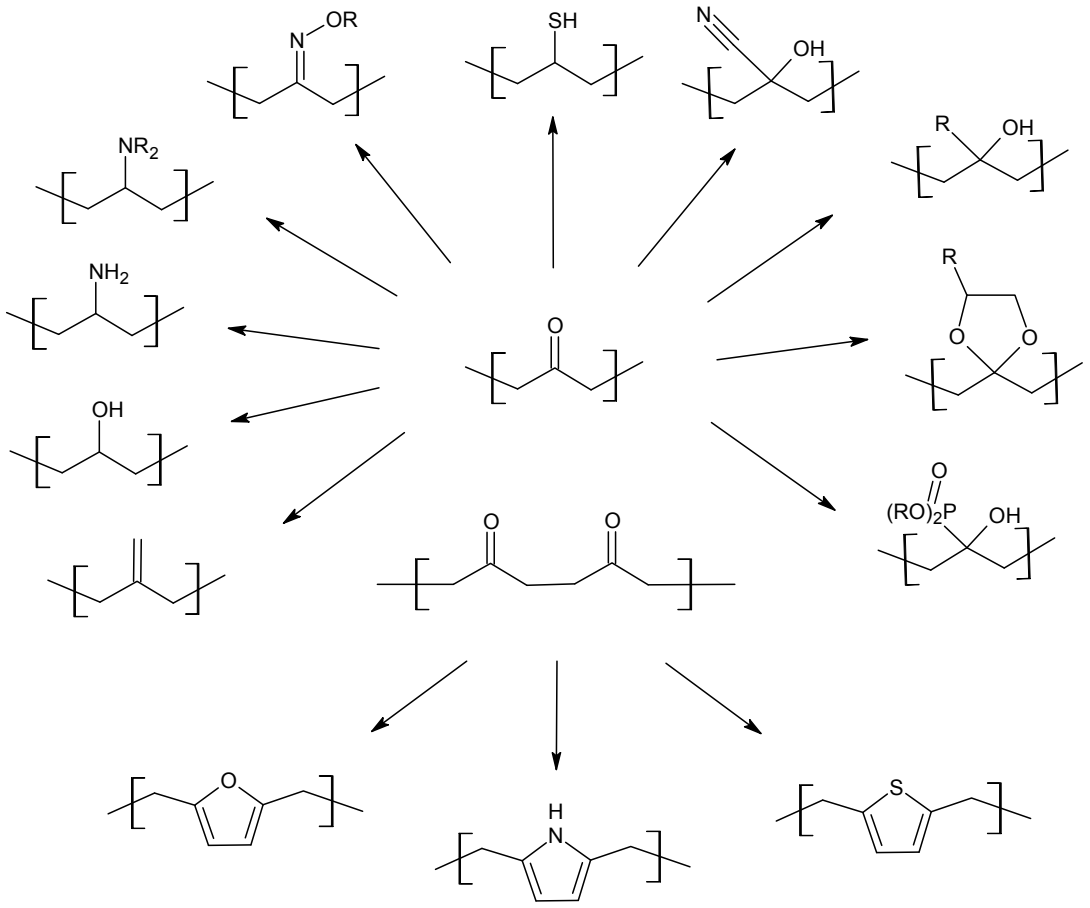

Figure 1.3: Scheme of several reported chemical modifications of polyketone, showing three additional pathways for 1,4-arranged systems (based on [69])

In recent years, a specific alternating aliphatic polyketone prepared by a homogeneous palladium catalyst has been shown to be non-toxic and highly biocompatible [74]. *In vitro* experiments demonstrated no damage in the tested organelles and cell structures after 60 days [74a], as well as increasing mineralization activities with decreasing polarity of the polymer in bone marrow cells [74b]. A particular motivation to use polyketone for such studies was reported to be the lack of admixtures (plasticizers, fillers) and impurities in the synthetic polymer, which normally cause difficulties in the use of synthetic polymers as implant on or body tissue [74a]. A follow-up study showed that similar polyketone-based polymers are biocompatible materials for urothelial cells *in vitro* and *in vivo* [84][84]. Hypothesized was that integrating more bioactive groups into the polymers might enhance their biocompatibility: the ideal CO-alkene polymer would combine a nonbiodegradable 'backbone' with pendant bioactive groups such as fibronectin or laminin [84]. Other recent studies have shown that bioactive moieties such as monosaccharide fragments and

protected tyrosine groups could be linked to the backbone of the polyketones by palladium catalyzed insertion polymerization [85,86][85,86].

1.5 Thesis outline

Given the recent advances in modifications of alternating aliphatic polyketones and subsequent successful utilization as wood adhesives [61,62], as well as the discovery of promising biocompatibility for specific alternating aliphatic polyketones [74,84], it appears to be worthwhile to examine if polyketone can be modified for use as a biocompatible adhesive (bioadhesive type IV). A successful application as such in a biomedical (or pharmaceutical) context would also require water-resistant adhesion [87-89][87,88,89]. In order to achieve biocompatibility and water-resistant adhesion characteristics, inspiration from nature can be drawn from the advances in understanding the adhesion utilized by aquatic organisms [50,58]. One popular biomimetic strategy in this context uses the finding that many mussel adhesive proteins (MAPs) identified to date are polyphenolic, non-toxic and biodegradable [50]. Marine and freshwater MAPs have high levels of a peculiar, modified amino acid L-3,4-dihydroxyphenylalanine (DOPA) [90][90], which has been found to play a critical part in the adhesive system [54,91-94][91,92,93,94]. Because the popular chemical modification of Paal-Knorr for alternating polyketones proceeds less well for sterically hindered amines [95,96][95,96] the use of the structurally similar compound dopamine seems recommendable. This molecule incorporates the reactive catechol group, but has a more freely available amine group for executing Paal-Knorr reactions (see Figure 1.4). As a final, the fundamental polymeric research part described previously can be regarded as part of a broader technology-push chemical product design project, which in turn is related to existing theories on chemical product engineering frameworks [7]. The possibility of benefiting from applying such frameworks not only for finding the most profitable [37] or most desired [6,7,8] chemical product, but also for integrated product and process design [32,33], should not be disregarded.

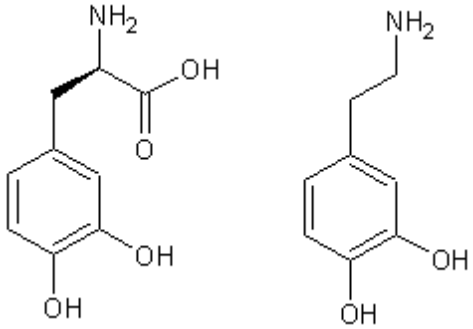

Figure 1.4: Chemical structures of L-3,4-dihydroxyphenylalanine (DOPA, left) and dopamine (right)

The central research question thus faced in this thesis is the following:
Can alternating aliphatic polyketones be modified with dopamine and used subsequently as or in an effective water-resistant adhesive product that resembles the adhesion characteristics found in aquatic organisms and meets market requirements?

In order to address this central question, three main sub questions have been formulated, which will be treated in the following chapters.

Chapter 2: Aquatic adhesion
What chemical and physical strategies are found in aquatic organisms for acquiring water-resistant adhesion capabilities?

Chapter 3: Aquatic-inspired adhesives
Which strategies exist in the development and manufacture of synthetic adhesives inspired by aquatic organisms?

Chapter 4: Novel polyketone-based adhesives
Can polyketone be used as a polymer backbone for acquiring a water-resistant adhesive which is inspired by aquatic organisms?

2 Aquatic adhesion

This chapter introduces the phenomena of adhesion in general, after which the theoretical requirements for aquatic adhesion are discussed briefly. Where relevant, a focus is applied on bioadhesives and water-resistant adhesives in particular. Following a short introduction on the various aquatic organisms currently under investigation for their adhesive capabilities, an overview is presented of the available knowledge concerning the (bio)chemical strategies and molecules involved. The physical phenomena encountered in these systems are treated next in order to provide a more complete picture on the matter. As a final, existing practical methods for assessing the quantitative performance of aquatic adhesives are discussed.

2.1 Adhesion theory

Adhesion is the physical attraction of the surface of one material for the surface of another [41,97],[97]. These attractions are the same as those used normally to describe the state of matter, i.e. van der Waals forces and electrostatic forces [41]. However, there is more than meets the eye here. To begin with, the science of (polymeric) adhesion can be divided into two distinct parts: (i) the formation of the adhesive bond (bond making) and (ii) the physical strength of the adhesive bond (bond breaking) [41]. The latter is also referred to as practical adhesion and is found to be determined primarily not by adhesion itself, but by the physical properties of the adhesive and adherends [97]. The implications of this finding are discussed below, following a brief overview of some of the fundamental concepts, parameters and equations used in adhesion science and aquatic adhesion.

2.1.1 Fundamental forces and energies in adhesion

As stated, fundamental ('physical') attraction forces are also relevant to the phenomenon of adhesion. In addition to the collection of three such forces called van der Waals forces (encompassing dipole-dipole, dipole-induced dipole and dispersion forces), several so-called chemical forces can play a role in the surface properties of a material [97]. These are usually of larger energy of interaction than the van der Waals forces and include: (i) acid-base interactions, including hydrogen bonding and donor-acceptor interactions, (ii) ionic bond formation and (iii) covalent bond formation [97] (see Table 2.1).

Table 2.1: Bond types and typical bond energies [111][98]

Type	*Energy (kJ/mol)*	*Distance (nm)*
Dipole-dipole	4-21	0.35-0.45
Induced dipole	2	0.40-0.50
Dispersion forces	0.08-42	0.35-0.45
Hydrogen	10-26	0.25-0.30
Ionic	590-1050	0.15
Covalent	63-710	0.15
Metallic	113-347	0.15

The translation of all these forces into equations for quantitative use in adhesion occurs by defining first the parameter of surface energy. The difference between atoms in the bulk, surrounded by 6 nearest neighbours in a simple 3D-lattice, and an atom on the surface, surrounded by only 5 nearest neighbours, results in an energy expended to create surface per molecule

$$E = \frac{1}{a_0} \cdot \left(E_S - E_B \right) = \frac{(5-6) \in}{2 a_0} \qquad \textbf{Equation 2.1}$$

in which E = total energy of attraction, a_0 = cross-sectional area on the surface occupied by the atom or molecule, E_S = energy of the molecule at the surface, E_B = energy of attraction in the bulk, $\in$ = energy of attraction between any pair of atoms or molecules and γ = surface energy [97]. Surface energy thus stands for the amount of energy necessary to create a new surface per unit area and typically has the units of millijoules per square meters (mJ/m^2).

If the substance in question is a liquid, the surface appears to exhibit a tension due to the same energetic effect described above. The surface energy is then numerically identical to the surface tension [97]. The relevance of fundamental physical attraction forces in this context is illustrated more clearly by the method of Fowler and Guggenheim. This method is used to calculate the total energy of attraction between two van der Waals surfaces in general (not only for liquids) to find an equation functionally equivalent to (2.1), namely

$$\gamma = \frac{\pi n^2 A}{32 r_0^2} \qquad \textbf{Equation 2.2}$$

The second equation bears great resemblance to the maximal theoretical strength of a material in which the forces of attraction are entirely the result of van der Waals forces (F_{max}; calculated by taking the derivative of the Lennard-Jones potential and setting it equal to zero)

$$F_{\max} = \frac{1}{9} \frac{\pi n^2 A}{\sqrt{3} r_0^3} \qquad \textbf{Equation 2.3}$$

where in both (2.2) and (2.3) A = attractive constant containing all information regarding the forces of attraction between atoms and molecules, n = density of atoms or molecules in the material and r_0 = equilibrium distance of separation of the atomic or molecular species [97]. Although taking into account that contributions of chemical forces alter the above equations (making them significantly more cumbersome), it is clear that the attractive constant A is directly proportional to the surface energy γ, illustrating the intimate relationship between both [97].

When expanding the scope of an adhesive system to include all noncovalent interactions along an interface and their energies, a different equation can be used to illustrate the effect of water on adhesive forces

$$E = \frac{Q_1^a Q_1^b}{k\left(4\pi\varepsilon_0\varepsilon\right)^d r^f} \qquad \textbf{Equation 2.4}$$

in which E = interaction energy, $Q_{1,2}$ = charge or tendency for electropolarization in each type of interacting functionality, ε_0 = permittivity of space, ε = dielectric constant, r = interatomic distance, a, b, d and f are exponents whose magnitude is defined by the type of interaction and k is a constant also dependent on the type of interaction [54]. For example, in charge-charge (Coulombic) interactions the parameters k, a to d and f are all equal to 1 [54]. Because water has a dielectric constant 80 times higher than a vacuum at 20 °C, interaction energies are reduced dramatically [54].

2.1.2 Work of cohesion and adhesion

When one considers the creation of two equal surfaces by splitting a material into two parts at an imaginary plane, illustrated in Figure 2.1, the amount of energy necessary to create this situation must be

$$W_C = 2\gamma \qquad \textbf{Equation 2.5}$$

in which W_C = work of cohesion (and γ = surface energy) [97]. If the process of separation would (theoretically) create two different materials however, the required amount of energy is described by the Dupre equation

$$W_A = \gamma_1 + \gamma_2 - \gamma_{12} \qquad \textbf{Equation 2.6}$$

in which W_A = work of adhesion, γ_i = surface energy of material i, and γ_{12} = interfacial energy between the two materials (energy required to create a unit area of interface) [97]. Important to note here is that: (i) the two equations above are only valid for reversible systems with elastic materials and (ii) it appears that adhesion will be greatest for high values of the two surface energies and a small value for the interfacial energy [97].

Now, the forces of attraction between polymer chains can be described for most polymeric materials by van der Waals attractions [41]. The result of this finding is that the cohesive energy density of a polymer and the surface energy of a polymer are low relative to most inorganic materials (in which other – stronger – intermolecular forces may dominate). To illustrate: the room temperature surface energy of polymers varies from 12 mJ/m² to 70 mJ/m² approximately, whilst the surface energy of aluminium oxide is 638 mJ/m² [41]. Thus, when applying a polymer to an inorganic surface, the work of adhesion is generally low and should be increased through (e.g.) chemical interactions at the interface [41].

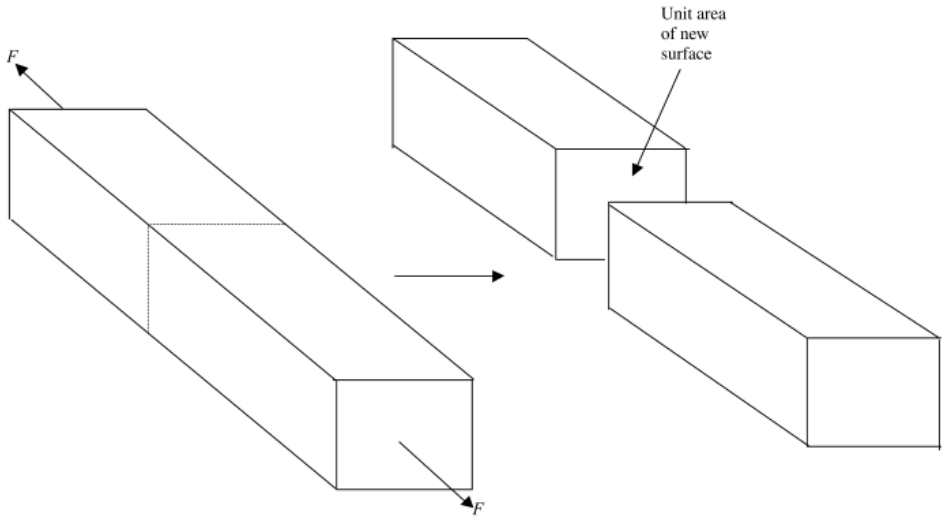

Figure 2.1: Illustration of the creation of two new surfaces by breaking a material at an imaginary plane in its interior [97]

2.1.3 Wetting

The role of chemical bonds between adhering phases is often discussed, especially when biological materials are involved [53]. From the theoretical demonstration that the energy involved in physical adsorption is more than adequate to produce adhesive forces greater than the cohesive strength of either adherend, it has been concluded that the quality of adhesion is strongly linked to the spreading of the adhesive (in the liquid phase) and wettability of the surface [53]. The theoretical basis of this statement, generally referred to as the adsorption theory, is only one of four main theories of adhesion dealt with in (bio)adhesives [99,100][99,100]. However, the fundamental tenet is that the two substrates must be in intimate contact for maximum adhesion strength [100]. This prerequisite applies to the other adhesion theory mechanisms as well and is described by the so-called wetting properties [100].

The wetting description is derived from the situation where a drop of liquid is placed on a smooth surface. The drop will assume a shape characteristic of the interaction of the liquid with the solid surface [97]. If it spreads on the surface, this is called wetting. Young originally derived an equation relating the angle of contact (θ) between the liquid and solid to the surface tensions of the solid and liquid (see Figure 2.2)

$$\gamma_{lv} \cos \theta = \gamma_{sv} - \gamma_{sl} \qquad \textbf{Equation 2.7}$$

where γ_{ij} = interfacial energy between phase i and phase j (s = solid, l = liquid, v = vapour) [97]. Although this equation remains the fundamental equation in the science of wetting, it is only valid for ideal solid surfaces where the influences of roughness, chemical heterogeneity, surface reconstruction, swelling and dissolution are neglected [55]. Nevertheless, combined with the Dupre equation (2.6), this yields

$$W_A = \gamma_{lv}(1+\cos\theta) \qquad \textbf{Equation 2.8}$$

showing that (i) the work of adhesion is maximized when $\theta = 0$ and (ii) the value of it can be at most twice the surface energy of the liquid involved in the wetting process (for water this is 144 mJ/m^2) [97]. Although the equations above indicate that complete wetting is required for strong adhesion, this prerequisite has been found to be neither definitive [101][101] (see section 2.2.3) nor sufficient [97]. Other adhesion theories formulate additional requirements and their effects on the actual bond strength attainable [100]. For example, the ultimate in intimate contact only occurs when the adherend and the adhesive are so compatible that they dissolve (diffuse) into one another, which forms the basis of the diffusion theory of adhesion [97]. For diffusive adhesive bonding to occur, the molecular interactions in the two materials to be adhered must be very similar so that their solubility parameters are the same (or the enthalpy of solution must be negative, e.g. through an acid-base reaction or hydrogen bonding) [97].

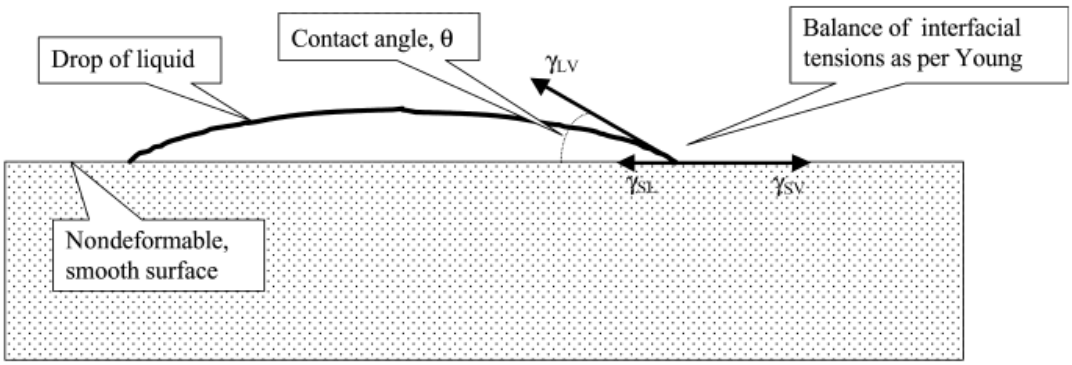

Figure 2.2: Schematic representation of contact angle measurement, including the force balance by Young [97]

2.1.4 Increasing practical adhesion

As stated earlier, the actual physical strength of the adhesive bond depends more on the physical properties of the adhesive and adherends than on the adhesion force at the interface. In fact, the energy needed to break a polymer-based adhesive bond is almost always much more than the energy of interaction at the interface [41]. One explanation for this finding is that materials in general have many ways of dissipating mechanical energy other than cracking to generate surface [97]. Much of the stress that can be placed on an adhesively bonded assembly can be dissipated by various mechanisms in the adherends or in the adhesive before that stress can be transferred to the interface [97]. The key for polymers to perform as adhesives is thus their ability to dissipate mechanical energy [41].

If the energy of interaction between a polymeric adhesive and an adherend (adhesive strength) is more than the energy of interaction between polymer segments (cohesive strength), the polymer will disentangle and dissipate mechanical energy as heat rather than separate from the surface [41]. To attain such a desired situation, practical adhesion can be increased through several techniques, including:

1. Mechanical roughening of the surfaces. This forces a crack to propagate through a more energy demanding non-sharp interface as it will favour the least stiff phase (where energy can be dissipated more easily through plastic deformation) or to cause mechanical interlocking if the adhesive has the correct viscosity to flow into the microcavities and subsequently solidify [97].
2. Removal of a weak boundary layer, which might be present and inhibits strong attachment between adhesive and adherend [97]. For instance, any surface in water becomes quickly coated with a monolayer of polymeric material commonly referred to as conditioning film. The adhesive strength of this biofilm to the substratum or the ability to remove such a film is thought to be crucial for adhesion of aquatic organisms [53].
3. Priming. This is a process in which a chemically distinct layer is placed upon an adherend prior to adhesive bonding in order to provide increased adhesion or increased durability of the resultant bond [97].

2.1.5 Requirements for aquatic adhesion

The challenge of attaining and sustaining high practical adhesion for adhesives in wet environments has been summarized some time ago in Figure 2.11. It illustrates that (i) the cohesion of an adhesive is weakened by swelling, plastification, erosion and hydrolysis, and (ii) the adhesion at the interface is dramatically reduced as the polar groups abundant in the adhesive interact with the polar water molecules through weak boundary layers, wicking and crazing [54,98,102][102].

The strategies to face the challenges of aquatic adhesion described above logically follow to counter these effects and include: (i) remove weak boundary layers, (ii) get the adhesive spread on the surface, (iii) develop numerous and strong interfacial interactions and (iv) cure or set the adhesive [98]. Aquatic organisms, such as epifaunal bivalves, have evolved strategies to successfully deal with the challenges of adhering underwater. Understanding these strategies can be seen to constitute an important background for the adhesive engineer. Although the specific strategies are discussed in the next section, it is practical to point out the general requirements here in advance.

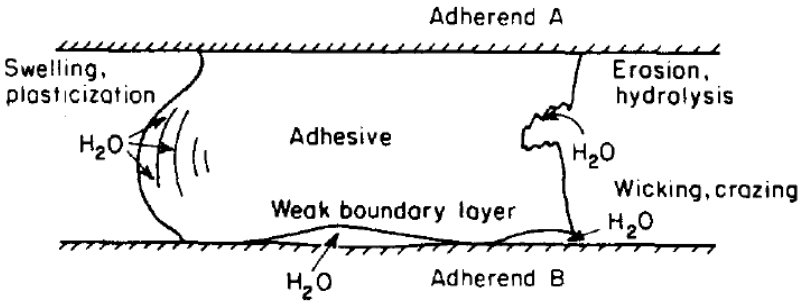

Figure 2.3: Four pathways by which water undermines the performance of adhesive bonds [98]

Aquatic adhesives clearly have to fulfil several functions, which also include preventing premature curing, shielding from aqueous erosion and microbial degradation [53]. All subfunctions can be

classified roughly into surface functions and bulk functions [103][103]. The surface functions include (i) displacement of the water layer, (ii) spreading the adhesive, (iii) coupling to diverse materials and (iv) cleaning the substrate (from biofilm) [103]. The bulk-functions include (i) self-assembly, (ii) curing to suitable toughness and (iii) protection from microbial degradation [103].

Because aquatic organisms are forced to formulate their underwater adhesives as water solutions or water suspensions, this has three important consequences [58]:

1. Polar sidechains in the adhesive are required to displace the water at the interface of the substrate, which leads to exchange of the water at the interface into the water carrier. If non-polar adhesives – or adhesives carried in non-polar solvents – were used, a thin layer of water at the interface would be trapped and subsequently form an interfering weak boundary layer.
2. The volume of the water carrier has to be minimized, because the water must be either expelled or stowed on board as the adhesive cures into a solid. Alternatively, the adhesive should be highly diffusible to water, which seems inconsistent with strong underwater adhesion.
3. The water-borne adhesive has to be delivered underwater without dissolving or dispersing before it sets. Note that a careful balance between cohesive and adhesive bonding is thus required: curing too much or too fast (cohesive bonding) yields a hardened material with little surface interaction, but too much adhesive bonding leads to surface monolayer coating with no connection to the bulk material above [104][104].

2.2 Aquatic organisms with adhesive capabilities

2.2.1 General overview

The underwater world shelters a fascinating array of creatures that utilize adhesion for their survival [105][105]. Aquatic organisms, both marine and freshwater, have developed various solutions to adhesively bond to dissimilar materials underwater [58]. Prime examples of these solutions are the enduring attachments of mussels and barnacles, the temporary attachment of starfish during locomotion and the construction of protective shelters by Sandcastle worms and freshwater larva [58,105]. The key features of several aquatic organisms and their adhesives are displayed in Table 2.2. It must be noted that microorganisms such as bacteria, algae and fungi are often mentioned in this context as these also operate in wet environments [49]. Indeed, advances in synthetic biomimetic adhesives based on e.g. algae have recently been reported [106,107][106,107]. This subfield is not addressed here.

Table 2.2: Key features of several aquatic organisms and their adhesives (based on [49])

Taxonomic group	*Organism/material*	*Type of adhesion**	*Main organic component***	*Typical range of tensile bond strengths (kPa)*
Molluscs	Mussel plaque	I	P	100 – 300 [105]
	Limpet mucus	R	P	75 – 225
	Periwinkle mucus	R	PC	-
	Land snail mucus	R	PC	-
	Slug mucus	R	PC	-
	Abalone shell	I	P	-
	Oyster cement [121][108]	I	P	-
Crustaceans	Barnacle cement	I	P	100 – 2000
Echinoderms	Sea star footprint	R	PC [109][109]	200 – 400 [110][110]
	Sea cucumber tubules		PC	25 – 150
Marine worms	Monogenean adhesive	R	P	2000 – 2500
	Polychaete cement	I		
Fish	Stickleback nest	I	P	-

*: I denotes Irreversible or long-term, R denotes reversible or short-term.

**: Main type of organic component in the adhesive is indicated by P (protein), C (carbohydrate) or F (lipid or fatty acid). Two letters denote two components in comparable amounts.

Five specific organisms (see Figure 2.4) are worth addressing in slightly more detail, before discussing the detailed strategies of the last three (see Figure 2.5). Note: the choice of these particular organisms is based on the amount of data available on their adhesives or recent developments in this area.

Figure 2.4: Pictures of oyster [108], starfish, barnacles, tubeworms [58] and mussel [104] (from left to right)

1. *Oysters: a new target*

   Researchers have very recently investigated the composition of oyster cement, which has shown in first instance to consist of a water-poor organic matrix of cross-linked, phosphorylated protein to harbor the inorganic component of their cement [108].

2. *Starfish: reversible adhesion*

   Reversible (temporary) adhesives of starfish are currently being studied particularly on their micro- and nanostructure. The adhesive material found in their footprints appears to be made up of globular nanostructures forming a meshwork deposited on a thin homogeneous film

[111][111]. Earlier work on its (bio)chemical composition showed that, inorganic residues apart, the protein moiety contains significant amounts of both charged (especially acidic) and uncharged polar residues (amounting to 52 % together) as well as of half-cystine (3.2 %) [109]. The carbohydrate moiety is also acidic, comprising both uronic acids and sulphate groups [109].

3. *Barnacles: strong and permanent*

   The permanent attachment devices of multiple species of barnacles have been studied in detail over the past decades [49]. Recent reviews [103,112],[112] highlight the unique chemical and physical properties that have been discovered over time. In general terms, the barnacles attach their own (hard) calcareous base to foreign materials with a cement layer of a few μm [112]. The cement of one thoroughly studied species is proteinaceous (>90% of its content), has two main macroscopic layers (surface coupling and inner bulk) and consists of more than six different proteins that do not seem to undergo (significant) post-translational modifications [112].

4. *Tubeworms: permanent but different*

   Members of the marine polychaete family *Sabellariidae* live within rigid composite tubes that they build by cementing together sand grains and other material such as mollusk shells [113][113]. The cement connects two hard particulates in water through a several tens of μm thick layer [112]. Also called honeycomb worms or sandcastle worms, the chemical [114-117][114],[115],[116],[117], biological [118][118], structural [119][119] and mechanical [120][120] properties of the adhesives of these organisms have been under close investigation during the last few years. The cement of *sabellariids* such as the California sandcastle worm is comprised of at least three proteins and significant amounts of Mg^{2+} and Ca^{2+} [115,116]. As opposed to the barnacle adhesive, the tubeworm proteins undergo extensive post-translational modifications [113,114,115]. Moreover, the known glue proteins constitute a set of oppositely charged polyelectrolytes at physiological pH. Together with other considerations it has led to the proposal of a complex coacervation model unique for adhesives [114,115].

5. *Mussels: the classic target*

   Mussels affix themselves underwater to a variety of surfaces by depositing several tens of small adhesive plaques connected to the animal using a long thread; an exogenous attachment structure called the byssus [50,104]. How mussels adhere is an active research topic with a respectable history. The undesired mussel attachments ('fouling') of offshore platforms, water-cooled power plants and hulls of ships has driven research initiatives in this particular area for at least 30 years [54]. Over the past ten years there has been a steady flow of reviews in journals [50,53,54,58,102,104,112,121][121] and books [49,52,59,60] either featuring or co-featuring the complex adhesive system.

In a first regard, the byssal thread of (marine) mussels has a modular structure with four proteinaceous parts: a proximal and distal part of the thread and a bulk and tip layer of the adhesive disk (or plaque) [54,112]. Of the more than 20 known proteins of mussel byssus [122][122], at least 10 different adhesive-related proteins from the marine mussel *Mytilus edulis* have been identified [50] and 6 different types of adhesive proteins have been characterized [102]. The exceptional strength of mussel adhesives is deemed the result of the repetitive nature of many of the individual proteins, the post-translational modification of individual amino acids and the gradient nature of byssal attachment devices [50].

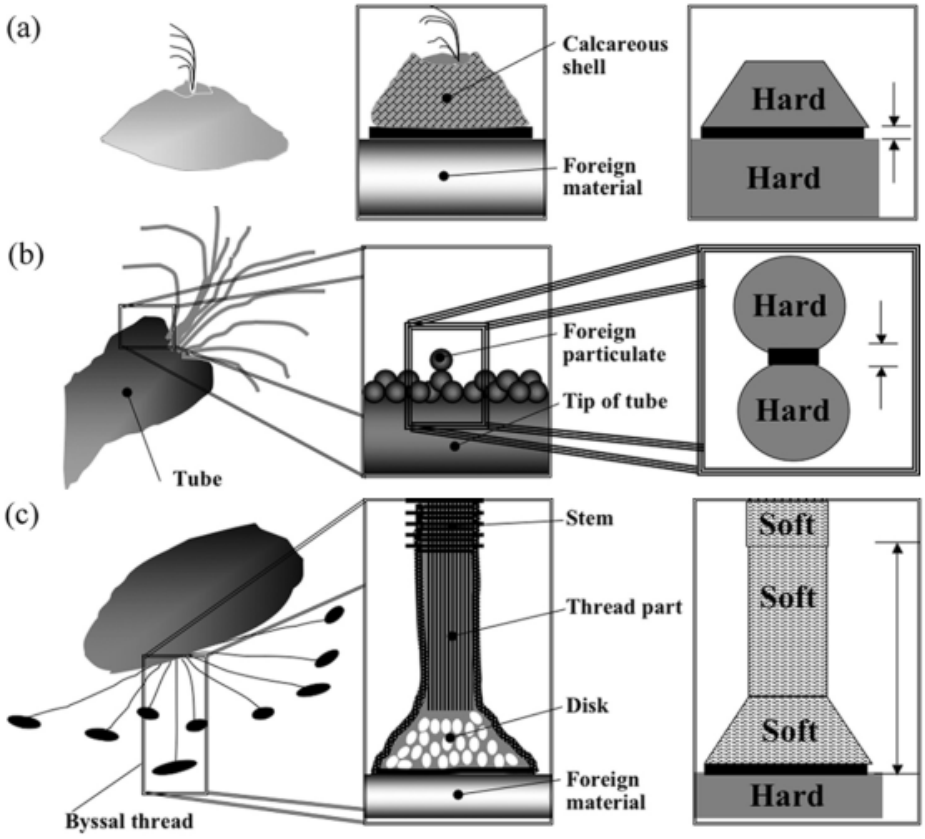

Figure 2.5: Modes of attachment of barnacle (a), tubeworm (b) and mussel (c) [112]

2.2.2 Chemical strategies

Sessile organisms generally produce a multiprotein complex for the multiple functions required for aquatic adhesion (formulated in section 2.1.5), suggesting that each component is linked to one or more of the subfunctions [103]. The specific chemical strategies are discussed in this section for each of three highlighted aquatic organisms.

Barnacles

The chemical composition of the cement of at least five species of barnacles has been determined [49]. Most work has been done on *Megabalanus rosa*, for which the adhesive protein characteristics are summarized in Table 2.3. A mixture of hydrophilic surface proteins (displacing water and forming strong adhesive interactions) and hydrophobic bulk proteins (mainly preventing dissolution) provides the overall required functionalities [103,112]. Especially noteworthy is the block copolymer-like structure of 'coupling agent' cp19k: it has STGA (Ser, Thr, Gly and Ala)-rich domains and smaller VK (Val, Lys)-rich domains [103,123][123]. Homologous genes for this protein were isolated from two other barnacle species and the amino acid compositions were very similar, although the overall sequence was not [103,123]. The four amino acids of Ser, Thr, Lys, and Val, are therefore thought to be essential as functional components to couple with diverse foreign material surfaces via hydrogen bonding, electrostatic interaction and hydrophobic interaction, whilst the small amino acid Gly (and Ala) provide chain flexibility to attain increased interfacial area [103,112,123]. Appendix I includes the chemical structure of these amino acids.

The barnacle *M. rosa* does not seem to rely on (quick) curing chemistry to obtain the cohesive strength in its cement. Neither evidence for intermolecular cross-linking (only intramolecular with Ser) nor any remarkable functional unit (such as DOPA) has been found in the cement [103]. From a functional point of view, it has been stated that curing may not be urgent with barnacle cement, because the adhesive layer that has already been formed would assist the holdfast to withstand physical impact [103]. Moreover, it has been found recently that amyloid-like sequences in the bulk cement protein of *M. rosa* can lead to drastic changes in the secondary structure and form a self-assembly under such stimuli as pH and salt concentration [123]. The control of hydrophobic interaction via conformational change of the bulk protein is therefore suggested to be a possible mechanism for the self-assembly of barnacle cement [123]. However, intermolecular (sulphur) cross-linking is not absent in all barnacle species [53] and cement of the settling stage of the barnacle *B. balanoides* has been proposed to contain 'tanned' protein (DOPA-crosslinks) [124][124]. The intermolecular cross-linking and curing chemistry should therefore not be disregarded for barnacle cement in general.

Table 2.3: Adhesive protein characteristics for barnacle *Megabalanus rosa* (based on [49,103,112])

Protein name	*Location*	*Molecular weight (kDa)*	*Key amino acid(s)*	*Hydropathy*	*Hypothesized function(s)*
cp19k	Surface	19	Ser, Thr, Gly, Ala, Lys, Val	Hydrophilic	Coupling with foreign material
cp20k		20	Cys, His, Glu, Asp	Hydrophilic	Coupling with calcite base plate
cp100k	Bulk	100	Leu, Gly	Hydrophobic	Viscosity lowering, protein-protein interaction, dissolution prevention
cp52k		52	Unknown	Hydrophobic	
cp68k		68	Ser, Thr, Ala, Gly	Hydrophilic	Unknown
cp16k	Unknown	16	Unknown	Unknown	Enzyme

Tubeworms

Most studies on the chemical composition of tubeworm cements have been conducted on the organism *Phragmatopoma californica* and the proteinaceous part of the adhesive [113,114,115,116], although very recently the inorganic elements in the cement of four other species of tubeworms have been studied as well [117]. Regarding the former, the adhesive of *P. californica* is a cross-linked mixture of three highly polar proteins [115,116] (see Table 2.4). The cement is known to be macroscopically heterogeneous, consisting of an outer skin, a porous interior and an adhesive interface [114,119], but it is currently unknown how the highly variable precursor cement proteins are distributed within these domains [116]. The overall mechanism of action is considered to be through a complex coacervate (as stated earlier). The adhesive is namely characterized by two groups of protein: at seawater pH one group is strongly cationic (Pc-1 and Pc-2), through high amounts of lysine (>20 mol%), and the other group is anionic (Pc-3s), through high amounts of phosphoserine (>40 mol%) [114,115]. These oppositely charged groups are thought to associate electrostatically with divalent cations (Ca^{2+} and Mg^{2+}; i.a. needed for charge neutrality) and condense into dehydrated granules at low pH inside the organism, preventing immediate dissolution when released into the seawater at higher pH [114,115].

Table 2.4: Adhesive protein characteristics for tubeworm *Phragmatopoma californica* (based on [114,115,116,119])

Protein name	*Location*	*Molecular weight (kDa)*	*Key amino acid(s) sequence (repeats)**	*Acidity (pI)*	*Hypothesized function(s)*
Pc-1	-	18	VGGY*GY*GGKK (15x)	Basic (9.7)	Coacervation, adhesive strength, cohesive strength
Pc-2		21	HPAVXHKALGGY*G (8x)	Basic (9.9)	
Pc-3a		10 - 52	pS, Y*, C	Acidic (0.5 - 1.5)**	
Pc-3b			pS, Y*		

: X denotes an intervening nonrepeated sequence, Y denotes a tyrosine modified to 3,4-dihydroxyphenyl- L-alanine (Dopa) and pS denotes phosphorylated serine [115]. **: If fully phosphorylated

In addition to the overall coacervate functionality of the protein complex design, the underwater adhesive forces are considered to originate from significant post-translational modifications [114,115,116]. The positively charged proteins (Pc-1, Pc-2) namely contain repeated sequence motifs rich in not only Gly and Lys, but also nearly 10 mol% of 3,4-dihydroxyphenyl-L-alanine (DOPA) [114,125][125]. This hydroxylated tyrosine has a catechol functionality and is known to strongly adhere to various surfaces [91,92,126][126]. The hypothesis of the adhesive role deemed for DOPA in tubeworm cement is also strengthened by the recent discovery of significant amounts of 2-chloro-DOPA in the material [116]. These halogenated catechols have lower pK_as due to the electronegative substituent and are thought to protect the similarly surface-active, but less acidic DOPA-catechols from oxidation by metals by coordinating these metals themselves [116]. Furthermore, the anionic proteins (Pc-3s) contain more than 40 mol% of phosphorylated serine and several phosphoproteins have been shown, or suggested, to bind strongly to calcareous minerals [114].

The curing process and cohesive strength of the tubeworm cement is thought to originate from the cysteine, DOPA and phosphoserine components [115,119]. Pc-1, -2 and -3 contain cysteine, some of which reacts to form 5-S-cysteinyl-DOPA cross-links during the setting process [115]. Other types of cross-links with DOPA have yet to be determined in the tubeworm adhesive [116], although diDOPA cross-links have been proposed to, at least partially, harden the cement after deposition on the particle [114]. The increase of pH from secretory gland (pH 5) to seawater (pH 8.2) is also considered to trigger a curing mechanism through the phosphate sidechains of Pc-3 [114]. First, deprotonation of histidine residues (pKa ~6.5) and the consequent loss of the positive charge would free up their phosphate counterions to interact with Ca^{2+}/Mg^{2+} cations [114]. Next, the nature of the interactions between Ca^{2+}/Mg^{2+} and phosphate groups would change from coulombic interactions between solvated ions to more ionic-like bonds in an insoluble salt, causing spontaneous hardening of the cement [114]. As a final, pSer may also be involved in protein-protein cross-linking as it is thought to condense with His to form histidinoalanine crosslinks with the loss of phosphate [127][127].

The chemical strategies for adhesion and cohesion (curing) are illustrated in Figure 2.6.

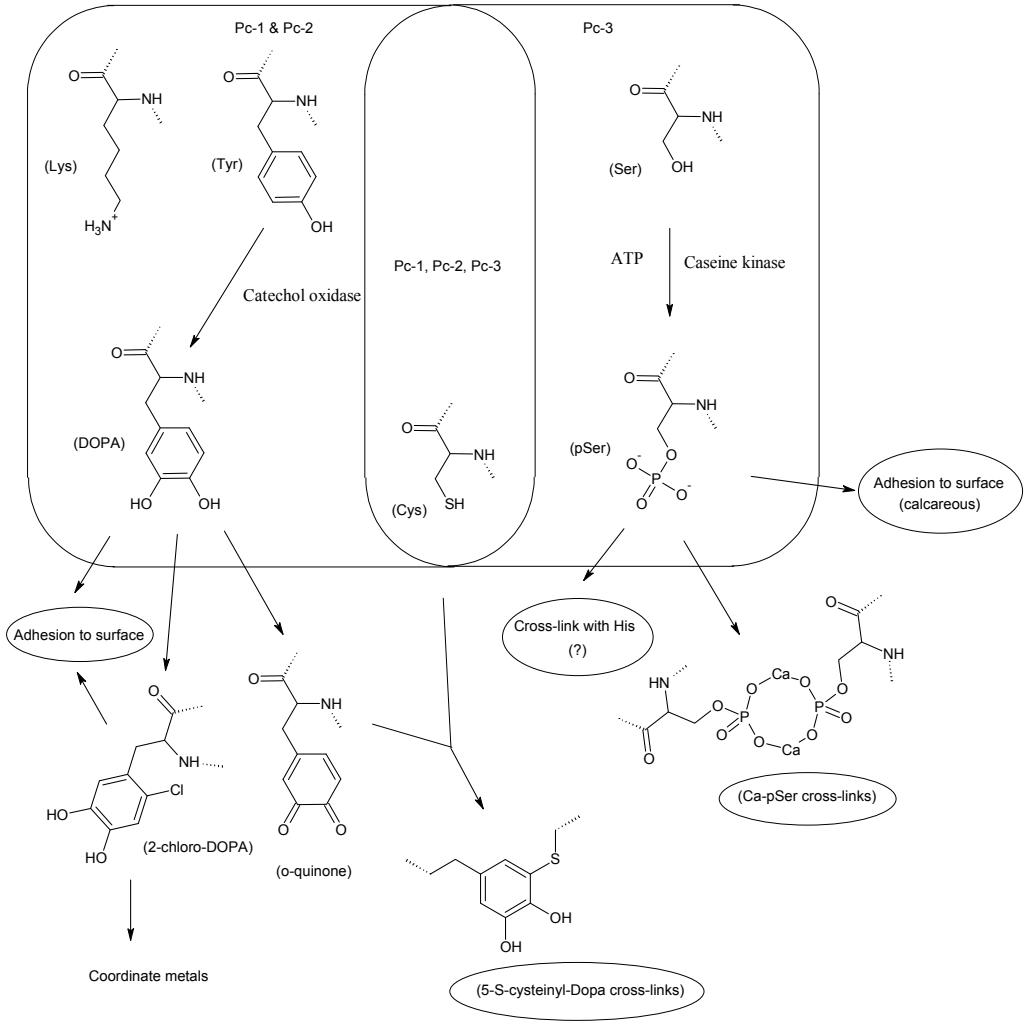

Figure 2.6: Schematic summary of chemical adhesion and cohesion strategies for tubeworms (based on [113,114,115,116,127])

Mussels[i]

Of the various different species of mussels, most studies on adhesion capabilities seem to have been directed on the marine mussel *Mytilus edulis* [49,50,54,112]. Although other species have been studied on their byssus proteins [50], it has recently been stated that potential differences in mussel attachment mechanisms between the freshwater and marine mussel species remain largely unexplored [128][128]. As another point in the case: not all species of mussels have the composite thread structure of *M. edulis;* some species have morphologically homogeneous threads [129][129]. Nevertheless, several adhesive proteins in other mussel species have been found analogous to those of *M. edulis* [50]. An overview of the proteins found in the byssus of this organism is displayed in Table 2.5. As is clear from this overview, the byssus consists of various specialized proteins providing adhesion, hardness, toughness and stiffness to the overall attachment structure. It has a unique overall strategy compared to tubeworms and barnacles as no acidic/basic coacervation mechanism or strongly hydrophobic proteins play a role [112]. Moreover, the extensive (selective) post-translational modifications to either hydroxylate (Tyr, Pro and Arg) or phosphorylate (Ser) the amino acids are a striking chemical feature of the adhesive device, in particular the high levels of DOPA (>20 mol% at the interface) [49,53,58].

Table 2.5: Byssus protein characteristics for mussel *Mytilus edulis* (based on [[49,50,54,102,121])

Protein name	*Location*	*Molecular weight (kDa)*	*Key amino acid(s) sequence (repeats)**	*Acidity (pI)*	*Hypothesized function(s)*
Mefp-1	Whole thread	110 – 115	AKPSYP*P*TY*K (80x), AKPTY*K	Basic (>10)	Protective coating
Mefp-2	Plaque bulk	42 – 47	C, Y*, EGF motif (11)	Basic (9)	Stabilization of plaque
Mefp-3	Plaque tip	5 – 7	R/NRY* (4x)	Basic (>11)	Surface primer
Mefp-4	Plaque bulk	79 – 80	G, R, H, Y, Y*	-	Thread-plaque junction
Mefp-5	Plaque tip	9.5	Y*K/Y*R/Y*H (>8), pS	Basic (9)	Calcareous binding
PreCol-P	Proximal thread	95	GPP*, H	-	Toughness, extensibility
PreCol-D	Distal thread	97	GPP*, H	-	Strength, stiffness
PreCol-NG	Whole thread	76	GPP*, H, Y		Mediator of preCols
PTMP	Proximal thread	50	-	-	Collagen binding

: Y denotes a tyrosine modified to 3,4-dihydroxyphenyl-L-alanine (Dopa), pS denotes phosphorylated serine, P* denotes hydroxylated proline (or Hyp) and R* denotes 4-hydroxyarginine.

[i] This section cites mostly recent review articles. The many original sources of work, which have been conducted over the last 30 years, can be found within these references.

The surface primers mefp-3 and mefp-5 most prominently display the adhesion characteristics of the mussel glue. These proteins are extremely polar and contain the highest levels of modified amino acids: 42% in mefp-3 and 37% in mefp-5 [54]. Both DOPA and pSer engage in interactions with mineral and metal surfaces that exceed the noncovalent possibilities in water [54]. The chelating of DOPA with metals, especially Fe^{3+}, can also lead to oxidation by molecular oxygen to generate quinone-like radicals that can react with the substrate [49]. The quinone-form can also engage covalent interactions with organic surfaces [126]. Furthermore, DOPA and amino acids such as hydroxyarganine can engage in pi-based interactions that allow binding to aromatic surfaces [49,53]. These last two mechanisms provide the remarkable ability of mussels to adhere to both organic and inorganic surfaces. This is deemed (partially) related to the equilibrium that exists between dopa and dopa-quinone at marine pH [126]. In addition, the numerous hydroxyl groups of the DOPA, Ser, Thr, Hyp, and Hyl (hydroxylysine) residues make it possible to displace surface-bound water molecules, leading to zipper-like chemisorption of the extended polypeptides [49]. As a final, the numerous basic residues (e.g. Lys) promote electrostatic interaction with natural underwater surfaces, which typically carry a net negative charge due to adsorption of acidic organic compounds [49,53].

Cohesive interactions within the adhesive of *Mytilus* are based on the same chemistry as adhesive interactions [53]. In general, hydrogen bonds and complex formations between DOPA and metal ions are proposed to contribute to cohesive strength within adhesive plaque and byssus thread [53]. DOPA cross-linking is pronounced in the superficial layer of the adhesive plaque formed by the cuticular protein Mefp-1, yielding some protection to the inner vulnerable foam-like adhesive [53]. As a side note, this protein was the first to be characterized for mussel byssus [130][130] and long thought to the one mainly responsible for the adhesion capabilities due to its high levels of DOPA [122]. Moreover, prior to the report of Sever et al. (2004) [131][131], the most important chemical pathway ensuring structural cohesive strength was thought to be the formation of covalent cross-links between DOPA containing proteins through a free-radical mechanism and enzymatically oxidized DOPA (*o*-quinones) [53]. In addition, it was thought that these o-quinones react with primary amines, such as the prominently available Lys groups, in a Michael addition reaction or to form a Schiff base [53]. These two pathways have even recently been mentioned as the main chemical cross-linking pathways for attaining cohesive strength [102]. However, it is now known that iron chelated DOPA complexes, mostly $Fe(DOPA)_3$, can account for much of the protein-protein cross-linking [49,131] and even for self-healing capabilities [132,133][132],[133]. A different recent review thus places iron central in cohesive (and both adhesive) mechanisms [104]. And to come to full circle: it currently thought that Lys does not participate in the primary mechanism of cross-linking, but does form Schiff bases with completed diquinone cross-links [49,122].

Because it is difficult to capture all chemical strategies for adhesion and cohesion into one clear illustration, only those in which DOPA plays a role are summarized in Figure 2.7.

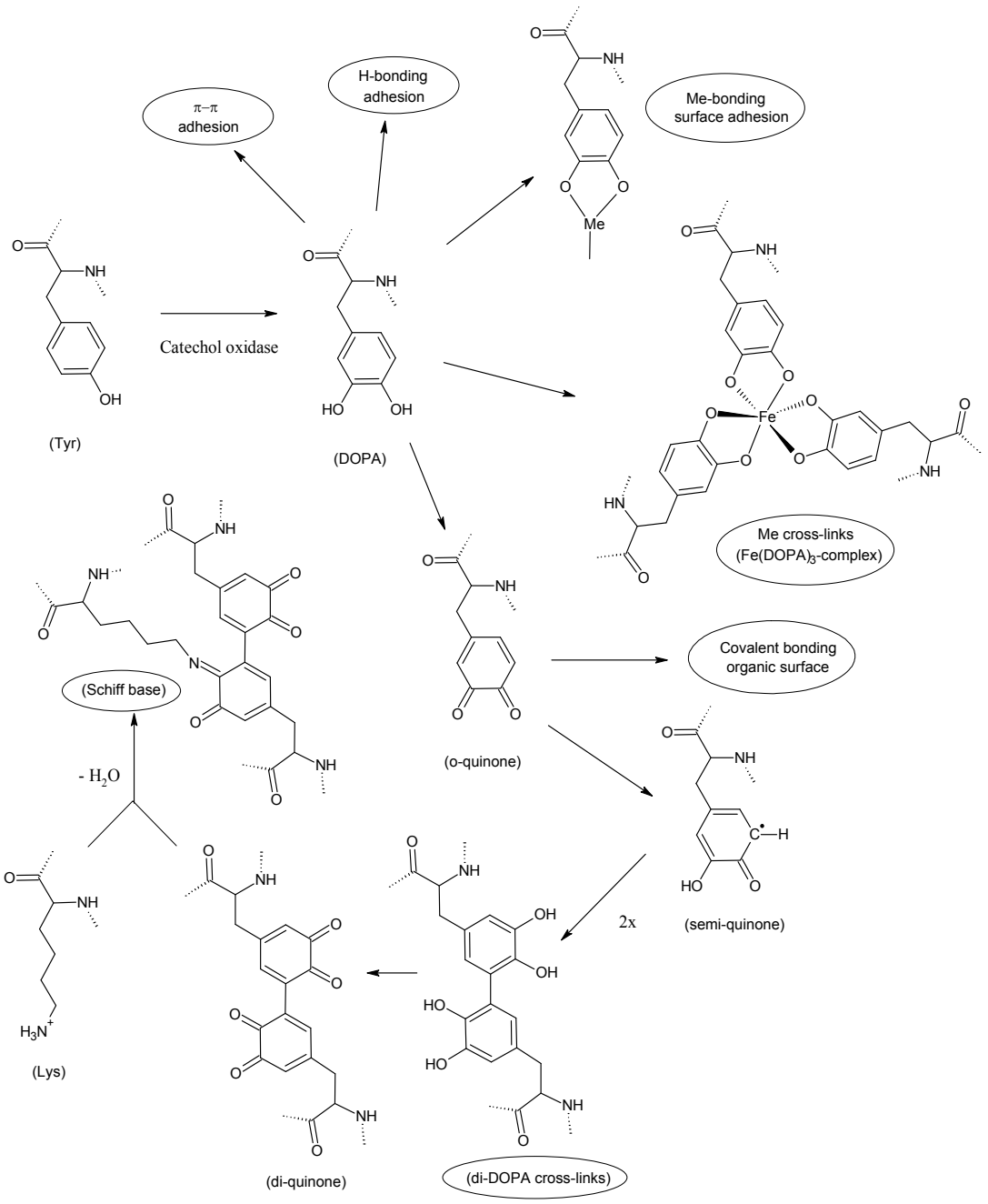

Figure 2.7: Schematic summary of chemical adhesion and cohesion strategies for mussels through DOPA (based on [49,53,54,104,121,126]). Note: resonance structures and strategies without DOPA not shown.

2.2.3 Physical strategies

In this section, five aspects of physical strategies will be briefly discussed: (i) surface preparation, (ii) spreading whilst preventing dissolution or dispersion of the adhesive, (iii) response to surface wettability, (iv) structural concepts of aquatic adhesives and (v) surface morphology.

Surface preparation

As stated earlier, any underwater surface in nature becomes quickly coated with a monolayer of polymeric material commonly referred to as conditioning film or biofilm [53]. Aquatic animals thus rarely experience the molecularly clean surfaces used in adhesive research in the lab (and adhesive literature) [58]. In order to prepare the surface for proper adhesion, sandcastle worms fondle particles physically before gluing them [119] and mussels appear to use their foot organ to clear away debri prior to thread formation [58].

Spreading without loss

Preventing the dissolution or dispersion of hydrophilic adhesive proteins has been explained partially in the previous section: barnacles combine these hydrophilic proteins with hydrophobic proteins [103,112] and tubeworms use a coacervation mechanism between oppositely charged proteins to phase-separate from the water [114,115]. In addition to these chemical strategies, mussels and barnacles use a physical process similar to injection moulding [58]. Mussels create a space protected from the surrounding seawater using the tip of their foot like a rubber plunger to form a seal, subsequently retracting to create low-pressure and then injecting the adhesive precursors, allowing them to set before exposure to the water [98]. Barnacles also inject cement into a confined space between the calcareous base plate and substrate (at later stages of their life) [58].

Response to surface wettability

Recent investigations on alga spores and mussel byssus depositions in response to variations in surface wettability discovered contradictory findings with respect to earlier studies and conventional Young-Dupré equations [101,134][134]. The standard thermodynamic theory (see section 2.1.3) would predict that a fluid adhesive would spread more easily ('wet') on a less wettable surface, but instead a positive correlation between surface wettability and adhesive plaque size was found [101,134]. The apparent contradiction (see Figure 2.8) could be explained by modifying the Young-Dupré equation (2.8) to the form using not the internal contact angle of a liquid on a surface (θ) but the contact angle of the adhesive (measured from the water side; θ_{LA})

$$W_{ALS} = \gamma_{LA}\left(1 + \cos\theta_{LA}\right) \qquad \textbf{Equation 2.9}$$

in which A = adhesive (protein), L = water, S = surface, γ_{LA} = interfacial tension between liquid and adhesive and W_{ALS} = work of adhesion between the adhesive and surface through water [134]. This equation was combined with the slightly expanded form of eq. (2.8), which includes the adhesive in the substrate-water system

$$W_{ALS} = (\beta - 1)\gamma_L(1 + \cos\theta) + W_{LL} - W_{AL} \qquad \textbf{Equation 2.10}$$

in which $\gamma_L = W_{LL} / 2$, $\beta = W_{AS} / W_{SL,}$ to obtain a theoretical explanation for the positive correlation between surface wettability (expressed as $\cos\theta$; higher for more hydrophilic surfaces as the internal angle is measured) and plaque size (correlated to θ_{LA}) [134]. In physical terms, the novel explanation

included the phenomenon that very polar adhesive proteins could indeed effectively compete with water to wet a hydrophilic surface by establishing stronger interactions (higher work of adhesion) between the adhesive and the surface than the energy required to dehydrate the liquid adhesive [101,134].

As a final, in the study with mussel byssus deposition the following sequence of events were proposed with regard to surface energies [101]:

1. A high energy surface is detected,
2. Identified as a good attachment site (strong bonding possible),
3. Mussel attaches and deposits byssi quickly,
4. Byssus plaque spreads well, resulting in high tenacity attachment,
5. Few byssi are required, so byssi attachment stops, conferring an energetic advantage to the organism.

The opposite might apply for low-energy surfaces [101]. However, it is stressed that one must take into account that surfaces of different materials might not just have different surface energies, but could also be heterogeneous in chemistry, polarity, topography (roughness) and modulus, influencing the results through these (possibly) relevant parameters [101].

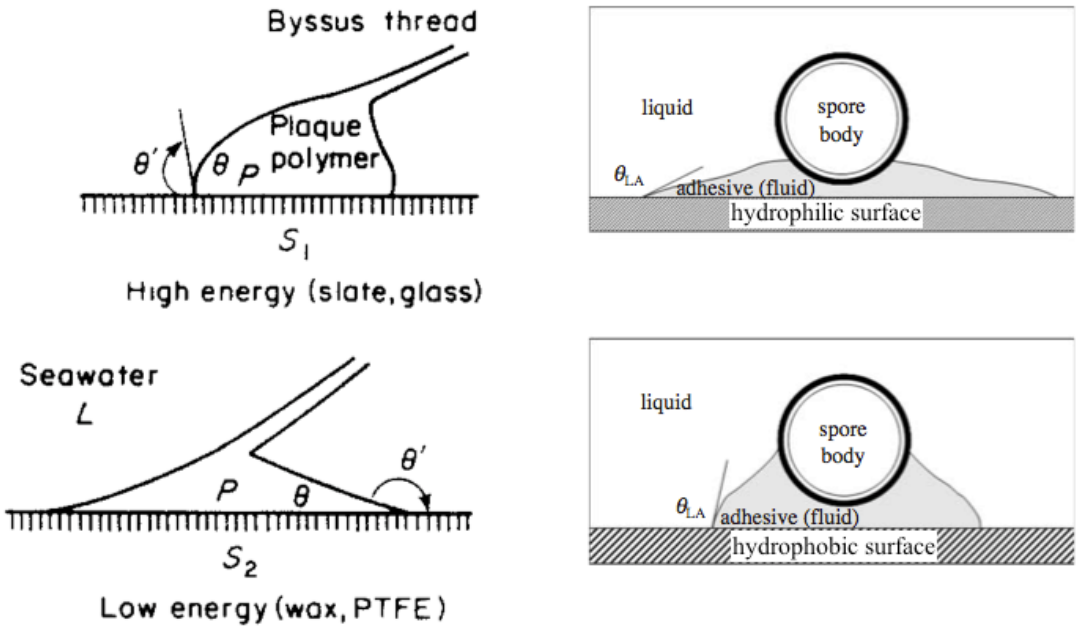

Figure 2.8: Difference between conventional interpretation of byssus adhesive spreading (left) [98] and novel interpretation of alga spore adhesive spreading (right) [134] on surfaces of different wettability

Structural concepts

Detailed macro- or microscopic details on the structural concepts of barnacles are scarce. One review states that the organism uses homogeneously coated nm-sized globules that form various macromolecular structures, depending on the substratum: tightly packed, foam-like, branching and/or loosely matted strands [53]. This macromolecular structure determines the physical characteristics, ranging from rigid cement films to elastic hydrated adhesive plaques [53].

Recent investigations into the structural properties of tubeworm cement (*P. californica*) revealed that the adhesive was a cellular solid [119]. Cell diameters ranged from 0.5 to 6.0 μm and were distributed to create a steep porosity gradient that ranged from near zero at the outside edges to about 50% at the centre of the adhesive joint [119]. The consequence of the adhesive gradient is to concentrate material at the edges where the stress (in shear) is maximal and to spare material in the centre of the joint where stresses are minimal, thus creating the highest quality joint whilst saving vital metabolic energy [119]. At the nanoscale, the adhesive appeared to be an accretion of trillions of deformable nanospheres, resembling a high-solids-content latex adhesive [119]. These deformable nanoparticles can absorb tensile strains and, together with the open cell microstructure, act as multiscale energy absorbing micro-dashpots [119].

Most information is available on the various structural concepts of mussel byssi. Mechanical studies on the byssus threads, both static and dynamic, have indicated complex yielding and stiffening behaviour for the different parts – in accordance with the heterogeneous structural design [135,136][135,136]. Three main concepts are utilized by the mussel [54]:

1. *An adhesive foam*

   Mussel use a solid foam structure in the adhesive in order to avoid contact deformation, defined as damage inflicted on the softer part of two joined materials (i.e. the softer thread versus the stiff and hard substrate) [54]. Two gradients are used to mitigate contact deformation damage: (i) a porosity gradient, from nonporous at the interface to mostly porous at the centre, and (ii) small projections of one material (rooted collagen fibres) extended into the other (foam) like tree roots, which increasing the contact area between the two [54]. Figure 2.9 illustrates both gradients in the foam.

2. *Graded block copolymers*

   The different block copolymer-like collagens (D, P and NG) of the stiffer fibrous threads are constructed in a gradient with silk (very stiff), elastin (soft) and amorphous (intermediate) flanking domains next to the kinked collagen core element [54].

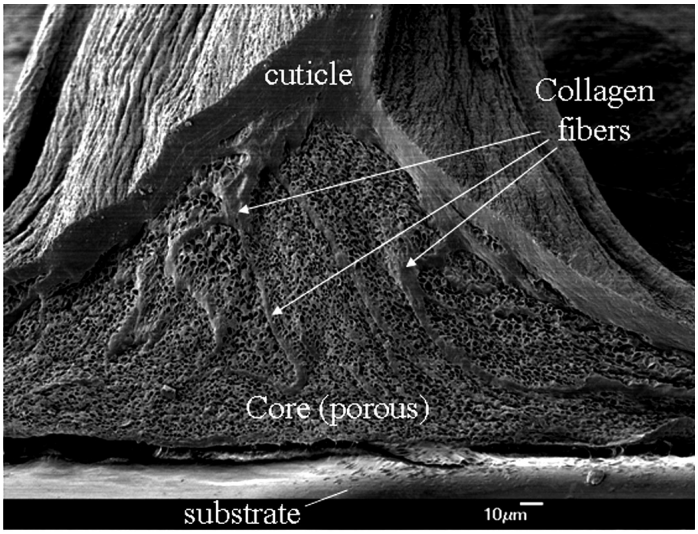

Figure 2.9: Solid foam structure of a byssal adhesive plaque [54]

3. *A durable coating*

   Because the intertidal habitat of mussels has a high particulate content and a wave velocity between 5 and 15 m/s, the exogenous byssus is exposed to an environment resembling cyclic sandblasting [54]. The solution to protecting the vulnerable adhesive to abrasion and erosion is to coat with a substance with a high hardness to stiffness ratio, which the mussel appears to do in a bumped/knobbed fashion (see Figure 2.10) [54]. Dense (metal-DOPA) cross-linking in cuticle granules was recently proposed to provide the hardness, whereas the less cross-linked matrix provides extensibility of the coating [132].

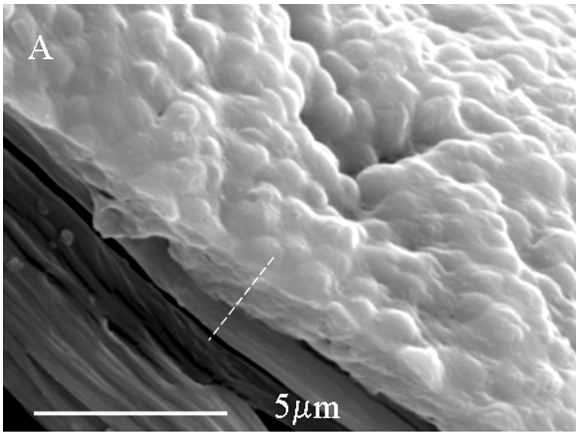

Figure 2.10: SEM of the protective coating of a distal byssal thread portion [54]

Surface morphology

A recent review states that the surface properties and external morphology of adhesives released by aquatic (benthic) organisms have received little attention compared to the biochemical content of these adhesives [137][137]. Although the focus of the review was on temporary adhesives of organisms

other than the three discussed here in more detail, the general conclusion was that an adaptive geometric match is made between the adhesive organ and the substratum from micro- to macroscopic levels [137]. Suggestions for increasing the adhesive performance of biomimetic (bio)adhesives thus included to investigate whether: (i) flexible and extensible bonds between two adhering surfaces increase adhesion, (ii) an adhesive could be patterned, or (ii) multiple isolated adhesive regions are better than an extended adhesive surface [137]. Indeed, little information could be found on the surface morphologies of any of the natural adhesives discussed in detail in this chapter. The only relevant remark found was that contact between the substratum and the mussel byssus adhesive is continuous [54].

2.3 Adhesive bond strength measurements

Consistently measuring and judging adhesive performance is as crucial a step in acquiring reliable data on the natural adhesive systems as it is for developing new ones. To this end, the following section addresses the general methods used for measuring (water-resistant) bond strength: the key performance property for an adhesive [41]. Note: biocompatibility is a second key performance feature for bioadhesives (type IV) [138][138]. This feature is reviewed in section 3.3 together with several other performance properties (e.g. durability and easy of application).

2.3.1 General methods and parameters

The primary performance characteristic of an adhesive is its adhesive bond strength, which forms the focus of this section. It is measured quantitatively by assessing the mechanical properties of an adhesive joint [97]. Specific tests have been developed to examine these properties under different modes of loading, the main four of which (tensile, shear, peel and cleavage) are displayed in Figure 2.11 [97]. Partially because tensile tests suffer from a non-uniform stress state and rarely mimic the true load on adhesive bonds in practice, lap shear tests are currently most often used [97]. Peel tests are used to test fractures, the propagation of an existing flaw at the edge of a specimen, when one or both adherends are capable of plastic deformation [97]. Cleavage tests assess the resistance to fracture when the adherends are thick enough to resist significant plastic deformation, resulting in the determination of the critical energy release rate (when appropriately applied) [97]. For all tests, adhesion data are typically reported in Pascals or Newtons of force to bring about detachment divided by the overlap area in square meters (Pa = N/m^2) [118].

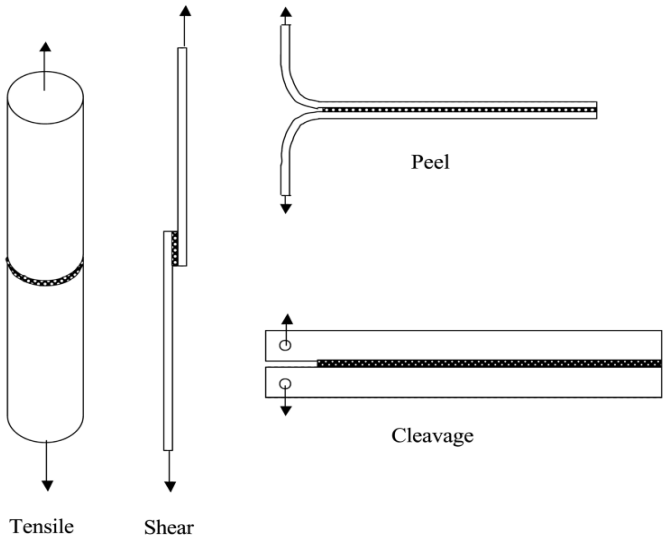

Figure 2.11: Schematic representation of main specimens used to determine adhesive bond strength: butt tensile, lap shear, T-peel and double cantilever beam (left to bottom right) [97]

In addition to the four methods described above, a separate technique called contact mechanics exists which allows the direct determination of the work of adhesion between two surfaces (typically expressed in mJ/m^2) at very low rates [97]. The use of this technique has increased significantly in recent years as it provides a means to connect the fundamental forces of adhesion to practical adhesion [97].

It is important to note that polymeric materials, including those used as adhesives, are sensitive to the rate of application of mechanical stress as a result of their viscoelastic properties [97]. Because this behaviour depends on temperature, the phenomenon is called time–temperature superposition [97][ii]. In addition, they can be subjected to increasing stress until failure (static mechanical tests), but also to multiple below-critical stresses during so called fatigue (or dynamic) tests. The latter type is for instance a more accurate predictor of clinical performance for bone cements, as these environments often encounter cyclical loading [49]. Thus: (i) type of specimen, (ii) type of loading, (iii) rate of mechanical stress and (iv) testing temperature are some of the first main items to consider when assessing adhesive bond strengths.

2.3.2 Use in aquatic (inspired) adhesives

A review of the literature on biological aquatic adhesives and aquatic-inspired (bio)adhesives indicated that many different methods have been applied to quantitatively evaluate their water-resistant adhesion properties. For the former group, a recent and comprehensive overview of method characteristics and results (mainly tensile and shear strengths) is available [49]. For the latter group,

[ii] This effect can be incorporated quantitatively into a so-called master curve. In this curve a shift factor is used to express the work necessary to break an adhesive bond as a function of the 'reduced rate of mechanical stress application' (which incorporates the temperature) [97].

no such overview could be found. To this end, a brief overview of several adhesive strength characterization methods for both types of adhesives has been devised in Table 2.6 for the case of mussel (inspired) adhesives. Generally, all adhesive systems have been aimed at biomedical applications, with the exception of the one tested on wood and a more theoretical proof-of-principle study

Table 2.6: Some characteristics of several mussel (inspired) adhesion bond strength determination methods

*Mussel (inspired) adhesive**	*Substrate(s)*	*Specimen type*	*Water in testing environment*	*Reference*
Natural system	Acrylic, PVC, Silastic ® T-2, aluminium, glass	Tensile	Tested in air within 7-10 min after removal of joint from cultivation tank	[105]
MAPs extract	Porcine tissue		Humid curing (80 % RH), tested in air	[139][139]
		Shear	Ambient curing, tested in air	[140][140]
Modified soy protein	Maple veneer (wood)		Hot press curing (20 kg/cm², 120°C, 10 min), soaked in water (at RT), dried in air (at RT), (repeated soak and dry), tested in air	[141-143] [141],[142],[143]
Synthetic polypeptide	Aluminium, steel, PMMA, PS, PE, glass	Tensile	Curing in oven, tested in air (no attempt to maintain hydration)	[91,92]
	Aluminium, steel, PS, glass, porcine skin, bone		Same as above, but also short cure in air, long cure in dialysis bag filled with water, tested in air	[144][144]
	HDPE, glass, alumina, iron		Curing at RT, dried under reduced pressure, tested in air (no attempt to maintain hydration)	[145][145]
Synthetic polymer	Glass	Shear	Adhesive applied to dried glass, clipped together (i) in air or (ii) under water, kept clipped together underwater, tested in air	[146][146]
	LDPE surface-grafted with hydrophilic monomers	Shear***	Clipped in air, cured in oven (25 °C), tested in air	[147][147]
	TiO_2-coated Si-wafer	Contact mechanics	Cured in air, dialyzed in 0.15 M HCl, equilibrated in PBS, tested while flooded with PBS Cured in N_2-rich glovebag, placed in HEPES buffer (for swelling), tested in HEPES buffer	[148][148] [149][149]
Synthetic polymer**	Aluminium	Shear	Cured at RT, 55 °C and RT, tested in air	[150][150]
Synthetic polymer	Bovine pericardium, Surgisis, CollaMend, Permacol	Shear, burst strength	Hydrated in PBS, activated with cross-linker solution, compressed (in air), conditioned in PBS, tested in air	[151][151]

*: All adhesives have been applied as aqueous polymer solution, except if noted otherwise.

**: Delivered as solution in an 1:1 acetone:dichloromethane mixture.

***: Called 'tensile shear,' to distinguish it from other (less commonly used) shear experiments, e.g. ring shear [97].

Examples of bioadhesives (type IV) in Table 2.6 – those which have also been tested on biological tissue – seem to confirm the statement that no standard test methods have been specifically designed for this particular type of adhesive [100]. Direct comparison of data between different research groups is therefore frustrated, as small variations in experimental variables have a substantial effect on the quantitative measurements (e.g. initial load, contact time, speed of testing and substrate preparation) [100]. Great care must thus be taken when designing adhesive assessment methods and comparing with existing data from the literature.

2.4 Conclusions

What chemical and physical strategies are found in aquatic organisms for acquiring water-resistant adhesion capabilities?

Although there have been huge developments in both the theory and applications of adhesives in air, limited endeavours have been made for the development of applications and theory of underwater adhesive technology [112]. Research into the chemical and physical strategies utilized by aquatic organisms has however been on-going for at least three decades, with a focus on mussels, barnacles and tubeworms. What is clear from these investigations is that aquatic adhesion is a multifaceted phenomenon. There are various requirements that adhesives have to meet in order to deal with the many disruptive influences water has on regular bond formation. Different organisms utilize common strategies to tackle these challenges, i.e. multi-proteinaceous hydrophilic complexes, post-translational modifications of amino acids and gradient-built structures. However, each has developed its own intricate and unique variant. An attempt to provide a concise summary of the information reviewed can be found in Table 2.7.

Table 2.7: Summary of chemical and physical adhesion strategies of aquatic organisms

Surface function	*Requirement*	*Solution characteristics*		
		Barnacle	*Tubeworm*	*Mussel*
1	Cleaning substrate	-	Fondle particles	Swipe with foot
2	Displacement of water layer	Hydrophilic primer proteins	Hydrophilic proteins	Hydrophilic and basic primer proteins
3	Spreading without dissolving	Complex of hydrophilic and hydrophobic proteins; protected spreading environment	Phase-separated coacervate	Protected spreading environment
4	Coupling to diverse materials	Amino acids with H-bonding, electrostatic and hydrophobic interactions; flexible chain conformation	Post-translation modified Tyr and Ser into DOPA and pSer	Post-translation modified Tyr and Ser into DOPA and pSer
Bulk function				
1	Self-assembly	Amyloid like sequences	Coacervation	Coacervation?
2	Curing to toughness	Conformational change of hydrophobic bulk proteins	Cross-links with DOPA, pSer and Cys	Cross-links with DOPA, Fe (, Lys)
3	Protection from degradation	Unknown	Hard outer layer	Highly cross-linked coating
4	Strong architecture	Unknown	Open cell microstructure, deformable nanoparticles	Bi-gradient adhesive foam, gradient thread

3 Aquatic-inspired adhesives

This chapter reviews existing approaches for developing synthetic mimics of aquatic adhesives. First the needs and market requirements for this chemical product category are briefly addressed, based on information from recent reviews in the academic literature. Next, a distinction is made between the chemical platforms utilized in the applied strategies. The biological systems that were attempted to mimic are mentioned and the discovered results in terms of mechanical and biological properties are treated subsequently. Where possible, the manufacturing and commercial aspects of these products will be mentioned at the end of this chapter.

3.1 The need for mimics

3.1.1 Market drivers

Developing new biomedical materials by mimicking or even using marine biological adhesives has been a general driver for many research activities in aquatic adhesion [104]. Researchers in this field typically emphasize qualitatively that new surgical adhesives, dental composites and/or orthopedic cements are still very much in demand [104]. The main description of tackling this demand for innovation has been: "*To develop effective adhesives for repair of wet living tissues [, as] 20th century mechanical fixation with stitches and staples remains very much the norm in medicine*" [58]. Slightly more specific, the challenge has been described as making adhesives that are simultaneously: (i) nontoxic, (ii) form strong bonds and (iii) are able to set in wet environments [104]. It is subsequently reported that no current man-made material is able to display all three properties, even though marine biology has largely solved such a problem [104].

The medical literature has been consulted briefly in order to investigate the claims of these authors, in addition to possibly providing complementary requirements. Recent reviews on surgical adhesives were found to discuss three categories of surgical adhesives: (i) hemostats (agents that stop bleeding), (ii) sealants (agents that seal small holes) and (iii) adhesives (agents that bond various tissues together) [152,153][152],[153]. An attempt to concisely summarize their findings is displayed in Table 3.1. Indeed, it can be observed from the overview that the primary combination of high bond strength and nontoxicity cannot be found in the currently available (and approved) surgical adhesives. The absence of any orthopedic adhesive can be noted as well, which is confirmed by a different recent study [154][154].

Table 3.1: Characteristics of currently used surgical adhesives (based on [152,153])

Origin	*Chemical system*	*Commercial name(s)*	*Type(s) of application*	*Disadvantage(s)*
Naturally derived	Fibrin glue: human derived fibrinogen, thrombin, factor III and bovine/artificial aprotinin	Tisseel, Evicel, Vitagel, Cryoseal, Artis	General as hemostat, colon sealant and skin graft adhesive	Risk of virus infection, low strength, rapid loss of strength, expensive, complex to prepare and use, requires low moisture when used as sealant
Semi-synthetic	Albumin-based glue: bovine serum albumin and glutaraldehyde	BioGlue	As sealant and adhesive in cardiac and vascular surgery	Toxicity of unreacted and leached glutaraldehyde, dense postoperative gel structure, expensive
	Gelatin-based glue: Gelatin-resorcinol-formaldehyde	GRF glue	Adhesive for acute aorta dissection	Toxicity of aldehyde
Synthetic	Cyanoacrylates: (1) Octyl cyanoacrylate (2) Butyl cyanoacrylate	(1) Dermabond, (2) Indermil, Histoacryl (Blue)	Skin adhesive: external surfaces only	(1&2) Toxicity of monomers and degradation product (aldehyde), only adheres top layer of skin (2) Poor tensile strength and brittleness
	Polyethyleneglycol (PEG): (1) PEG and oligotriethylene carbonate with acrylate ester end caps, triethanolamine and eosin Y (2) PEG-ester and trilysine amine (3) Two PEGs	(1) AdvaSeal (2) DuraSeal (3) CoSeal	(1&2) Sealant for pulmonary air leakage (EU) (2&3) Sealant for cranial surgery	Expensive, only moderate strength, swelling

Furthermore, a recent study extensively reviewed 14 carefully selected clinical studies (1152 patients in total) to assess the effects of various tissue adhesives for the closure of surgical wounds as compared to conventional skin closure techniques [155][155]. Sutures were found to be significantly better than tissue adhesives for minimizing dehiscence (wound re-opening) and were found to be significantly faster to use as well [155]. Besides assessing bond strength durability (in the form of dehiscence) and time to closure, this study also took into account the levels of infections, cosmetic appearance, patient satisfaction, surgeon satisfaction and relative cost in order to present a more complete comparison of performance characteristics [155]. In addition, researchers have recently commented on the absence of a standard technique to measure the adhesive performance of surgical glues [156,157][156,157]. General commentary on the performance of currently available surgical sealants included disappointing clinical adhesion and high prices, stressing in response efficient and cost-effective usage [157]. Based on these and the various other needs mentioned previously, an overview has been constructed for general (qualitative) market requirements (see Table 3.2).

Table 3.2: Qualitative market requirements for biocompatible, water-resistant adhesives

Category	*Nr.*	*Requirement*	*Reference(s)*
Biocompatibility	1	No immune response	[139]
	2	Biodegradable with no tissue toxicity and no accumulation	[139,158][158]
	3	Prevent wound infections	[155]
Physical	4	Liquid to apply	[152]
	5	Able to set in wet environments	[104]
	6	Rapidly curable	[152]
	7	As pliable as adherend tissue	[152]
Mechanical	8	Strong bonding[iii]	[104,158]
	9	Durable bonding in presence of physiological fluids	[139]
Other	10	Affordable	[153,157]
	11	Easy to handle	[139,153]
	12	Environmentally friendly /renewable production	[41,42,146]

3.1.2 Limits of the natural adhesives

Biological attributes have evolved by trial and error over a very long time to a specific (and changing) set of challenges [54]. The natural adhesives should however not be considered optimal biological solutions for underwater adhesion, let alone optimal material engineering solutions [58]. After all, adaptation is a multivariate optimization process under various constraints [58]. These constraints are different for the aquatic organisms than they are for adhesive producers targeting biomedical applications. More to the point, three limits to the natural underwater adhesive systems have been described:

1. *Low bond strength*

   Natural underwater adhesives seem to have bumped up against a bond-strength ceiling somewhere short of 1 MPa [58]. Mussel plaques rarely exceed 300 kPa [49,105], although the cement from barnacles and tubeworms can attain adhesion strengths of 2 MPA (see Table 2.2). Even though comparison between such bond strengths must be done with great caution (see section 2.3.2), these pale in comparison with the 20 MPa bond strengths of contemporary dental adhesives [58] and the 50MPa of high performance synthetics (polyimides) [54].

2. *Low production yield*

   Working with the natural adhesive proteins from aquatic organisms is hampered by the low extractability efficiency for obtaining them. For example, approximately 10000 *M. edulis*

[iii] Note that the prerequisites for strong bonding have been detailed in chapter 3.

mussels are needed to produce 1 g of Mefp-1 adhesive from byssal structures [50,159][159]. Earlier attempts of using native barnacle cement proteins has also required a whole week of collecting the organisms and resulted in only a few micrograms of the cement [58].

3. *Immune response*
   Previous studies on the use of mussel adhesive proteins (MAPs) as medical adhesives showed that both the proteins and the required oxidase enzymes caused significant toxicity and antigenicity in animal models [160][160]. However, other studies showed that mussel adhesive proteins are harmless to the human body and do not impose immunogenicity [161][161]. This stated limit is thus controversial.

3.2 Chemical platforms

How can one efficiently make stronger underwater glues? One popular approach has been to combine functional elements or design principles from the natural glues with the versatility of synthetic polymer chemistry and the gathered know-how of adhesive engineers [58]. The general allure of synthetic approaches is the broad range of polymer backbone chemistries, the diverse side chain functionalities that can be built in during polymerization, and cost-effective commercial scale-up [58]. Based on a detailed literature review, three categories of existing approaches have been identified: (i) protein based, (ii) polypeptide based and (iii) other polymer based. Obviously, the degree of modification of the chemistry of the mimicked natural systems increases in this line-up.

3.2.1 Protein-based

The recombinant versions of the barnacle adhesive cement surface proteins (cp19k and cp20k; see Table 2.3) have been used in larger quantities to assess the adsorption to various materials [123,162][162]. However, these have not been used to assess their direct performance as a synthetic adhesive. Indeed, recent reviews do not mention certain applications [103,112], although the native adhesives were shown to be able to cement particles of different materials together underwater in an artificial way [112]. Over the last ten years only one patent application could be found on barnacle adhesive proteins and possible technical exploitation [163][163]. Earlier Japanese patents on the matter, published between 1995 and 1998, have never been transferred into an international or US patent [53]. In contrast, MAPs have been a more popular source of inspiration to develop synthetic mimics. Table 3.3 details the chemical features of protein-based systems, using only sources that included macro-scale adhesive bond strength data (given the scope of this study).

Table 3.3: Chemical features of protein based mussel-inspired adhesive systems developed over the past decade

Protein system	*Substrate(s)*	*Main reactant(s)*	*Protection chemistry**	*Crosslinker/oxidant*	*Ref.*
Dopamine and cysteine modified soy protein	Maple veneer (wood)	Dopamine-HCl, cysteamine, soy protein isolate	Yes	None (hot-press)	[141,142, 141]
MAP (acidic solution)	Glass, pig and cattle muscle	MAP	No	None	[164][164]
				$NaOH$ / Na_2CO_3	[165][165]
				$NaIO_4$	[166][166]
MAP (slightly basic solution)	Eye	MAP, heparin, sutures		H_2O_2	[167][167]
MAPs (paste)	Porcine skin	MAP		None	[139]
	Small intestinal submucosa			$KMnO_4$, $Mn(OAc)_3$, $K_2Cr_2O_7$, $NaVO_3$, $Fe(NO_3)_3$	[140]
Recombinant hybrid MAP	PMMA	Recombinant hybrid MAP	No	None	[159]
	Aluminium			$Fe(NO_3)_3$, $Mn(OAc)_3$, $NaIO_4$	[168][168]
Recombinant hybrid MAP coacervate		Recombinant hybrid MAP, hyaluronic acid		None	[169][169]

*: The use of protection chemistry in incorporating the aquatic-inspired chemical component.

It can be observed from the overview above that only a limited number of macro-scale adhesive systems have been developed. The use of soy proteins and modifying them by mussel-inspired groups (using dopamine) for use as a more water-resistant wood adhesive [141,142,143] stands out as a distinct technology with regard to the others. The second group consists of using extracted native proteins, dealing with low yields (thus neither environmentally friendly nor economically practical [50]) and clearly aimed at biomedical applications. These technologies show a development from using a non-oxidant using system [139,164] to an oxidant using system in order to increase adhesive bond strengths and reduce curing times [140,166]. The third group uses recombinant hybrid proteins in order to attain a more facile scale-up of using marine adhesive proteins as a bulk-adhesive [159,168,169]. In addition, effective incorporation of the tubeworm-inspired coacervation principles has been demonstrated recently by using hyaluronic acid as the cationic partner to the negatively charged MAPS; a two-fold increase in adhesive bond strength was observed with regards to using the MAPs alone (albeit in a dry curing environment) [169].

Using a recombinant hybrid approach is the most recent technological development in the field and a lot is expected in terms of enabling endless commercial applications [50]. However, significant challenges remain. These include attaining: (i) similar levels of the extensive post-translational modifications found in the native tubeworm and mussel adhesives (see Chapter 3) whilst keeping

purification simple, (ii) minimal toxicity to the expression host, (iii) high expression levels, and (iv) sufficient solubility of the purified proteins [58].

3.2.2 Polypeptide-based

Synthetic polypeptide systems have been used to clarify the role of certain amino acids and amino acid sequence in aquatic adhesion. Most notable studies in this regard are those that concluded that: (i) amino acid functionality is key to replicate bulk adhesion, not amino acid sequence [91,92]; (ii) Lys and Tyr residues are the key amino acids for (nonspecific) mussel-mimicking adhesion [87,170][170]; (iii) DOPA-containing decapeptides based on the sequence of mefp-1 are effectively cross-linked following oxidation to quinopeptides, whilst Lys residues may participate in intramolecular side reactions with the cross-links formed [171][171]; (iv) mussel adhesive proteins have a meaningful primary structure, enabling adherence to both high and low surface free energy surfaces in a watery environment [145]; and (v) strong adhesion and cohesion in mfp-3 mimicking films can be attributed to DOPA groups favorably oriented within or at the interface of these films [172][172].

Although synthetic polypeptides in aquatic-inspired adhesive research have clearly proved to be valuable systems from an academic point of view, their polyelectrolyte nature causes the polymers to swell considerably in aqueous solutions [160]. This swelling severely limits their utility as medical adhesives and sealants [160]. Nevertheless, a small number of the studies on model sequential and random polypeptides also tested the bulk adhesive properties of these sequential polypeptides directly. An overview of these specific studies is given in Table 3.4.

Many of systems mentioned above have prepared polypeptides via the ring-opening polymerization of α-amino acid-*N*-carboxyanhydrides (NCAs), using novel initiators that allow the living polymerization to form well-defined structures (see Figure 3.1) [160]. Of all four systems described above, only the one with poly(Lys-DOPA) was used recently in a more application-oriented type of study [144]. Important to note from the chemical perspective is that Lys was not only chosen just because of its – somewhat controversial – reacting role in aquatic adhesion (see section 2.2.2). It was chosen more importantly to make the polypeptide physically water-soluble, thus facilitating use as a tissue adhesive [144]. The authors discussed that the undesired cohesive failure within the adhesive bond observed in previous poly(DOPA-Lys) systems (and related to the swelling behaviour; see also section 2.1) was a difficult problem to solve. Other amino acids could render the cured adhesive less hydrophilic and thus less vulnerable to swelling, but would also render the original polypeptide less water-soluble, frustrating (facile) biomedical application. A second difficulty was the slow oxidation needed to avoid rapid consumption of the surface-binding catechol groups, leading in turn to undesired high curing times to attain sufficient bond strength. Using glutaraldehyde as an additional component in the system was successful in decreasing water uptake and degradability, but only at the cost of adhesive strength. A better solution was found in the compound ferric citrate. This oxidant increased resistance to swelling and degradation of the cured polymer together with a more acceptable loss of adhesive strength [144].

Table 3.4: Chemical features of polypeptide based aquatic-inspired adhesive systems developed over the past decade

Polypeptide system(s)	*Substrate(s)*	*Main reactant(s)*	*Protection chemistry*	*Crosslinker/ oxidant*	*Ref.*
Poly(Lys-DOPA)	Aluminium, steel, PMMA, PS, PE, glass	(Di)carbobenzyloxy-protected L-lysine and L-DOPA N-carboxyanhydrides	Yes	air (O_2), H_2O_2, pH=12, tyrosinase, $NaIO_4$, $Fe(H_2O)_6^{3+}$ (*)	[91,173] [173]
	Aluminium, steel, PS, glass, porcine skin, porcine bone			H_2O_2, ferric citrate, $NaIO_4$, chymotrypsin, O_2, glutaraldehyde/H_2O_2	[144]
Poly(Lys-DOPA), poly(Glu-DOPA)	Aluminium	Same as above, also: poly(γ-benzyl-L-glutamate)		H_2O_2	[92]
Polyoctapeptides (X/Y-Gly-Tyr-Ser-Ala-Gly-Tyr-Lys)$_n$ (X = Thr, Ala; Y = Thr:Ala = 3:2)	Aluminium, iron, HDPE, glass	Boc-, Nps-,O-Et, ONp- and Bzl-protected amino acids	Yes	Tyrosinase (mushroom)	[145]
Poly(X-Tyr-Lys) (X = Gly, Ala, Pro, Ser, Leu, Ile, Phe), poly(Y-Lys) (Y = Gly, Tyr), poly(Gly-Tyr)	Porcine skin	Nps-,ONp- and Bzl-protected amino acids			[87]
Poly(Cys-Tyr-Gly-Lys)	Aluminium, iron	Carbobenzyloxy-protected Cys, Tyr, Gly and Lys N-carboxyanhydrides	Yes		[174] [174]

*: This ferric oxidant is mentioned in the patent [173], but not explicitly referred to in the examples provided, nor in the scientific articles referred to [91,92].

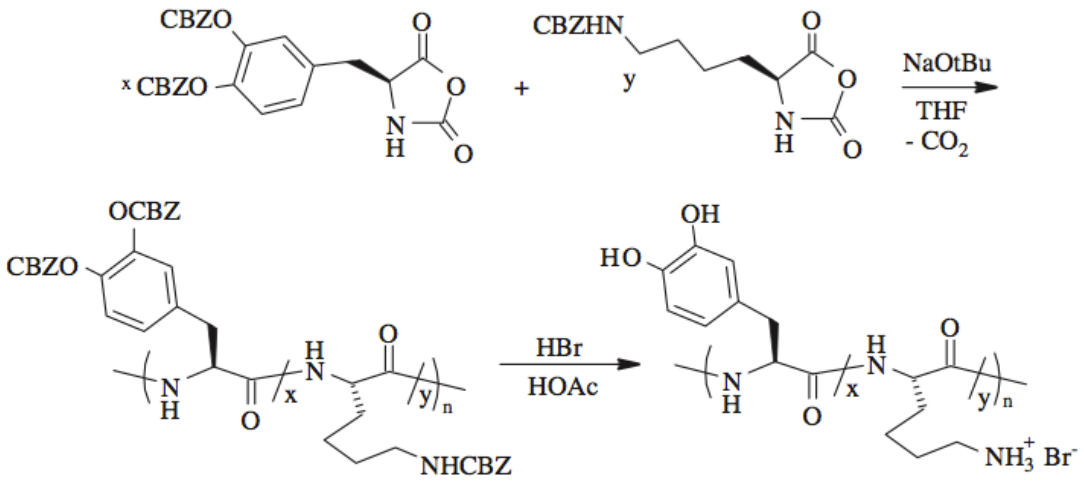

Figure 3.1: Synthesis of adhesive DOPA-Lys copolypeptides using NCA monomers [160]

3.2.3 Other polymer based

Using non-protein and non-peptide based polymeric systems has been by far the most popular chemical route chosen in recent years for developing (possible) new aquatic-inspired biomedical adhesive materials. Analogous to the previous two overviews, Table 3.5 summarizes the key chemical features of mussel-inspired systems and Table 3.6 for those of tubeworm-inspired systems. Note: recently developed pressure-sensitive poly(dopamine methacrylate-co-2-methoxyethyl acrylate) (coated) systems [175-177][175,176,177] based on a gecko-mussel structured adhesive [178][178] are relevant to mention, but have been excluded from this overview due to the distinctly different adhesive application orientation.

Table 3.5: Chemical features of other polymer based mussel-inspired adhesive systems developed over the past decade.

Polymer system(s)	*Substrate(s)*	*Main reactant(s)*	*Protection chemistry*	*Crosslinker/ oxidant*	*Ref.*
DOPA-PEG, Oligo-DOPA-PEG, Oligo-(DOPA-Lys)-PEG, DOHA-PEG, DMe-PEG (ester-linked dopamine-PEG)	Ti-coated glass, porcine skin	N-Boc-DOPA, 3,4-dihydroxy-hydrocinnamic acid (DOHA), branched PEG-NH_2 and PEG-OH, DOPA-NCA, Fmoc-LYS-NCA, dopamine-HCl, succinic anhydride	Yes	$NaIO_4$ and phospholipid encapsulated $NaIO_4$	[179][179]
DOPA-$(PEG\text{-}PLA\text{-}MA)_2$, Oligo-(DOPA)-$(PEG\text{-}PLA\text{-}MA)_2$, Oligo-(DOPA-Lys)-$(PEG\text{-}PLA\text{-}MA)_2$	Ti-coated silicon	TBDMS-MPD, EO, lactide, methacrylic anhydride, N-Boc-Gly, DOPA, Fmoc-Lys		DMPA & UV-irradiation	[149]
DOHA-PEG-PCL, Dopamine-PEG-PCL	Bovine pericardium	PEG-NH_2 and PEG-OH, polycapro-lactone (PCL), succinic anhydride, N-Boc-Gly-OH, DOHA, dopamine-HCl	No	$NaIO_4$	[151]
DOPA-PEG-dextran	Mice duodenum	PEG-NH_2, linear dextran, L-DOPA		None (air?)	[180][180]
Poly(hyaluronic acid-dopamine-co-thiol-terminated Pluronic)	Mice skin	Hyaluronic acid, dopamine-HCl, pluronic, cysteamine			[181][181]
DOPA modified PMMA-PMAA-PMMA	TiO_2	MMA, *t*BMA, DOPA methyl ester HCl	Yes	pH=10 and self-assembly in H_2O	[88,182][182]
DOPA modified PMMA-PMAA-PMMA, Boc-DOPA-PS-PEO	TiO_2-coated quartz, porcine skin	Same as above, also: PS-PEO-OH, N-Boc-L-DOPA dicyclohexyl-ammonium salt		$NaIO_4$	[183][183]

(Continued on next page)

(Continued from previous page)

Quinone modified chitosan	Glass	Chitosan, dopamine-HCl, tyrosinase	No	Mushroom tyrosinase	[146]
Quinone modified chitosan with PEG		Chitosan, dopamine-HCl, tyrosinase, PEG			[184][184]
Quinone modified chitosan		Chitosan, dopamine-HCl, tyrosinase		*MelB* tyrosinase	[185][185]
	MAA, AA, and MAAm grafted LDPE			Mushroom tyrosinase	[147]
Quinone modified chitosan-dextran	Bovine cortical bone	Chitosan, dextran, L-DOPA, H_5IO_6		H_5IO_6	[138]
Phenolics-laccase modified chitosan	Maple veneer (wood)	Chitosan, various phenolic compounds, laccase		Laccase	[186][186]
Poly(4-vinylphenol)		4-vinylphenol	?*	1,6-hexane-diamine, DETA	[187][187]
Poly(*N*-acryloyl dopamine), polyethyleninime (PEI)		Dopamine-HCl, acryloyl chloride, PEI	Yes	PEI	[188][188]
Tannin, PEI		Condensed tannin, PEI	No		[189][189]
Soluble decayed wood, kraft lignin, PEI		Soluble decayed wood, kraft lignin, PEI, $NaBH_4$, H_3BO_3, $Na_2B_4O_7$			[190-192][190], [191,192]
Poly((3,4-dimethoxystyrene)-co-styrene)	Aluminium	Styrene, 3,4-dimethoxystyrene	Yes	$Fe(acac)_3$ $[(C_4H_9)_4N]IO_4$ $[(C_4H_9)_4N]_2Cr_2O_7$	[150]
Dopamine modified polyurethane (PU)	Iron	Polyether polyols, isophorone diisocyanate, dimethylol propionic acid, dopamine-HCl	?*	?*	[193][193]
Polymerized TDA-$(EO)_2$-DOPA-C_2-OH, TDA-Gly-OMe	PMMA, glass, SiO_2	TDA, 2-hydroxyethyl-amine-2-chlorotrityl, Fmoc-DOPA, EO	Yes	UV-irradiation	[194][194]

*: indicates information could not be obtained from the article abstract in case full-text was unavailable.

Table 3.6: Chemical features of other polymer based tubeworm-inspired adhesive systems developed over the past decade

Polymer system(s)	*Substrates*	*Main reactant(s)*	*Protection chemistry*	*Crosslinker/ oxidant*	*Ref.*
Poly(acrylamide) coacervate with (i) phosphate and dopamide sidechains, (ii) lysine sidechains	Bovine cortical bone	Dopamine-HCl, methacryloyl chloride, monoacryloxyethyl phosphate, acrylamide, N-(3-aminopropyl) methacrylamide-HCl, Ca^{2+}, Mg^{2+}	Yes	$NaIO_4$	[154]
Coacervate with (i) poly(acrylamide) with phosphate and dopamide sidechains, (ii) amine modified gelatin	Aluminium	Dopamine-HCl, methacryloyl chloride, monoacryloxyethyl phosphate, acrylamide, gelatin, ethylene-diamine dihydrochloride, Ca^{2+}, Mg^{2+}		$NaIO_4$	[195][195]
				$NaIO_4$ / 1,2-O-isopropylidene-a-D-glucofuranose	[196] [196]

The different polymer backbones utilized in the systems detailed by the previous two overviews can be classified roughly into five groups:

1. *Polyethyleneglycol (PEG)*

   PEG is made by polymerization of ethylene oxide and the resulting hydrophilic polyether is miscible with water. It is applied in medicine as a hydrogel wound dressing, tablet excipient and denture fixative [52]. The polymeric system has been studied fairly extensive by the Messersmith group (a.o.) for use as an aquatic-inspired bioadhesive (type IV). Linear and branched PEGs have been modified initially with DOPA or DOPA-mimicking end-group functionalizations to obtain rapidly gelating and adhesive hydrogels upon mixing with an oxidant [179,197][197]. Photo-curable amphiphilic block-co-polymers were developed subsequently, which utilized methacrylate end groups to photopolymerize and poly(lactide) (PLA) segments to render them biodegradable (by virtue of the hydrolysation) [149]. Advanced biological and adhesive evaluations were published recently on similar systems that did not require protection-chemistry [151,180]. These systems incorporated either hydrophobic hydrolysable (ester-linked) polycaprolactone (PCL) segments [151] or used the water-soluble poly(glucose) dextran as an additional bio-based component in the hydrogel system [180]. All systems have in common that they swell in the presence of water – hence the name hydrogel – resulting in mechanical properties comparable with native soft tissue [180].

2. *PMMA-PMAA-PMMA*

   Poly(methyl methacrylate)-poly(methacrylic acid)-poly(methyl methacrylate) (PMMA-PMAA-PMMA) triblock copolymers have recently been used in a similar way as the PEG-based hydrogels as an aquatic-inspired adhesive. These polymers can be completely dissolved in toxicologically acceptable solvents such as NMP, EtOH and DMSO [88]. Self-assembled hydrogels were obtained by exposing the triblock copolymer solutions in dimethyl sulfoxide (DMSO) to water vapour [182]. As water diffused into the solution, the hydrophobic end blocks (from PMMA) formed aggregates that were bridged by the water-soluble midblocks (from PMAA) [182]. This self-assembly strategy was deemed advantageous with regards to physical crosslinking, because it removes the necessity of a potentially harmful oxidizing agent and would be less sensitive to oxygen (or DOPA) inhibition of alternative cross-linking strategies (e.g. pH, temperature, UV) [182]. However, when modifying the hydrophilic mid-block by the relatively hydrophobic DOPA, a buffer solution at pH=10 was needed to attain similar swelling behaviour [88,182]. This did induce some oxidation and physical cross-linking due to the auto-oxidation of DOPA under these basic conditions [182]. A follow-up study utilized periodate oxidation and also used a system with DOPA functionalized end groups of a polystyrene-poly(ethylene oxide) (PS-PEO) copolymer to investigate the effect of the morphology [183]. Unfortunately, the focus of this study was on the developed method of adhesion characterization (through films, not hydrogels) and not particularly on the (spatial) chemistry [183].

3. *Chitosan*

   Chitosan is a bio-based polymer obtained by deacetylating chitin (a polysaccharide), which is extracted from the exoskeleton of *Crustacea* (e.g. craps and shrimps) [52]. It is cationic as it contains glucosamine and N-acetyl glucosamine units, rendering it water soluble at lower pHs (at which the amine group is protonated and more hydrophilic) [52]. Not surprisingly, the material has been used in developing aquatic-inspired adhesives for the reason that it is made from abundantly available bio-based material and that it is able work without using organic solvents [146,147]. Mussel-inspired (and insect cuticle curing-inspired) systems have been developed from this polymer using enzymatic dopamine-oxidation in order to implement water-resistant adhesion [146,147,185]. PEG [184] and dextran [138] have been used recently as additional components; the first to increase the adhesive strength at shorter reaction times by virtue of its enzyme-protecting capabilities (it restrains decrease in activity), the second to enable the formulation of a two-component biocompatible (bone) adhesive based on amine-aldehyde interactions. In contrast to the first, the second study used an inorganic oxidant (H_5IO_6) [138]. As a final, chitosan has been used in a proof-of-principle study for a mussel-inspired wood adhesive using a different enzyme (laccase) and various phenolic compounds [186].

4. *Polyacrylamide*

Polyacrylamide has been used as the 'backbone' material in a two component systems with polyethyleneimine (PEI) for a wood adhesive[iv] [188]. Analogously, it has recently been used together with an amine-modified acrylamide [154] or an amine modified gelatin [195,196] for a two component bioadhesive (type IV) inspired by tubeworm coacervates (see Figure 3.2). In these studies dopamine-HCl was reacted with an acroyl chloride to develop polymerizable monomers containing the desired catechol groups, requiring either diphenyl [188] or borate-complex [154,195,196] protection of the alcohol groups. Similarly, monoacryloxyethyl phosphate and *N*-(3-aminopropyl)methacrylamide-HCl could be used to mimic the pSer and Lys groups of the tubeworm coacervate adhesive [154,195,196]. The choice of polymerizable acrylate monomers was further explained by stating that water-soluble methacrylates are not expected to elicit immune responses [154]. A general advantage of using acrylamide is known to include its favourable reactivity ratios with many co-monomers, allowing a substantial variety of polymers to be tailor-made [198][198].

5. *Other*

The remainder of aquatic-inspired adhesive systems utilized a variety of polymers. Hyaluronic acid and Pluronic, two biocompatible copolymers, have recently been used to create injectable and robust thiol-catechol reacting hydrogels for biomedical applications [181]. Formaldehyde-free wood adhesives have been by mussel-inspired chemistry using poly(4-vinylphenol) [187], tannin [189] and soluble decayed wood [190-192] as (bio-based) polymeric sources of phenolic or catechol groups. Polystyrene [150] and polyurethane [193] were recently modified to contain DOPA mimicking catechol groups and assessed on their adhesive capabilities in proof-of-principle studies. These studies were driven to combine the unique chemistry of marine adhesive proteins with the flexibility/designability, easy synthesis, and low cost of simple bulk polymers [150,193]. As a final, an advanced low-viscosity aqueous solution containing UV-induced polymerizable vesicles was recently developed [194]. Linear peptide amphiphiles based on photopolymerizable diacetylenic fatty acids, ethylene oxide spacers and DOPA functional groups constituted the main building blocks. It is beyond the scope of this study to discuss the detailed chemical aspects of all these systems beyond their main advantages summarized above.

[iv] Strictly speaking, the (long-term) goal of this research was to develop a more effective wood-plastic coupling agent through use of Poly(*N*-acryloyl dopamine) (PAD). "PAD should be able to serve as a wood-binding domain for a wood-plastic compatibilizer because N-acryloyl-O,O- diphenyldopamine can be used to prepare a PP–PAD diblock copolymer" [188].

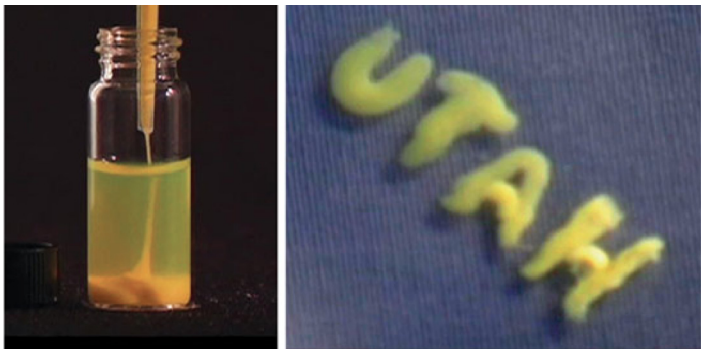

Figure 3.2: Pipettable synthetic complex coacervate (l) and fully submerged application thereof (r) [58]

To facilitate the interpretation of the chemistry of the different groups identified, the chemical structures of representative examples of each group are presented in Figure 3.3.

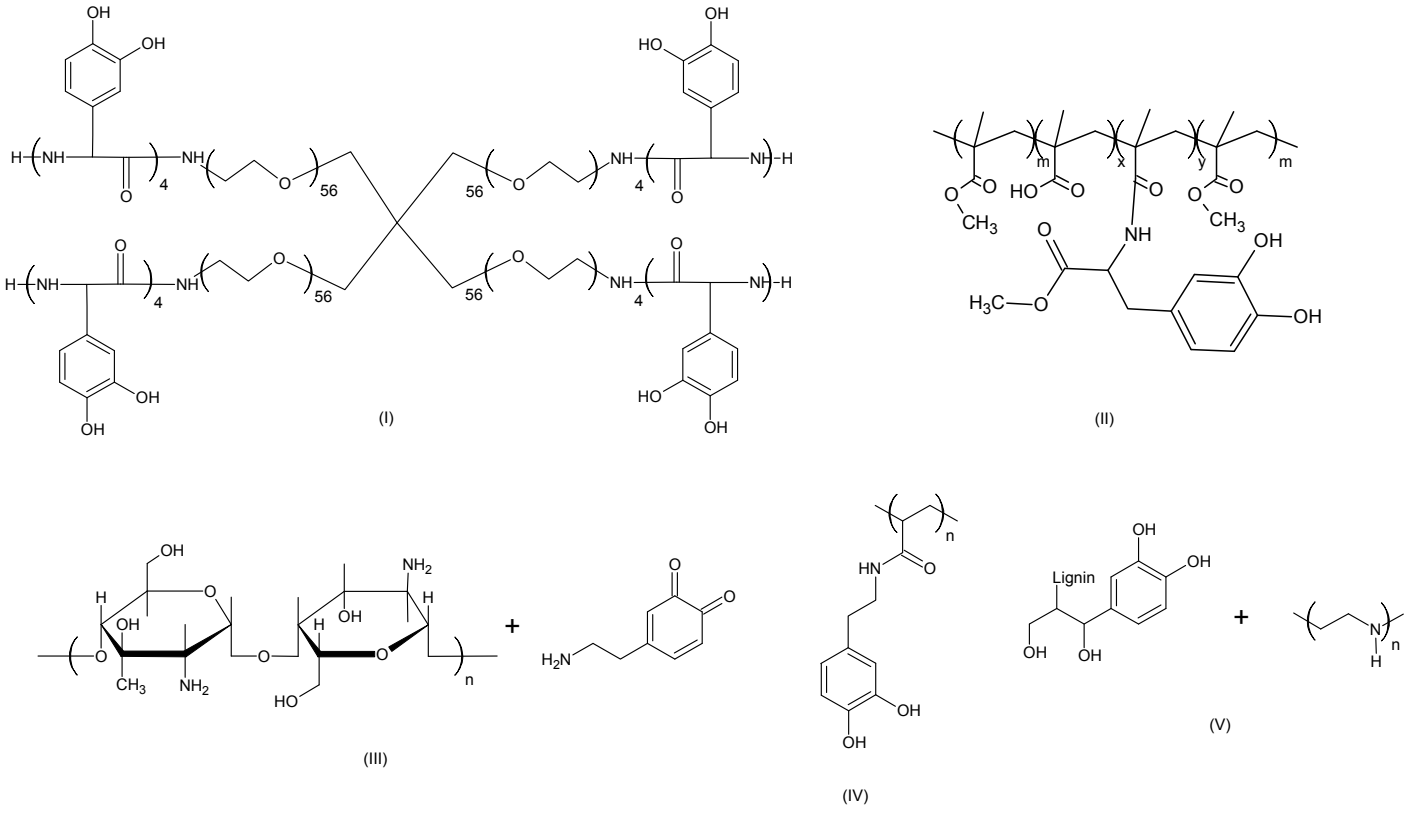

Figure 3.3: Chemical structures of several developed aquatic-inspired adhesive systems with non-protein and non-polypeptide polymers. (i) DOPA-PEG [179],(ii) DOPA modified PMMA-PMAA-PMMA [182], (iii) quinone tanned chitosan [146], (iv) poly(*N*-acryloyl dopamine) [188], (v) soluble decayed wood with PEI [190]

3.2.4 Extent of mimicking functional groups

An intriguing question confronting the adhesive researcher is to what extent the aquatic-inspired polymer has to contain the mimicking adhesive groups, particularly DOPA, for optimal adhesive strength performance. Some factors that are relevant to consider when addressing this question are listed below:

1. Single-molecule experiments with DOPA-modified AFM tips have demonstrated that the catechol group forms bonds to wet titanium oxide surfaces with the strongest non-covalent reversible binding interaction ever reported involving a small biological molecule (dissociation energies of 22 kcal mol^{-1}) [126]. The catechol bound approximately four times stronger than the quinone and approximately eight times stronger than tyrosine [58].
2. Native primer proteins of the *Mytilus edulis* (mefp-3 and mefp-5) contain 20-30% DOPA [161].
3. The fact that not higher levels of DOPA are utilized by the organism has only recently been explained with increased theoretical detail [199][199]. The authors of this study used the freely-jointed chain model in combination with AFM experiments and concluded that mussel can have one group that is highly adherent to a particular surface spaced by several monomers with other functionalities without losing its adhesive power. The conditions for attaining this effect include solubility of polymer and the distance between functional groups being smaller than a factor including the Kuhn length and contour length of the polymer chains [199].
4. Functional groups other than DOPA are required to make a polypeptide physically water-soluble [144].

Given the complex challenge of attaining aquatic adhesion (see chapter 2) and taking into account general considerations on biomimetics with respect to the limits of the natural aquatic adhesives (see section 3.1.2), one can expect that the optimal modification degree is highly system-dependant. To briefly test this hypothesis, the optimal adhesive performance of ten different systems was compared with the amount of DOPA or DOPA-mimicking groups present in the polymeric materials used (see Figure 3.4). Although one must be aware of the difficulty surrounding comparison of adhesive performances determined through different methodologies (see section 2.3.2), this overview is only for general illustrative purposes. Indeed, it can be observed that DOPA or DOPA-mimicking content varies widely between 2 mol% (for a specific hydrogel [179]) and 25 mol% (for a 1:3 quinone:chitosan adhesive mixture [147]) for optimum adhesive performance. Somewhat surprisingly, the synthetic systems contain mostly lower molar amounts of the key DOPA (mimicking) component than the mussel itself appears to use in its primer proteins (see section 2.2.2). It must be noted though that some data points were estimated based on weight percentages (e.g. [151, 188]) or other data provided such as number of residues per protein [140].

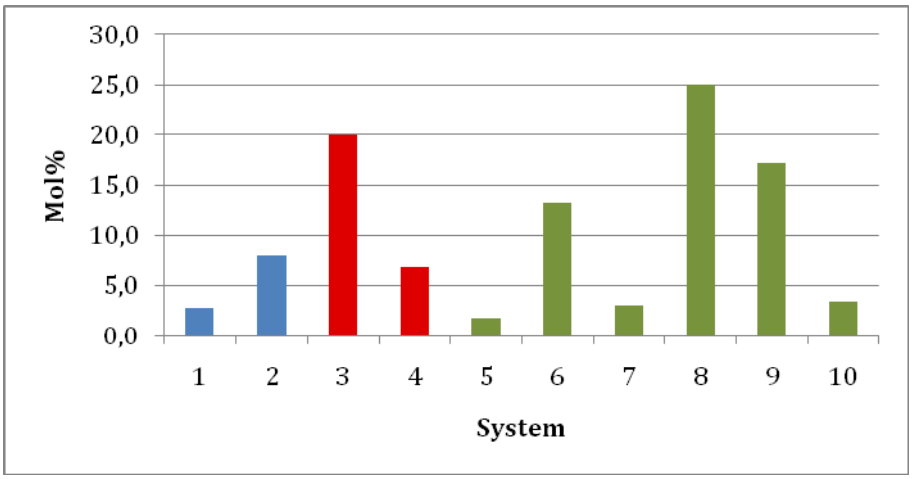

Figure 3.4: Comparison of (optimal) DOPA or DOPA-mimicking content in aquatic-inspired adhesives with respect to maximal adhesive strength under wet conditions (if applicable). Blue pillars signify protein based systems, red pillars polypeptide based and green pillars other polymer based. References of systems: 1=[140], 2=[168], 3=[144], 4=[174], 5=[179], 6=[183], 7=[151], 8=[147], 9=[188], 10=[150]

3.2.5 Oxidants

From the overviews presented in the previous sections it is clear that a variety of different chemical oxidants have been tested in aquatic-inspired adhesive research. Three aspects are relevant to address:

1. *No chemical oxidation*

   Oxidation chemistry has not been applied in wood adhesive research, where amine-catechol reactivity at increased temperatures (hot-pressing) is key and adding a particular oxidant is not (e.g. [141,142,143,143,187-192]). Recent studies on developing bioadhesives (type IV) also focused on synthetic systems that do not require chemical oxidants (e.g. [88,149,182,194]). These have mentioned drivers originating from (i) the stronger adhesive properties of unoxidized DOPA and (ii) the expectation that oxidizing reagents may complicate the future *in vivo* applications of these materials [182]. It cannot be said however that these sophisticated systems signify a general trend. The opposite of the first statement is testified by evidence that the oxidized DOPA/catechol groups may have functional [126] or even superior [146] adhesive capabilities in aquatic(-inspired) adhesives. The second statement is rejected by the appearance of more recent studies that do make use of oxidants and moreover do so successfully for *in vivo* application (see point 3).

2. *Enzymatic oxidation*

   As the natural adhesive system in mussel byssi make use of an oxidative enzyme in their hardening mechanisms [174,184], a commercially available mushroom tyrosinase analogue has been used in many studies (e.g. [87,145-147,174,184]) to either selectively oxidize tyrosine residues to DOPA and/or to oxidize the DOPA-residues into o-quinones [174]. One might

expect biocompatibility driven motivations for using enzymes, but these are not mentioned in the published articles. In contrast, Yu et al. recalled that older work on extracted mussel adhesive proteins in bioadhesion showed that the proteins were nontoxic, but that the toxicity of the enzymatic oxidizing agent was problematic [91]. As a final, the only exception for the statement that wood adhesive researchers have not used oxidants in developing aquatic-inspired systems is from Peshkova and Li (2003) [186]. In this study laccase was used as an enzymatic oxidant for various phenolic compounds, but the system appears to have had little to no follow-up.

3. *Chemical oxidation*

Yu and Deming (1998) started the investigation into inexpensive oxidizing agents for their synthetic polypeptides as an alternative to the existing systems with oxidizing enzymes and marine adhesive proteins [91]. Air (O_2), hydrogen peroxide (H_2O_2), pH = 12 and sodium periodate ($NaIO_4$) were studied in their published work [91], whilst ferric ion in the form of $Fe(H_2O)_6^{3+}$ was patented in addition [173]. The choice of oxidant was found to be relevant in curing times below 1 day, H_2O_2 being the most versatile [91]. However, a follow-up study with the same system conducted more recently attained better results with other oxidants [144]. Moreover, H_2O_2 has been applied since then only once [167]. Inspired by the published finding by Monahan and Wilker (in 2004) that oxidizing metal ions, particularly Fe^{3+} and Mn^{3+}, were most effective in curing mussel adhesive precursors [200][200], protein based adhesives have recently been cured with $KMnO_4$ [140] and $Mn(OAc)_3$ [168], $Fe(NO_3)_3$,[140, 168] and $K_2Cr_2O_7$ [140]. Analogously, $[(C_4H_9)_4N]MnO_4$, $Fe(C_5H_7O_2)_3$ and $[(C_4H_9)_4N]_2Cr_2O_7$ have been used to cure hydrophobic styrene mimics [150].

As it appears, no oxidant has been identified to perform best in general terms. However, the periodate ion (IO4-) has been used most extensively overall: as $NaIO_4$ in protein based system [166,168], polypeptide based systems [91,173,144] and in other polymer based systems [151,154,183,195,196]. Periodate has also been used in the last category as an intermediate oxidation reactant for DOPA, starting from periodic acid (H_5IO_6) in a first step (to oxidize dextran) [138]. A particular invention has been patented in the form of thermally triggered liposome encapsulated $NaIO_4$, created to be able to store an adhesive formulation at room temperature and later polymerize it at a wound site by the increase of temperature from body heat [179]. Indeed, $NaIO_4$ has recently been shown to be biocompatible [201][201] in curing a synthetic tubeworm complex coacervate [195] mimic at a 1:2 ratio to DOPA side chains.

3.3 Performance characteristics

3.3.1 Adhesive bond strength

It was mentioned in section 2.3 that the primary performance of an adhesive is its bond strength. No consensus has however (yet) been established on a universal methodology for assessing this important characteristic, which was also found to the case in the field of aquatic-inspired adhesives (see Table 2.6). Although the consequence is that reported values of different systems are often very difficult to compare directly, an attempt is made in this section to provide an overview of reported bond strength ranges in order to discover generic trends. Regarding the devised summaries (Table 3.7 and Table 3.8), three topics are discussed below:

1. *Substrate and application*
   The reported values seem to correspond in general to the application envisioned and thus also with the substrate(s) tested. For wood adhesives, reported adhesive bond strength values are typically several MPa for both dry and wet curing circumstances (e.g. [143,188]). Similar values are sometimes reported on inorganic substrates such as aluminium (e.g. [92,169]), but systems developed for biomedical applications generally tend to show adhesive bond strengths in the kPa range when tested under humid, wet or physiological conditions. This is particularly the case when biological substrates are used (e.g. [139,179,180]).

2. *Testing methods*
   Testing methodologies can by themselves be expected to significantly influence the adhesive bond strength results reported (see section 2.3). It has been discussed recently in the context of surgical adhesives that shear strength test results are also strongly dependent on the size and quality of the specimens, rather than on the intrinsic adhesion strength of the glue itself [156]. Measurements thus have to be performed at least four or five times to obtain a reliable average and this amount increases for inhomogeneous interfaces such as biological skin [156]. In addition, shear tests have been criticized for the lack of their ability unambiguously differentiate between cohesive and adhesive contributions to the measured shear strength values [149,156]. Crack-initiation (at the maximum strength) governs the overall (sudden) failure of the bond, which corresponds with a higher adhesive bond strength than for crack propagation, but shear tests are unable to distinguish between both phenomena [156]. As discussed in section 2.3.1, contact mechanics has been devised as an advanced method to address this inability. Although the group of Messersmith has used this method (e.g. [88,149,182]) and a resembling membrane inflation method [183], the vast majority still uses shear tests (e.g. [144,150,159,168,169,179,194]).

3. *Contact area and surface morphology*

Adhesive bond strength is typically reported as the force required to separate divided by the contact area (MPa = N mm^{-2}) [105,194]. In section 2.2.3 it was remarked that surface properties and external morphology of adhesives released by aquatic organisms have received little attention. The same can be said for (macro-scale) aquatic-inspired adhesives, when disregarding micro-scale systems such as the previously mentioned gecko-mussel structured adhesive [178] and a gecko-inspired bioadhesive (type IV) [202][202].

To the knowledge of the author, there are only two recent exceptions. The first is a study that utilized two different polymeric materials and surface morphologies (see Figure 3.5), but unfortunately only discussed in the detail the membrane inflation method devised ([183], see also section 3.2.3, point 2). The second recent exception is a study in which polymerizable biomimetic vesicles with controlled local presentation of adhesive functional DOPA groups were applied [194]. The latter reported higher adhesive strength at bond rupture for assembled and polymerized vesicles compared to that for disordered and nonpolymerized assemblies (e.g. 3.7 N versus 2 N) [194]. Adhesive performance was reported unconventionally in Newtons, because "the adhesive contacts in this system are established only in a discrete number of nanoscopic points and hence the real contact area is smaller than the apparent macroscopic contact area" [194]. This consideration is also important when reviewing systems for which contact areas are not reported well defined (e.g. [164-166]), as this parameter greatly influences outcomes calculated in MPa.

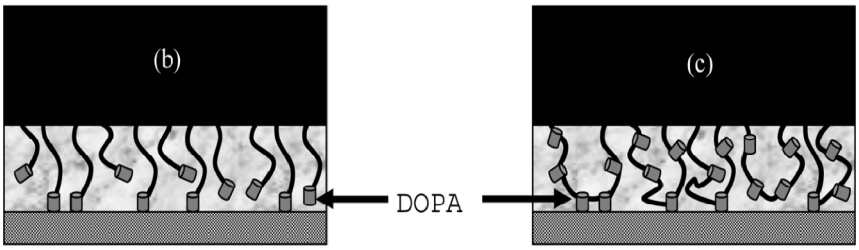

Figure 3.5: Schematic illustrations of the interfacial structure for membranes modified with a PS-PEO-DOPA copolymer (l) and a DOPA20 acrylic triblock copolymer (r) [183]

Table 3.7: Macro-scale adhesive bond strength data reported on protein and polypeptide based aquatic-inspired adhesive systems developed over the past decade. Numbers are only indicative, as different methodologies have been utilized for strength determination.

Platform	*System*	*Substrate(s)*	*Dry adhesive strength (MPa)*	*Humid/Wet adhesive strength (MPa)*	*Ref.*
Protein	Dopamine and cysteine modified soy protein	Maple veneer (wood)	2.5 – 4.5	2.5 – 4.5	[141,142, 143]
	MAP (acidic solution)	Glass, pig and cattle muscle	0.0087 – 6.8 (*)	0.0087 – 0.026 (*)	[164]
			0.01 – 9.8 (*)	0.016 – 0.041 (*)	[165]
			0.0038 – 2.2 (*)	0.020 – 0.040 (*)	[166]
	MAPs (paste)	Porcine skin	0.04 – 0.60	0.0 – 1.4	[139]
		Small intestinal submucosa		-	[140]
	Recombinant hybrid MAP	PMMA	1.7 – 2.0	-	[159]
		Aluminium	0.42 – 1.13		[168]
	Recombinant hybrid MAP coacervate		3.0 – 4.5		[169]
Polypeptide	Poly(Lys-DOPA)	Aluminium, steel, PMMA, PS, PE, glass	0.1 – 4.7	-	[91,173]
		Aluminium, steel, PS, glass, porcine skin	0.2 – 5.7	-	[144]
		Porcine bone	0.3	0.15	
	Poly(Lys-DOPA), poly(Glu-DOPA)	Aluminium	1.8 – 5.7	-	[92]
	Polyoctapeptides $(X/Y\text{-Gly-Tyr-Ser-Ala-Gly-Tyr-Lys})_n$ (X = Thr, Ala; Y = Thr:Ala = 3:2)	Aluminium, iron, HDPE, glass	0.098 – 0.74	-	[145]

*: an estimated number on the basis of peak force (g or N) and overlap area (cm^2)

Table 3.8: Macro-scale adhesive bond strength data reported on other polymer based aquatic-inspired adhesive systems developed over the past decade. Numbers are only indicative, as different methodologies have been utilized for strength determination. Values have been converted to MPa where possible. Units are displayed in parentheses if this conversion was not possible or straightforward.

Polymer system(s)	*Substrate(s)*	*Dry adhesive strength (MPa)*	*Humid/Wet adhesive strength (MPa)*	*Ref.*
DOPA-PEG, Oligo-DOPA-PEG, Oligo-(DOPA-Lys)-PEG, DOHA-PEG, DMe-PEG (ester-linked dopamine-PEG)	Ti-coated glass, porcine skin	-	0 – 0.070	[179]
DOPA-$(PEG\text{-}PLA\text{-}MA)_2$, Oligo-(DOPA)-$(PEG\text{-}PLA\text{-}MA)_2$, Oligo-(DOPA-Lys)-$(PEG\text{-}PLA\text{-}MA)_2$	Ti-coated silicon		25 – 550 (mJ m^{-2})	[149]
DOHA-PEG-PCL, Dopamine-PEG-PCL	Bovine pericardium		0.007 – 0.110	[151]
DOPA-PEG-dextran	Mice duodenum		0.0053 – 0.011	[180]
Poly(hyaluronic acid-dopamine-co-thiol-terminated Pluronic)	Mice skin		0.0012 – 0.008	[181]
DOPA modified PMMA-PMAA-PMMA	TiO_2		0 – 135 (mJ m^{-2})	[88]
			5 – 2200 (mJ m^{-2})	[182]
DOPA modified PMMA-PMAA-PMMA, Boc-DOPA-PS-PEO	TiO_2-coated quartz, porcine skin		0 – $4.0 \cdot 10^{-4}$	[183]
Quinone modified chitosan	Glass		0 – 0.5	[146]
Quinone modified chitosan with PEG				[184]
Quinone modified chitosan				[185]
	MAA, AA, and MAAm grafted LDPE	0.1 – 0.95	-	[147]
Quinone modified chitosan-dextran	Bovine cortical bone	-	0.01 – 1.22	[138]
Phenolics-laccase modified chitosan	Maple veneer (wood)	0.5 – 2.1	0 – 1.7	[186]
Poly(*N*-acryloyl dopamine), polyethyleninime (PEI)		2.8 – 6.4	1.7 – 5.2	[188]
Tannin, PEI		4.7 – 6.2	0.86 – 6.9	[189]
Soluble decayed wood, kraft lignin, PEI		1.4 – 5.5	0 – 4.0	[190]
		2.0 – 6.5	0 – 6.7	[191]
		0.7 – 7.2	0 – 4.1	[192]

(Continued on next page)

(Continued from previous page)

Poly((3,4-dimethoxystyrene)-co-styrene)	Aluminium	0.4 – 1.7	-	[150]
Polymerized TDA-$(EO)_2$-DOPA-C_2-OH, TDA-Gly-OMe	PMMA, glass, SiO_2	-	0 – 45 (N)	[194]
Poly(acrylamide) coacervate with (i) phosphate and dopamide sidechains, (ii) lysine sidechains	Bovine cortical bone	-	0.05 – 0.11	[154]
Coacervate with (i) poly(acrylamide) with phosphate and dopamide sidechains, (ii) amine modified gelatin	Aluminium		0.075 – 0.875	[204]
			0.34 – 0.68	[205]

3.3.2 Biocompatibility

In contrast to the lack of a standard methodology for measuring (bio)adhesive strength, assessing biocompatibility is strictly regulated and well established through the ISO 10993 protocol [156] (see Figure 3.6). Two parts of this protocol are particularly important. Part 4 governs tests examining the interactions with blood, e.g. through thrombogenicity and haemolysis (together with the ASTM F 756-00 norm) for a bioadhesive [203][203]. Part 5 governs tests for cytotoxicity (cell toxicity), e.g. used recently to examine bone glue effects on MC3T3 cells [138] and tissue sealant effects on fetal membrane cells [204][204]. Analogous to the latter part, endothelial cells and MC3T3-E1 osteoblast cells have been used to assess the *in vitro* biocompatibility of a mussel-inspired (polypeptide based) tissue sealant [144] and a tubeworm-inspired coacervate for gluing craniofacial bone [205][205], respectively.

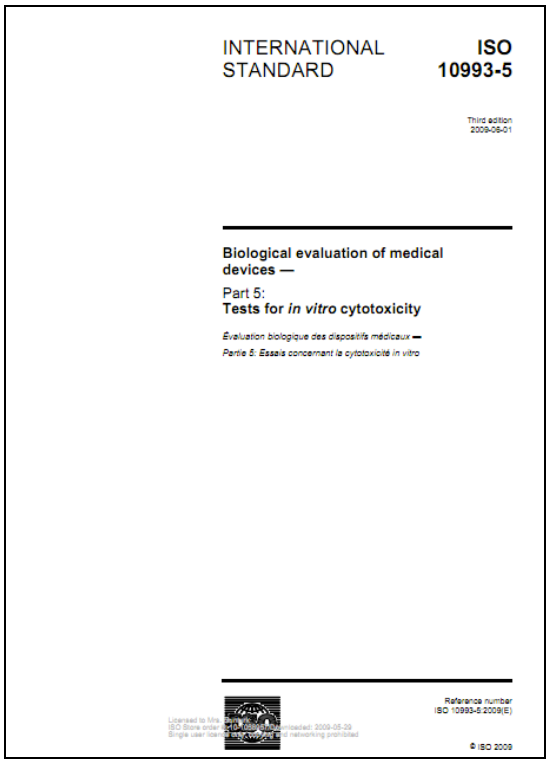
INTERNATIONAL STANDARD

ISO 10993-5

Third edition
2009-06-01

Biological evaluation of medical devices —

Part 5:
Tests for *in vitro* cytotoxicity

Évaluation biologique des dispositifs médicaux —
Partie 5: Essais concernant la cytotoxicité in vitro

Reference number
ISO 10993-5:2009(E)

© ISO 2009

Figure 3.6: Front page of the most recent ISO 10993-5 standard (2009)

In vitro tests are a relatively facile method for assessing biocompatibility. However, *in vivo* studies using animal models are required as a more accurate predictor of clinical performance when promising results are attained in first screenings. *In vivo* biocompatibility has in fact recently been determined successfully in the field of aquatic-inspired. Examples of the animal models utilized include: (i) a living pig for closing an incision in the skin [206][206], (ii) mice for general biocompatibility [180] as well as hydrogel stability [181] and for specific extrahepatic syngeneic islet transplantation adhesive performance [89] and (iii) rats for craniofacial bone reconstruction [205].

It is relevant to point out that the absence of an (direct) immune response is only one factor of biocompatibility, as mentioned in section 3.1.1. Biocompatibility is accomplished as a whole through the material being absorbable (and removable) by the body and its degradation products being non-toxic as well [138,139,158]. Generally referred to here as biodegradability, proteins and polypeptide materials (natural or synthetic) logically seem to have the advantage on this point. Indeed, (weakly) adhering fibrin sealants are clinically favoured on this criterion [138]. Chemical strategies to achieve this characteristic in other polymer based materials have been outlined to include poly(lactid acid) segments [149] and ester-linked poly(caprolactone) segments [151] in PEG (see section 3.2.3). A slight variation of this theme has been to use hydrolysable phosphoester groups in a poly(acrylamide) [154], although this can be seen more as a synergistic effect with its specific surface adhesion capability. Another clear strategy is to use bio-based polymers (that degrade well) as backbone materials, such as hyaluronic acid [181], gelatin [195,196] and chitosan [138].

Unfortunately, experimental methods and results to determine the rate of biodegradation and the biocompatibility of the degradation products are scarce to come by for aquatic-inspired adhesives. Those of a gelatin-based adhesive complex coacervate have been reported to be currently in progress [195]. Degradation of adhesive polymers has been characterized only physically by thermal analysis [138] or by assessing weight loss *in vitro* when incubated in phosphate buffered saline (PBS) at pH = 7.4 and 37 °C over an extended period of time [151,181]. The only study that truly assessed the effect of degradation on both mass loss and immune response used an *in vivo* procedure over a period of 21 days [151].

It is clear that biocompatibility is a prime requirement for developing a novel high-potential water-resistant (aquatic-inspired) adhesive. However, a further in-depth review of the assessment methodologies and outcomes thus far reported is outside the scope of this study given the general consensus on the ISO 10993 protocol in recent years and the specific expertise required in this field.

3.3.3 Durability

It goes without saying that the adhesive performance should be sufficient over a required period of time. Functionally, this durability aspect could be assessed by (i) repeated cyclic loading below the critical bond strength (see section 2.3.1), (ii) determining the thermal stability of the adhesive (e.g. by Thermal Gravimetric Analysis, [138]) and/or (iii) the physical stability when exposed to a mimicking

environment (e.g. assessing weight loss *in vitro* when incubated in phosphate buffered saline (PBS) at pH = 7.4 and 37 °C [151,181]). The third method shows the intricate balance that is required between both degradability and durability when using bioadhesives (type IV). As a final, the ultimate proof of durability is to expose adhesive bonds to either the natural application environment or to an extreme exponent of it. An example of the former is to assess the adhesive performance at the application site at various points in time *in vivo* [89], examples of the latter include exposing wood adhesives to boiling water [142,143,189,190,191].

3.3.4 Ease of application

As identified in section 3.1.1, adhesives should be easy to apply and, together with the wettability prerequisite (see section 2.1.3) this requires them to be liquid before setting. Indeed, recent articles characterize their adhesives as injectable to stress this property [181,204]. The physical property governing this flowability behaviour is viscosity, which makes quantitative calculations and characterization possible. Increasing this measurable property by adding an oxidant (or other cross-linker) has been used as a predicative phenomenon to determine desired curing/gelation behaviour [91,147] and even adhesive strength performance [146,184-186] (see e.g. Figure 3.7). A specific example of this technique is by use of the Hassan method, which estimates mucoadhesion (adhesion to mucin) through straightforward viscosity measurements [207][207]. Other methods include simply measuring the time required to attain a sol-gel transition through use of a spinning stir-bar [179], vial-tilting [179,181] or vial-inversion [89]. Alternatively, penetration experiments can provide similar insights. These are carried out on hardening or hardened material by driving a steel rod into the gelatinous sample at a constant velocity and measuring the force required to do so [150,200].

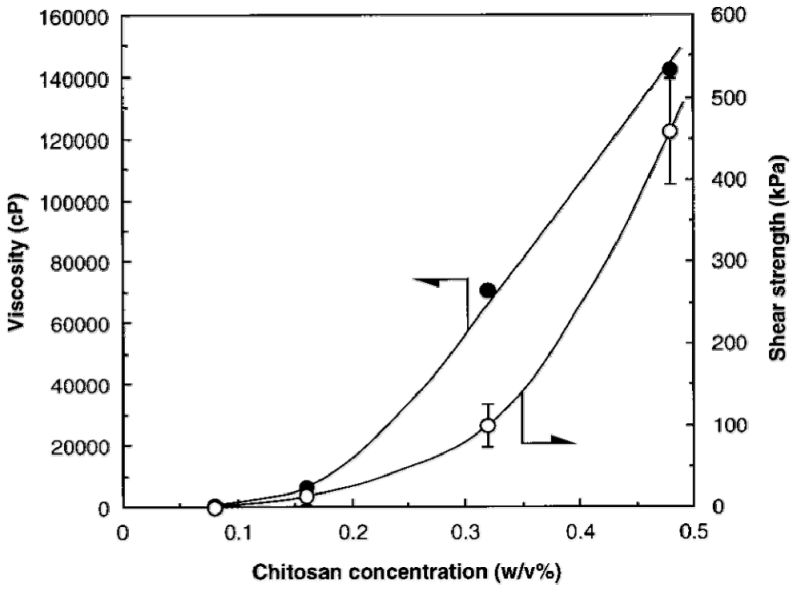

Figure 3.7: Relationship between viscosity and water-resistant adhesive strength [146]

Determining what the initial viscosity should be for applying the adhesive appropriately is not trivial. Low-viscosity solutions have for instance been appraised for being injectable in a clinical environment

[181,204], making nanopad glues available [194] and improving interfacial contact on rough surfaces [97]. The latter has also lead to a common strategy of depositing a primer (see section 2.1.4) from a low-viscosity carrier before applying a high viscosity adhesive on a microscopically surface rough adherend [97]. On the other hand, many studies recall qualitatively that adhesive have to be sufficiently viscous to allow practical adhesion applications [144,159], e.g. to prevent flowing out of a bonded assembly [139]. A recent comparative review concluded that in the clinical performance of various surgical adhesives high viscosity adhesives were less time consuming to use than low viscosity tissue adhesives (and all other outcomes were not statistically effected) [155]. Moreover, increases in concentrations have been correlated in other studies to higher viscosities and higher adhesive performances [91,146,208][208]. There is a limit to this trend though. One possible cause for this is the limited solubility of the active ingredient [208]; another is the occurrence of heterogeneous cross-linking at high viscosities [184,185].

From the discussion above it can be stated that the optimal initial viscosity is a multivariate optimization problem depending on the substrate chosen, the ease of use for a particular application and the concentration required to attain sufficient bonding strength for a specific component (mixture). Examples of initial viscosities for various adhesives vary significantly and this finding is thus non-surprisingly: 28 cP and 292 cP for commercial cyanoacrylate tissue adhesives [209][209], 755 cP for a novel siloxane adhesive [209], and 50 cP for a bovine serum albumin adhesive [208]. For polyketone-based wood adhesives, viscosities of emulsions have been reported to be anywhere between 1 and 175 Pa·s, corresponding to 1000 – 175000 cP (1 Pa·s = 10 P = 1000 cP) [61,62]. Figure 3.7 shows comparable viscosities.

3.3.5 Other characteristics

The remaining performance characteristics required identified in Table 3.1 mainly include environmentally friendly / renewable production and being affordable. Both are discussed briefly:

1. *Environmentally friendly / renewable*
   Creating adhesives in an environmentally friendly or renewable fashion has been stressed (i) by some researchers in aquatic-inspired adhesive research using bio-based polymers (chitosan) [146,184] and no organic solvents [185], and (ii) in general considerations on adhesive production prospects [41,42,47]. These considerations also apply for more low-tech wood adhesives, which do not have to meet the challenging biocompatibility requirement. Accordingly, research in this field can focus more on using low-cost and bio-based materials [143,189-192]. On the other hand, the fact that researcher in the field of biomedical/surgical applications rarely discuss this factor suggests that meeting the other challenging performance requirements seems to be much more important, at least in the short term.

2. *Affordable*

   A similar reasoning as the one above can be applied to the factor of costs. Although physicians are the first to take affordability specifically into account [152,153,155] and emphasize that surgical adhesives should become much less expensive [157], it does not seem to be a research priority in this area. The opposite is true for general low-grade water-resistant [146,184,185] or wood-adhesive [189-192] applications.

3.4 Commercial and manufacturing aspects

Chemical engineering has traditionally focused on the scale-up and efficient production of functional chemicals (or chemical products). To investigate which aquatic-inspired adhesive systems identified in this chapter have shown such promise to enter this stage of product development, the patent literature has been examined in more detail. The findings are discussed shortly in this section.

3.4.1 Protein based products

It has been stated recently that neither native mussel foot proteins nor barnacle cement mimics are used in eye surgery or any other medical procedure [58]. The mussel foot proteins are commercially available in milligram quantities (Cell-Tak, BD Biosciences), but "are priced like lifesaving medicine" [58]. This is not surprising considering the inefficient extraction process (see section 3.1.2). Patents have been filed through use of these extracted proteins [164-167] and the company Stryker has acquired the system using $NaIO_4$, but no more information than that could be found. Recombinant fusion proteins are also patented [210][210], commercially available in milligram quantities (Kollodis, Inc) and less expensive than the native proteins [58]. Figure 3.8 shows images of both commercial products. Silverman and Roberto expected a few years ago that "the production-scale availability of recombinant mussel adhesive proteins will enable researchers to develop formulations for adhesives in which there exist endless applications for the commercialization of water-impervious, ecologically safe adhesives derived from mussels" [50]. Indeed, it has been reported more recently that Fraunhofer IFAM is currently developing an innovative Mefp-based adhesive for dental implants using this approach [102].

Figure 3.8: Commercially available native mussel proteins (l) [211][211] and recombinant fusion proteins (r) [212][212]

As a final, the dopamine-modified soy protein system developed for attaining a formaldehyde-free wood adhesive has been patented [143]. The idea is commercially applied in plywood manufacturing through Columbia Forest Products and Hercules Inc, albeit through a different 'curing' process because this alternative route is cheaper than the chemical modification route patented [213][213].

3.4.2 Polypeptide based products

Polypeptides have been deemed to be not very suitable as aquatic-inspired adhesive products due to their swelling behaviour (see section 3.2.2). The only patent identified [173] appears to have had little follow-up indeed. However, a final screening of the patent literature did reveal a recent patent on a mussel-inspired formulated medical (haemostat) adhesive utilizing a Lys-Tyr oligopeptide (n=5 or n=10), 2,5-dihydroxy-N-(2-hydroxyethyl)-benzamide as a bridging molecule, laccase as enzymatic oxidant and (optionally) natural zeolites [214][214]. This system [170] appears to resemble the polyphenolics-laccase-wood adhesive system developed several years ago [186] together with the earlier (X-)Lys-Tyr system [87] and is property of Stryker Trauma GmbH. No macro-scale bond strength data was reported (only qualitative observations for bonding on collagen and polystyrene), but more information can be expected to appear in the near future.

3.4.3 Other polymer based products

The most studied aquatic-inspired adhesive system over the past decade in this category seems to be PEG-based systems (see sections 3.2 and 3.3). Several patents have been granted which are targeted at various medical applications [88,179]) and some are still in the application process (e.g. specifically for fetal membrane repair [215][215]). Kensey Nash has been traced to be the current commercial developer of both adhesive and coating technologies based on catechol-PEG systems [216][216], following Nerites Corporation [179] as an earlier host. Other systems targeted at biomedical applications described in this chapter could not be traced to specific patents or companies. Correspondingly, it has been stated in 2008 that no mussel-based system has been approved for use in surgical procedures [49]. In 2010, a mussel-catechol (PEG) system was described as still being experimental [204].

For the wood adhesives developed, the patented system of Li and Geng [192] does not seem to have attained the same matter of success as the soy-protein system (from the same inventor) discussed in section 3.4.1.

3.4.4 Considerations on manufacturing

Due to time constraints, the technology governing (theoretical) larger-scale manufacturing of aquatic-inspired adhesive products has not been examined in detail yet. More will follow in a later stage, when integrated product and process design have become relevant to address.

3.5 Conclusions

Which strategies exist in the development and manufacture of synthetic adhesives inspired by aquatic organisms?

The development of synthetic mimics of natural aquatic adhesives has been motivated mainly by the search for biocompatible, strong adhesives that can operate in wet environments. No currently approved medical adhesive satisfies all these requirements. The natural adhesives by themselves suffer from limited bond strengths, but even more so from their limited availability. Creating easily bulk producible and cheaper analogues has thus been the target of various research groups around the globe. Based on a detailed literature review, three categories of approaches on developing man-made mimics have been identified: (i) protein based, (ii) polypeptide based and (iii) other polymer based. It is important to mention that these systems have not solely been aimed at creating biocompatible medical adhesives, but some have also targeted creating water-resistant (formaldehyde-free) wood adhesives. For such an application, cost factors and using bio-based products are key drivers instead of achieving biocompatibility.

The catechol functionality of DOPA found abundantly in mussel foot primer proteins has been mimicked most commonly, although recently synthetic coacervates utilizing the tubeworm cement system have also been developed. The mimicked catechol group levels employed to attain highest bond strengths have been found to be in the range of 2-25 mol%, which is lower than for the natural adhesive primer proteins (20-30 mol%). From a chemical perspective, many polymer backbone materials and protecting chemistries have been applied to fine-tune additional properties as solubility and biodegradability whilst preserving the reactive catechol groups during chemical modifications and polymerization reactions. In addition, different oxidizing agents and cross-linking methods have been employed to attain hardening (curing) of the adhesive. Sodium periodate seems to be applied mostly, but alternatives include enzymes, hydrogen peroxide, Fe^{3+}, Mn^{3+} and avoiding the use of an oxidant altogether. The latter is applied in sophisticated UV-triggered, heat-triggered and/or vapour exchange self-assembly systems. However, it is also common for wood adhesives, as these are commonly cured at elevated temperatures (hot-pressed) and/or use a separate polyamine ingredient.

The results attained through these systems vary between a few kPa and multiple MPa. It must be said though that the lack of a universally applied bond assembly, curing and testing method frustrates direct comparison. Nevertheless, the higher bonding strengths are generally only attained for wood adhesives and through use of (rigorously cleaned) inorganic adherends. When wet or physiological conditions are applied and biological tissues are used, several hundred kPa seems to be the common limit thus far. As a final, some details of promising or already commercially successful systems are summarized in Table 3.9.

Table 3.9: Summary of promising or commercially successful aquatic-inspired systems

Platform	*System*	*Application*	*Curing*	*Commercial participator(s)*
Protein	Extracted mussel protein	General medical	$NaIO_4$	Stryker, BD Biosciences
	Recombinant fusion protein	Dental adhesive	Unknown	Fraunhofer IFAM, Kollodis Inc.
	Modified soy protein	Wood adhesive	Unknown	Columbia Forest Products, Hercules Inc.
Polypeptide	Tyr-Lys oligopeptide, briding agent, natural zeolites	Haemostat	Laccase	Stryker Trauma GmbH
Other polymer	Catechol-PEG hydrogel and coating	General medical	Unknown	Kensey Nash

4 Novel polyketone based adhesives

This chapter details the experimental work and results obtained on the attempts to obtain polyketone based adhesives through chemical modifications with a DOPA-mimicking molecule: dopamine. The results of further research into the properties and usability of the synthesized components as an aquatic-inspired adhesive are also treated.

4.1 Introduction: considerations on synthesis

This section summarizes several important considerations on the chemical synthesis of the envisioned novel polymers, based on available information from the academic literature.

4.1.1 General synthetic goal

The following Paal-Korr pyrrole synthesis is attempted first in order to obtain a low molecular weight product of the reaction between dopamine and a model compound of polyketone, namely 2,5-hexanedione (see Figure 4.1). Similar experiments have been done previously to aid in the identification of product structure and reaction kinetics, because the polymeric nature of polyketone prohibits obtaining high resolution spectra [96,217,218][217,218]. Important to note is that dopamine is only commercially available as its hydrochloride salt and must thus be used as a starting material in this form.

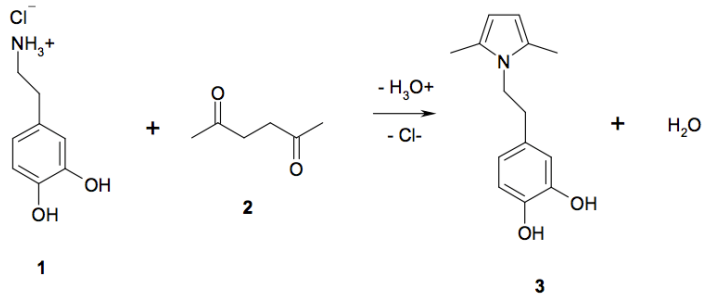

Figure 4.1: Model compound reaction between dopamine-HCl (1) and 2,5-hexanedione (2) for obtaining Paal-Knorr pyrrole product (3)

When sufficient data is obtained on the feasibility of the reaction and the characterization of the product structure, the following novel Paal-Korr pyrrole synthesis is attempted for the particular polymeric compound (see Figure 4.2).

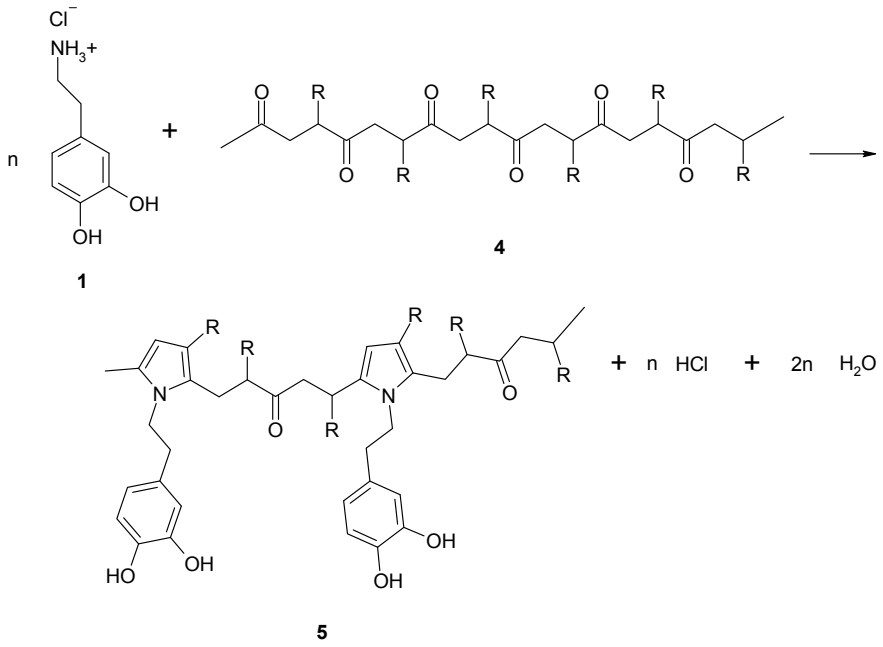

Figure 4.2: Reaction between dopamine-HCl (1) and polyketone (4; R = H or CH_3) for obtaining Paal-Knorr pyrrole product (5)

4.1.2 Dopamine stability

It is critical to take into account the conditions under which dopamine is stable, in any form, in order to attain a successful synthesis. This topic will be reviewed here briefly.

Oxidation issues and mechanistic pathways

One of the challenges in manipulating dopamine is that it is readily oxidized to dopamine quinone, especially under basic conditions [219][219]. This quinone molecule is susceptible to nucleophilic attack by amines and thiols. The reaction with an amine can also occur intramolecular to form a bicylic compound called aminochrome, a red coloured compound which in turn polymerizes (with other compounds) to form dark coloured neuromelanin [220][220]. It is long known that the mechanistic pathways through which dopamine can be oxidized are complex; these depend on i.e. the pH of the environment and the particular oxidant involved [221,222][221,222]. The former will be discussed in more detail in the next section. Regarding the latter: it is known that catecholamine neurotransmitters such as dopamine may undergo auto-oxidation in the presence of molecular oxygen or be oxidized by peroxidative enzymes and metal-ions [223][223]. Even though specific research in this field dates back to 1927, the precise mechanism by which molecular oxygen oxidizes catecholamines to the o-quinone is still unsettled [220]. Nonetheless, in general it can be been concluded from electrochemical investigations [224-226][224,225,226] and studies with the model compound 4-methylcatechol [220] that the initial quinone oxidation product promotes overall catechol oxidation by oxidizing more reactive intermediate products such as 5,6-dihydroxyindoline (indicated in the centre of Figure 4.3) or 4-methylcatechol semiquinone.

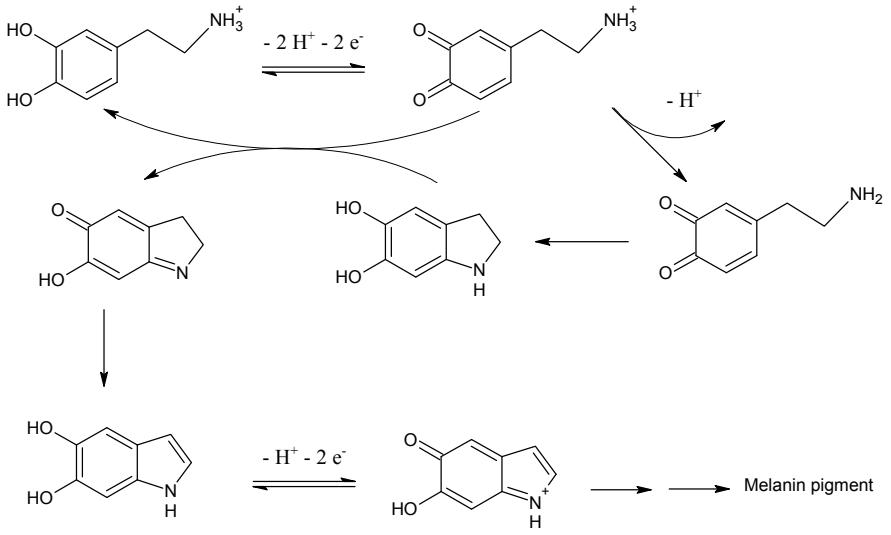

Figure 4.3: A proposed oxidation pathway of dopamine to melanin pigment [226]. Note that irreversible cyclization occurs after deprotonation of the amino-group.

From a kinetic point of view, dopamine oxidation has been described as (relatively) slow because ring closure removes the dopamine quinone, hindering further oxidation [220]. It is important to note in this regard that the relative rate between (i) intramolecular cyclization, (ii) addition of external nucleophiles and (iii) rereduction to the original catechol determines the fate of the catechol [225]. For instance, reduction caused by ascorbic acid is faster than cyclization and prevents aminochrome formation when present in sufficient quantities [225]. Other reductants/antioxidants have also been used to prevent such oxidations, notably including sodium (meta) bisulfite [227,228][227,228].

Influence of pH on structure and oxidation reactions

Dopamine has an amino group that can accept a proton and a phenolic hydroxyl group that can donate a proton, with the second phenolic group having a pK_a value greater than 12 [229][229]. Therefore, except at extremely basic pH values where both hydroxyl groups can be dissociated, dopamine can exist as a cation ($^{+}H_3NDOH$, with D for dopamine skeleton), a zwitterion ($^{+}H_3NDO^{-}$), a neutral form (H_2NDOH), or an anion (H_2NDO^{-}) [229]. With pK_{a1} and pK_{a2} values of 8.86 and 10.5, it can be calculated that at physiological pH (~7.4), dopamine exists mostly as a cation [229]. Prior to providing a short quantitative illustration of this statement, it is important to note here that the first pK_a governs the transition from the cationic form to the mixture of zwitterion and neutral form (both overall neutral species) rather than representing the dissociation of the amino group only [229]. Similarly, the second pK_a describes the transition of the two neutral species into the anion and not just the dissociation of the hydroxyl group [229]. Now, using the well-known Henderson-Hasselbalch equation to approximate [230][230] the ratio of the ionic forms of dopamine around the first transition in an aqueous solution

$$pH = pK_{a1} + \log\left(\frac{^{+}H_3NDO^{-}/H_2NDOH}{^{+}H_3NDOH}\right) \qquad \textbf{Equation 4.1}$$

results in the following general percentages (see Table 4.1). The outcome shows indeed that for pH = 7.4 and pK_{a1} = 8.86 the cation concentration is >90% (96.6% when approximated in more detail).

Table 4.1: Approximated relative amounts of the ionic forms of dopamine at different pH around pK_{a1}. Note: the effect of pK_{a2} has not been accounted for.

$pH - pK_a$	$\frac{^+H_3NDO^- / H_2NDOH}{^+H_3NDOH}$	$^+H_3NDOH$ (%)	$^+H_3NDO^- / H_2NDOH$ (%)
3	1000 / 1	0.10	99.90
2	100 / 1	0.99	99.01
1	10 / 1	9.09	90.91
0	1 / 1	50.00	50.00
-1	1 / 10	90.91	9.09
-2	1 / 100	99.01	0.99
-3	1 / 1000	99.90	0.10

It is tempting to theorize from (i) the previous calculations and (ii) the fact that dopamine oxidizes easily under basic conditions (pH >7) that the zwitterion and neutrally charged forms of dopamine are 'unstable' in the presence of oxidants such as air and thus unsuitable for chemical modifications under these conditions. However, the reality is more complex. For instance, it is long known that (initial) oxidation reactions of dopamine can occur even under strongly acidic conditions (pH 0-1) when using lead dioxide as oxidant [231][231]. Subsequent cyclization, further oxidation (to 5,6-dihydroxyindole) and accompanying colour transition from orange-yellow to deep-red occurs rapidly at only slightly lesser acidic conditions (pH >2) [231]. When using ferrocyanide as oxidant, oxidation occurs down to pH 4 if zinc ions are present [232][232]. Similarly, studies on the enzymatic catalysed oxidation of dopamine with tyrosinase (in the presence of molecular oxygen) or through use of sodium periodate also indicated both general and specific oxidation activities over a wide range of pH [233][233]. It is thus difficult to construct a generic operating window in terms of the thermodynamic and/or kinetic stability of dopamine towards oxidation, depending on the acidity of the reaction medium. Other system variables such as type of oxidants presents, concentration levels of oxidants, reaction temperatures and reaction times appear necessary to be included.

Reactivity towards other compounds

Like other beta phenylamines, dopamine readily undergoes Pictet–Spengler condensations with aldehydes and ketones to produce tetrahydroisoquinolines [219], which can be undesired in either main synthesis reactions or in attempted intermediate protection chemistry (see Figure 4.4).

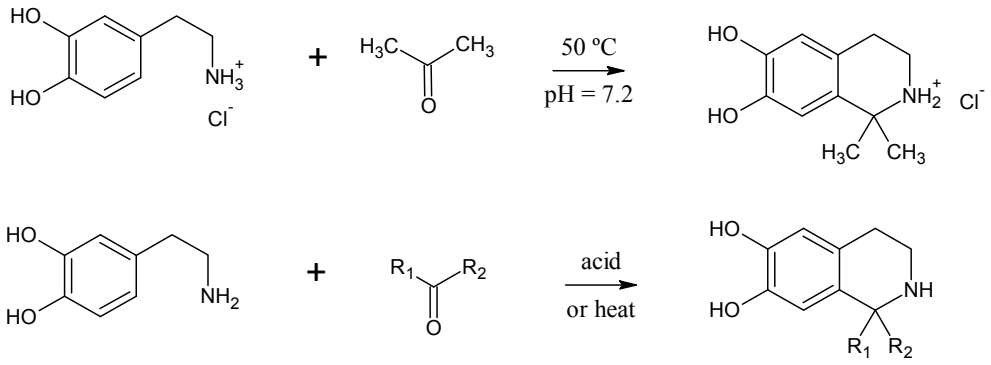

Figure 4.4: Pictet-Spengler condensations with dopamine as first discovered (top) [234][234] and later generalized (bottom; R_1, R_2 = H, alkyl, Ar, carbonyl) [235,236] [235,236]

The nucleophilic amino group of dopamine can react in many other ways, some of which have been applied as desired protection chemistry. A short overview of these applications is given below in Table 4.2, in which two popular catechol-protection strategies in adhesive research have also been included.

Table 4.2: Some chemical protection strategies for dopamine

Subject of protection	*Protecting agent*	*Deprotection*	*Reference*
Amino-group	*N*-carbethoxyphtalimide	H_2NNH_2	[219]
	CF_3COOMe	LiOH	[219]
	Fluorenylmethyloxycarbonyl chloride (FMOC)	$O(CH_2CH_2)_2NH$	[237][237]
	Di-tert-butyl dicarbonate (BOC)	HCl/dioxane	[238][238]
Catechol-group	Ph_2CCl_2	HBr/AcOH/TFA	[141,188]
	$Na_2B_4O_7$ (aq)	pH reduction	[175,178]

4.1.3 Paal-Knorr pyrrole synthesis

Discovered more than a century ago, the Paal-Knorr (PK) pyrrole synthesis is an intermolecular condensation of a primary amine (or ammonia) with a 1,4-diketone (or 1,4-dialdehyde) to give a pyrrole (see Figure 4.5) [236].

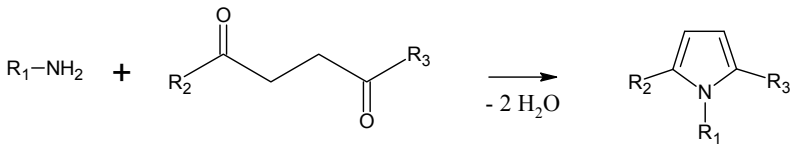

Figure 4.5: Paal-Knorr pyrrole synthesis, R_1-R_3 = H, alkyl, aryl [236]

Mechanism of pyrrole synthesis

In spite of the apparent simplicity of the PK reaction scheme, the mechanism through which it proceeds has long remained a mystique [236]. The specific pyrrole obtained by reacting ammonia with 2,5-hexanedione (R_1 = H, R_2 = R_3 = CH_3) is currently thought to be formed by the mechanism

illustrated in Figure 4.6, but the mechanisms of other PK pyrrole formations are often dependent on pH, solvent and reactant structure [236].

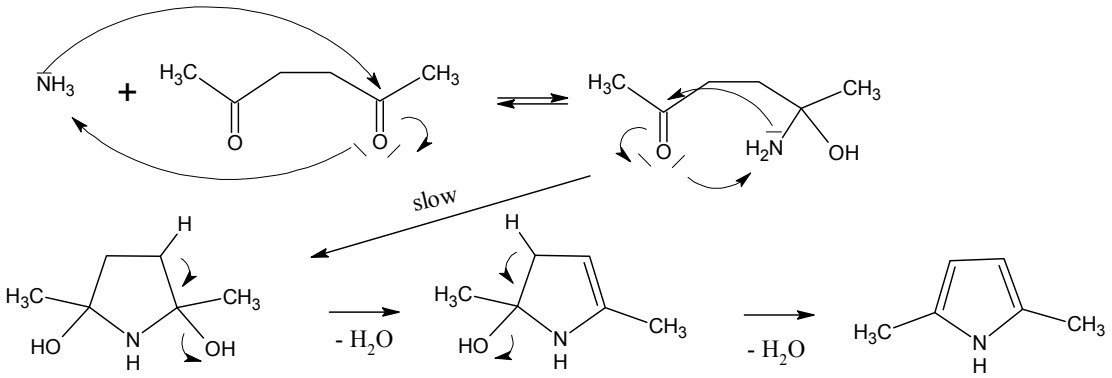

Figure 4.6: Simplified mechanism of specific Paal-Knorr pyrrole synthesis based on [239][239]. Arrows have been included to emphasize the nucleophilic addition of the amine, but ignore the role of solvent and catalyst in proton exchanges.

Role of amine reactant structure, catalyst and solvent

A quick review of the literature on successful PK pyrrole syntheses indicated that almost all protocols utilized neutrally charged amines. This can be rationalized from the nucleophilic addition step in the reaction mechanism and the critical role that steric hindrance plays in the reactivity of the amine for PK reactions [67,96,239,240,241][240],[241]. Two apparent exceptions to this rule were found in the studies of Artico et al. [242][242] and Werner et al. [242][243], in which respectively high reaction temperatures (150 – 160 ^{o}C) or 1.5 mol equivalents of the base triethylamine (TEA) were used when dealing with hydrochloric ammonium salt forms of the amine. The latter strategy is widely used for neutralizing inorganic acids (such as HCl) that are liberated during chemical reactions, as the resulting trialkylaminium salt is water-soluble and therefore easily separated from the organic phase [244][244].

TEA has also been used by Hamarneh [218] when using amino acids as PK reactant, referring to the patent of Sinai-Zingde [245][245] in which the compound is believed to function as a catalyst in similar syntheses. Both authors use TEA (mainly) in a 1.5 – 3 times molar excess with respect to the amine reactant, but do not discuss its more specific functionality or effects on the chemistry involved. Interestingly, catalysts for the PK pyrrole synthesis generally include protic acids and certain Lewis acids, not bases [246][246].

Regarding the solvent, two remarks are important to make. The first is that the solvent of choice depends on the type of amine used and can range from polar protic to dipolar aprotic all the way to nonpolar solvents [246]. Secondly, relatively basic alkylamines do not react if the acidity of the reaction medium is below pH 5.5, while aromatic amines usually undergo the desired cyclization step only when pH <8.2 [246]. It has been stated in this regard that PK pyrrole reactions can be conducted under neutral or weakly acidic conditions, where addition of a weak acid such as acetic acid

accelerates the reaction, but the use of amine/ammonium hydrochloride salts or reactions at pH <3 leads to furans as main products [247][247]. Because virgin polyketone oligomers are only slightly soluble in protic solvents such as methanol and ethanol [96], successful solution modifications through PK will thus most probably require (i) protic solvents which are also compatible with the (dop)amine and (ii) appropriate acidity.

4.1.4 Use of tyramine as alternative reactant

Given all constraints described in the previous two sections on Paal-Knorr reactions and the use of dopamine in chemical syntheses, the structurally similar compound of tyramine (see Figure 4.7) might be useful to incorporate in this research. Although it lacks the desired catechol functionality deemed necessary for attaining (water-resistant) adhesion, it is commercially available in its pure (non-organic salt) form and has previously been used successfully in a (different) Paal-Knorr synthesis [248][248].

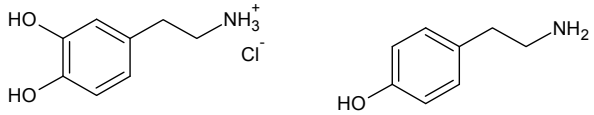

Figure 4.7: Dopamine-HCl (left) and tyramine (right)

4.2 Experimental section

4.2.1 Materials

Chloroform ($CHCl_3$, Lab Scan, ≥99.5%; Fisher Scientific, ACS), dimethyl sulfoxide (DMSO, Fisher Scientific, ACS), ethyl acetate (EtAc, Jose Miraz Pereira, ≥99.5%), 2-(3,4-dihydroxyphenyl)ethylamine hydrochloride (dopamine-HCl, Sigma-Aldrich, ≥98%; 3-hydroxytyramine-HCl, Acros, 99%), 2,5-hexanedione (Sigma Aldrich, ≥99%), hydrochloric acid (HCl, Merck, 37 wt%), iron(III) acetylacetonate ($Fe(acac)_3$, Sigma, 99.9%), methanol (MeOH, Lab Scan, ≥99.8%; Panreac, 99.5%), salicylic acid (Himedia, 99.5%), sodium hydroxide (NaOH, Merck, ≥99%; Panreac, 98%), sodium dichromate ($Na_2Cr_2O_7{\cdot}2H_2O$, Baker, 99.5-100.5%) sulphuric acid (H_2SO_4, Merck, 95-97%), tertbutylammonium (meta)periodate ($Bu_4N(IO_4)$, Sigma), tetrahydrofuran (THF, Acros, ≥99%), triethylamine (TEA, Sigma, 99%) were used as received.

Alternating aliphatic polyketones with 30% ethylene (PK30, M_n = 2797 Da), and 50% ethylene (PK50, M_n = 5072 Da) based on the total olefin content were synthesized according to a reported procedure [249][249] and used as received.

Deuterated chloroform ($CDCl_3$, Sigma Aldrich, ≥99,8 atom%), deuterated water (D_2O, Sigma Aldrich , ≥99,9 atom%) and deuterated dimethylsulfoxide (DMSO, Sigma Aldrich, ≥99,9 atom%) were used as solvents for NMR measurements and used as received.

4.2.2 Analytical measurements

Nuclear Magnetic Resonance (NMR)

Spectra were recorded in Groningen on a Varian Mercury Plus 400 or 500 MHz spectrometer, in Cambridge on a Bruker Avance 400 QNP Ultrashield spectrometer (by the Department of Chemistry NMR service) and in Coimbra on a Bruker Ultrashield Plus 400 MHz spectrometer (by the Nuclear Magnetic Resonance Laboratory of the Coimbra Chemistry Centre). MestReNova (v6.2.1) software was used to analyse and export the data. Peak assignment was done based on references from the literature and ChemBioDraw Ultra (v12) computer simulations.

Fourier Transform Infrared Spectroscopy (FT-IR)

A Jasco FT/IR 4200 ATR was used to record the infrared spectra of starting materials and reaction products. Samples were placed on a diamond plate and 128 scans were recorded for each sample over a range of 4000-550 cm^{-1} with a resolution of 1 cm^{-1}. Background signals were recorded by measuring only the air present in the room.

Ultraviolet-visible spectroscopy (UV-Vis)

A Jasco V550 UV/VIS spectrometer was used in Coimbra to record the UV-Vis spectra of starting materials, reaction products and for oxidation studies. Samples were placed in a quartz cuvet and spectra were recorded for each sample over a range of 800-250 nm with a resolution of 1 nm at a scan rate of 400 nm/min. The reference cuvet contained only solvent and was kept in place during measurements. Jasco Spectra Manager (v2.08.01) software was used to export the data.

A ThermoSpectronic Aquamate 4.60 UV/VIS spectrometer was used in Groningen to record the UV-Vis spectra of the reaction products in DMSO. These spectra were analysed to determine the catechol-content of reaction products based on a calibration curve constructed from known concentrations of dopamine and the maximum absorbance wavelength of this compound (λ_{max} = 286 nm) [151]. Samples were placed in a quartz cuvet and spectra were recorded for each sample over a range of 600-250 nm with a resolution of 0.5 nm at a scan rate of 350 nm/min. Visionite Scan v 2.1 software was used to export the data.

Elemental analysis (EA)

The elemental composition of synthesized compounds with respect to carbon, nitrogen and hydrogen was analysed in Groningen using a Euro EA element analyser and in Coimbra with a EA 1108 CHNS-O Fison Instruments element analyzer. The data were used to calculate the conversion of the carbonyl groups and the amine reactant [218] according to the following equations (see Appendix II for the derivation):

$$X_{CO} = \frac{N(wt\%)\cdot(8-2x)}{C(wt\%)\cdot 1.1662 - N(wt\%)\cdot 8} \qquad \textbf{Equation 4.2}$$

$$X_{A} = \frac{X_{CO}}{2\cdot r} \qquad \textbf{Equation 4.3}$$

in which X_{CO} and X_A are the conversion of carbonyl units and amine reactant respectively, N(wt%) and C(wt%) are the mass percentages of nitrogen and carbon respectively (as outcome of elemental analysis), x is the fraction of ethylene in the polyketone copolymer (e.g. 0.3 for 30% ethylene) and r is the initial molar ratio between the amine reactant and the carbonyl groups.

Thermal analysis

Thermal analysis, i.e. simultaneous thermogravimetric analysis and differential scanning calorimetry, of several acquired polymers was carried out using a SDT Q600 analyzer in Coimbra between room temperature and 300 °C under N_2 with a heating rate of 10 °C/min. TA Instruments Universal Analysis V 4.2E software was used to analyse the data. Differential scanning calorimetry was also carried out in Groningen using a modulated DSC Q1000 V9.8 and the same software package. Two cycles were recorded for each sample, consisting of equilibration at -50 °C for 10 minutes and heating to 100 °C at a rate of 10 °C/min. Intermittent cooling was executed at 10 °C/min and experiments were conducted under a nitrogen flow of 50 mL/min.

4.2.3 Model compound reactivity: determination of kinetics by ^{1}H-NMR

Several reactions between the polyketone model compound 2,5-hexanedione and dopamine or tyramine were performed in a 5 mm diameter NMR tube. Spectra were recorded at various time intervals (typically at 0, 2, 4, 8 and 24 h), temperatures (20 °C and 60 °C) and with two different activating agents for the dopamine-salt: NaOH and TEA. In a typical experiment 2,5-hexanedione (8 mg, 0.07 mmol) was reacted with either tyramine (10 mg, 0.07 mmol) or dopamine-HCl (13 mg, 0.07 mmol) by dissolving both components in 0.6-0.8 mL deuterated DMSO. To activate the dopamine salt, TEA (7 mg, 0.07 mmol) was added or NaOH (2.8 mg, 0.07 mmol) was dissolved in 0.2 mL deuterated water and added to the reactants solution. In all experiments, the total amount of solution was 0.8 mL. The compounds were stirred in a vial for one minute at room temperature and the contents were transferred into an NMR tube. The tube was kept at room temperature or placed in a temperature-controlled oven at 60 °C and removed temporarily for NMR analysis during the course of reaction. The total reaction time was 24 h.

4.2.4 Model compound synthesis

Pyrrolic dopamine was obtained by the reaction of an excess amount of 2,5-hexanedione (24.07 g, 0.211 mol) in 400 mL of MeOH with dopamine-HCl (10 g, 0.0527 mol) in a 1 L round-bottom flask equipped with a magnetic stirrer and a reflux condensor. The dopamine-salt was first activated by dissolving the white crystals in 240 mL MeOH and adding an equimolar amount of NaOH (2.108 g, 0.0527 mmol). Upon dissolution of the components, the colour of the dopamine-mixture changed from clear yellow to orange to brown in several minutes. The activated dopamine was added to the hexanedione, a spatula point of salicylic acid (approx. 25 mg) was added as a catalyst and the mixture was refluxed for 21 h under stirring at 250 rpm. The bulk of the solvent was evaporated after the

predetermined reaction time by removing the reflux condenser and continuing to heat for 3 h, after which the remaining viscous content was dried in a vacuum oven for two days at 40 °C.

Water-soluble by-products, mainly NaCl, were removed by dissolving the dried red-brown solids in 300 mL EtAc and washing once with 150 mL H_2O, three times with 50 mL H_2O and once with brine. The organic layer was dried with sodium sulphate, filtered and the solvent was evaporated at ambient conditions (bulk) and in a vacuum oven (40 °C). Recrystallization from chloroform (carried out by Diego Wever) unfortunately yielded degraded products and all other organic solvents attempted displayed either insufficient solubility at boiling point (e.g. cyclohexane, toluene and DCM) or too high dissolution at room temperature (e.g. methanol, ethanol, and acetone). An alternative final purification step was therefore devised. This procedure consisted of removing the excess amount of water-miscible 2,5-hexanedione by dispersing the material in 250 mL milli-Q water, collecting the solids over a Büchner funnel, drying in a vacuum oven (40 °C) and grinding the powder to a attain smaller sized granules. The process was repeated three times to yield practically hexanedione-free solid, maroon-coloured (purple) pyrrolic dopamine (7.0 g, 57% yield). ^{1}H-NMR (400 MHz, DMSO-d_6, δ) 8.71 (s, 2H, OH), 6.62 (d, J = 8.0 Hz, 1H, ArH), 6.54 (d, J = 1.9 Hz, 1H, ArH), 6.38 (dd, J = 8.0, 1.8 Hz, 1H, ArH), 5.57 (s, 2H, pyrrole), 3.81 (t, J = 7.5 Hz, 2H, CH_2), 3.34 (br s, H_2O), 2.61 (t, J = 7.6 Hz, 2H, CH_2), 2.08 (s, 6H, CH_3). ^{13}C-NMR (200 MHz, DMSO-d_6, δ): 145.07, 143.70, 129.42, 126.34, 119.44, 116.21, 115.49, 104.76, 45.00, 36.30, 12.10. FT-IR: ring stretching from pyrrole rings ~ 3350 cm^{-1}. Elemental analysis for $C_{14}H_{17}NO_2$: Calcd: C, 72.70; H, 7.41; N, 6.06; Found: C, 71.60; H, 7.17; N, 5.72.

4.2.5 Polyketone modifications

Polyketone modifications and purifications were based on the developed synthesis strategy for the pyrrolic dopamine model compound, a published polyketone modification procedure [218] and a patented dopamine/PEG-modification [179]. Reactions were performed in a glass reactor (100 – 250 mL) equipped with a magnetic stirrer or a U-type anchor impeller, a reflux condenser and an oil bath for heating. In the first step the polymer (3.0 – 4.0 g PK30, 22.8 – 30.4 mmol dicarbonyl-units) was inserted into the reactor and heated to 65 °C to facilitate stirring. Dopamine-HCl or tyramine (intakes between 1.14 mmol and 15.2 mmol, equivalent to 5 – 50 % aimed conversion) was dissolved in methanol (50 – 75 mL) and an equimolar amount of either NaOH or TEA was added to activate the HCl-salt of dopamine. When NaOH was added, a distinct colour change was observed: the mixture turned from clear beige to clouded dark brown. No visual change occurred upon addition of TEA. Next, the activated amine in methanol was added to the heated polyketone, a spatula point of salicylic acid (approx. 25 mg) was added as a catalyst and the mixture was refluxed for 21 h under stirring at 100 rpm (impeller) or 250 rpm (magnetic stirrer). No colour change could be observed over the course of the reaction when NaOH was used to neutralize the dopamine, but use of tyramine or TEA showed a transition from clear yellow/beige to orange-brown or red to brown over several hours. The bulk of the solvent was evaporated after the predetermined reaction time by removing the reflux condenser and continuing to heat for 3 h, after which the remaining viscous content was dried in a

vacuum oven overnight (50-100 mbar, 40 °C). The crude products obtained were brown or black coloured and their physical appearance ranged between viscous (5%), viscous-solid (10%), soft solid (25%) to rigid solid (50%).

Although polymers modified up to 10% (aimed conversion) displayed reasonable solubility in ethyl acetate, those modified up to 25% were significantly better soluble in chlorinated solvents such as dichloromethane and chloroform. 50% modified PK30 could only be dissolved in water-miscible solvents such as THF and DMSO. Given these solubility constraints, 5%, 10% and 25% modified PK30s were purified by dissolving in 100 – 300 mL of DCM or $CHCl_3$, decanting into a separation funnel, washing twice with 50 – 100 mL distilled water, twice with 50 – 100 mL 10 mM HCl and once with brine. Care was taken to minimize the formation of emulsion, which was easily triggered upon vigorous mixing. These emulsions did not separate effectively by themselves, but did so reasonably swift upon the addition of several millilitres of brine. The organic layers were subsequently dried over sodium sulphate, filtered and the solvent was evaporated in bulk at ambient conditions, followed by drying for 48 hours in a vacuum oven (50 – 100 mbar, 50 °C). 50% modified PK30 was purified in a similar fashion using THF and 5 – 10 mL of brine added each time to the homogeneous mixture to force phase separation. Moreover, the solid morphology of the modified polymer enabled a final purification step in which the product was precipitated from 50 mL THF in 1 L of cold deionized water and 10 mL of brine, filtered over a Büchner funnel and dried in a vacuum oven for 48 hours (50 – 100 mbar, 50 °C).

Between 1 and 3.5 g of final modified product was typically obtained (36%-72% yield), depending on the dopamine activation method (TEA or NaOH) and the amount of amine added.

The purified products were characterized by ^{1}H-NMR, ^{13}C-NMR, FT-IR, TGA/DSC, EA and UV-Vis. The latter two methods were used to independently determine the degree of modification through either the conversion of the carbonyl groups and the amine reactant (EA, Equations 4.2 and 4.3) or the catechol-content of the modified polymers (UV-Vis). ^{1}H-NMR (400 MHz, DMSO-d_6, δ) 8.70 (br, OH), 6.60 – 6.37 (br, ArH), 5.59 (br, pyrrole), 3.77 (br, CH_2), 3.34 (br s, H_2O), 3.0 – 0.7 (br, polymer backbone). ^{13}C-NMR (200 MHz, DMSO-d_6, δ): 211.47, 207.85, 145.12, 143.76, 129.16, 119.28, 116.10, 115.53, 48.56, 44.97, 43.64, 43.32, 33.53, 34.02, 17.32, 16.63, 16.02, 13.46.

4.2.6 Oxidation analysis

The reaction between the oxidants H_2O_2 and $NaIO_4$ and the novel dopamine-pyrrolic products, either in the model compound form or in the polymeric form, was studied with ^{1}H-NMR, FT-IR (ATR) and/or UV-Vis spectroscopy.

^{1}H-NMR

0.013 g of the dopamine-pyrrolic compound (56 μmol) was dissolved in 0.7 mL DMSO-d6. Next, 0.013 g NaIO4 (61 μmol) or one drop of H2O2 (approx. 0.025 g; 0.74 mmol) was added to the mixture

inside an NMR tube (5 mm diameter), the contents were shaken and spectra were taken within 5 minutes and after 1 hour.

FT-IR (ATR)

50 mg of dopamine-HCl, dopamine-pyrrolic compound or 25% dopamine modified polyketone (aimed conversion, TEA activated) was dissolved in 2 mL of acetone inside a test tube. Next, 25 mg of NaIO4 in 0.5 mL H_2O was added, contents were stirred with a magnetic stirrer for 5 minutes and the mixture was allowed to stand overnight. The solidified contents were dried on filter paper and subsequently freeze-dried for 48 h (dopamine and dopamine-pyrrolic compound) or dried inside an oven at 60 °C for 24 hours (25% dopamine-modified polyketone). After drying, the oxidized product was a black coloured brittle powder when dopamine-HCl or pyrrolic dopamine was used and a brown coloured paste in case of the modified polyketone. The dried products were analysed by using just enough sample material to cover the top of the FT-IR ATR diamond plate and subsequently running the background against air in the laboratory to baseline the spectra.

UV-Vis

1 mL of DMSO containing the novel dopamine-pyrrolic products, either in the model compound form or in the polymeric form, was placed inside a quartz cuvette using a Gilson pipette. Next, 1 mL of DMSO containing the oxidant H_2O_2 or $NaIO_4$ was added. Negative controls were devised in an identical fashion by adding only 1 mL of solvent (DMSO). A positive control was devised by using dopamine instead of the dopamine-pyrrolic products. After addition of the solutions and mixing by pipetting three times up and down, spectra were recorded for 24 hours (or longer) at various fixed time intervals.

First, a 1.0 mM model compound solution was used with a 50 mM H_2O_2 oxidant solution. Next, a 2.0 mM model compound solution was used with a 2.0 mM $NaIO_4$ oxidant solution. A less concentrated 1.0 mM $NaIO_4$ oxidant solution was used for the modified polymers. The solutions containing the dopamine-pyrrolic polymers were prepared at such a concentration as to (i) roughly match a 1:3 to 1:5 ratio with respect to the periodate oxidant (periodate in excess) and (ii) give readings in the 0 – 2 relative absorption range of the spectrometer at the start of the experiment. E.g. the amount of 50% modified PK30 (aimed conversion) was dissolved to attain a concentration of 0.018 mM, which equals approximately 0.19 mM of catechol groups based on a known (number) average degree of polymerization of 21.2 of the virgin PK30. 10% modified PK30 was added at a higher concentration of 0.12 mM to compensate for the lower amount of modified groups. In the first case the ratio between catechol groups and periodate was approximately 1:4.8, whilst in the latter the ratio was 1:3.7.

4.2.7 Biocompatibility analysis

The biocompatibility of the modified polyketones was evaluated *in vitro* according to the ASTM F 756-00 protocol [250][250]. More specifically, the haemocompatibility of the developed materials was studied in a preliminary fashion through haemolysis analysis ACD rabbit blood [203] brought into

contact with 25% dopamine-modified PK30 (aimed conversion, NaOH activated). Three samples of the solid material (0.35 g each) were placed in polypropylene test tubes and 7 mL of diluted blood solution was added. The tubes were incubated for 3h at 37 ºC and carefully inverted twice every 30 min to guarantee the contact between the blood and the material. Positive and negative controls were prepared by adding the same amount of ACD blood to 7mL of water and PBS, respectively. The contents of each tube were subsequently centrifuged at 2000 rpm for 15 min. A cyanmethemoglobin method was used to quantify the haemoglobin (Hb) present in the diluted blood (both erythrocytes and plasma haemoglobin) after contact with the polymeric material. The haemoglobin released by haemolysis was measured by the optical densities (OD) of the supernatants at 540 nm using a spectrophotometer UV–vis (Jasco V-550). The percentage of haemolysis was calculated according to the following equation:

$$\text{Haemolysis (\%)} = \left(\frac{OD_{test} - OD_{negativecontrol}}{OD_{positivecontrol} - OD_{negativecontrol}} \right) \cdot 100 \qquad \textbf{Equation 4.4}$$

The haemocompatibility tests were conducted by Luísa Filipe (in Coimbra).

4.2.8 Adhesive bond strength measurements

Adhesive bond strength measurements were conducted by using aluminium adherends (5754) in a lap shear configuration. The assessment was mostly based on a recently published procedure [251][251], which is a minor modification of the ASTM D1002 standard [252][252]. First, the aluminum adherends were treated with a mixture of water, H_2SO_4 (concentrated), and $Na_2Cr_2O_7$ (40:20:4) at 65-70 °C for 20 min [91]. They were then rinsed with deionized water and air-dried at room temperature in 30-60 min. Adhesive formulation, application and curing conditions depended on the environment chosen: either dry or underwater.

Under dry conditions, a polymer solution (0.3 g/mL) was made by dissolving the modified polymers in 50/50 (volume fraction) $CH_3OH/CHCl_3$. A negative control consisted of using unmodified polyketone (PK30). The polymer solution (22.5 µL) was applied atop each of two adherends by spreading the liquid over an area of 1.25 cm x 1.25 cm using the tip of the pipette. Next, 15 µL of either solvent alone, $Bu_4N(IO_4)$ or $Fe(acac)_3$ cross-linking solution in 50/50 $CH_3OH/CHCl_3$ was added to one of the aluminum adherends by depositing a central drop in the middle over the overlap area. The oxidant solution was formulated to deliver 0.3 eq of crosslinker per catechol group. Without any additional mixing, a second adherend was placed on top of the solutions in a lap shear configuration. A separate aluminium adherend was placed perpendicular at the outer end to support several upper adherends. No pressure other than the weight of the adherend itself was applied and the joints were allowed to cure for 1 hour at room temperature (20 °C), 22 hours at 55 °C, and 1 hour at room temperature (20 °C).

Under wet conditions, a polymer solution (0.3 g/mL) was made by dissolving the modified polymers in $CHCl_3$, which is denser than water. Adherends were submerged in artificial seawater (pH 8.0, ~3.3% salinity) and the polymer solution (45 µL) was applied underwater atop the lower adherend in the centre of the overlap area (1.25 x 1.25 cm). Next, 15 µL of either solvent alone, $Bu_4N(IO_4)$ or $Fe(acac)_3$ cross-linking solution in $CHCl_3$ was added to the polymer solution bubble. Without any additional mixing, a second adherend was placed on top of the solutions in a lap shear configuration. A separate aluminium adherend was placed perpendicular at the outer end to support several upper adherends and each joint was stabilized by using a 55 g weight (comprised of lead shot in a 15 mL test tube closed with a plastic stopper). The adherends were cured underwater at room temperature (20 °C) for 24 hours. The test samples were then removed from the water bath and blotted dry with paper just before testing.

The adherends were pulled apart using a Tinius Olsen H25KT materials testing system at a rate of 2 mm/min. The adhesive force for each assembly joint was obtained by dividing the maximum load (N) observed at bond failure by the area of the adhesive overlap (mm^2), resulting in the adhesive strength in Megapascals (MPa = N/mm^2). For each test, five samples were used. Values are reported as an average with standard deviation. All samples showed cohesive failure.

4.3 Results and discussion

4.3.1 Model compound reactivity: determination of kinetics by ^{1}H-NMR

To gain insights into the overall feasibility and reaction kinetics of the attempted Paal-Knorr pyrrole syntheses, several reactions with the polyketone model compound 2,5-hexanedione were carried out at a range of process conditions (see experimental section). The diketone to amine molar ratio was set to 1 for all experiments, similar to a previous investigation [218]. The conversion of tyramine versus time was determined from the ratio of the peaks around δ 6.9 ppm (aromatic H from reacted tyramine) and around 7.0 ppm (aromatic H from unreacted tyramine). Similarly, the conversion of dopamine was determined from the ratio of the peaks around 6.35 ppm (aromatic H from reacted dopamine) and around 6.45 ppm (aromatic H from unreacted dopamine) when TEA was used as the activation agent. In case of NaOH as an activation agent, the conversion of dopamine versus was determined differently due to overlapping spectra signals in this shift range. Here the ratio of the peaks around 3.75 ppm (CH_2 from reacted dopamine next to pyrrole ring) and around 2.7 – 2.8 ppm (CH_2 from unreacted dopamine next to pyrrole ring) could be used.

Moreover, in all experiments with tyramine and with TEA as the activation agent for dopamine the conversion of 2,5-hexanedione could also be determined from the ratio of the peak integrals around 2.05 ppm (CH_3 from reacted hexanedione) and round 2.09 ppm (CH_3 from unreacted hexanedione). These signals disappeared quickly altogether in the experiments with NaOH, although the formation of a distinctive peak around 6 ppm arising from the H atoms on the pyrrole rings [96,217,218] could be observed in all spectra.

The Paal-Knorr reactions with tyramine, which were expected to be unaffected by an activating agent such as TEA, were carried out with and without the presence of an equimolar amount of TEA. In this experiment, it was aimed to obtain a more detailed expression of the conversion versus time behaviour by repeating the experiment without use of TEA in a 500 MHz NMR apparatus and recording spectra every 30 minutes over a period of 14 h. The results are shown in Figure 4.8.

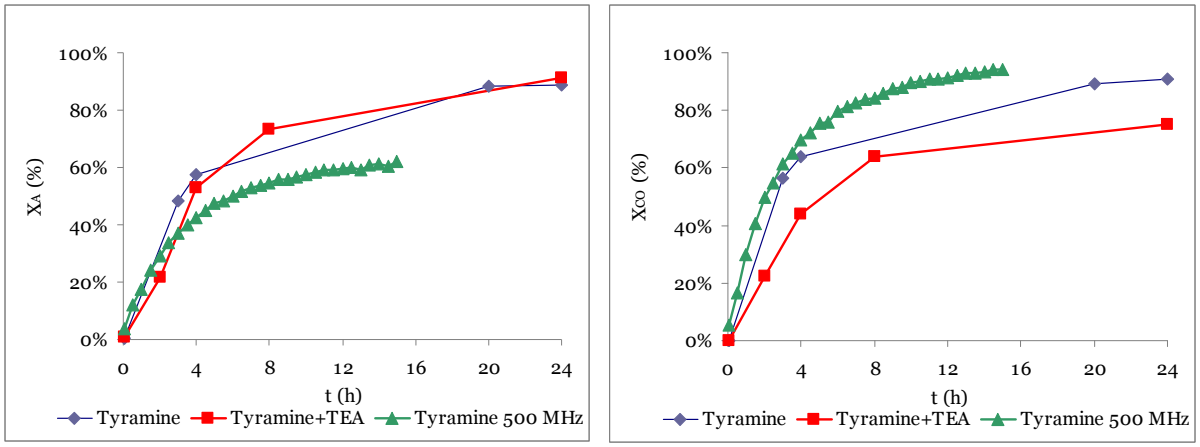

Figure 4.8: Effect of TEA and reaction time on the conversion of tyramine (left) and 2,5-hexandione (right) of model Paal-Knorr reactions in DMSO/water at 60 °C

The results shown in Figure 4.8 indicate that an amine similar to dopamine can react successfully in near quantitative yields at elevated temperatures of 60 °C over a period of 24 hours. A maximum amine conversion of 90% could be attained and TEA does not appear to affect this reaction significantly. However, the sensitivity of the reaction to proper weighing and mixing of the reactants before inserting into the NMR tube is clear, as testified by the difference between amine conversion and hexanedione conversion. This difference is most apparent in the 500 MHz experiment, in which it appears that a substoichiometric amount of hexanedione was added instead of an equimolar amount: carbonyl conversions are greater than 90% but the amine conversion was 62% at maximum.

The Paal-Knorr reactions with dopamine-HCl were carried out with and without the presence of the activating agents TEA and NaOH. The results are shown in Figure 4.9 and indicate that an activation agents is indeed required for the dopamine-salt in order to react successfully. Even the addition a weak protic acid (i.e. trifluoroacetic acid) as a catalyst did not result in a measurable conversion when no activating agent was used (data not shown). The stronger base NaOH resulted in a higher and faster conversion than the weaker base TEA when both are used in equimolar amounts (data shown as the average of two samples each). However, this difference is minimized when TEA is used in a three times molar excess, at which even a higher maximum conversion is actually achieved (94% at 24h, one sample tested). Interestingly, the model reaction with NaOH occurs to almost similar extent at room temperature. This indicates that utilizing elevated reaction temperatures might be useful in attaining

(slightly) higher and faster conversions, but might not be a crucial factor besides lowering the amount of solvent required to attain (and maintain) a homogenous reaction mixture.

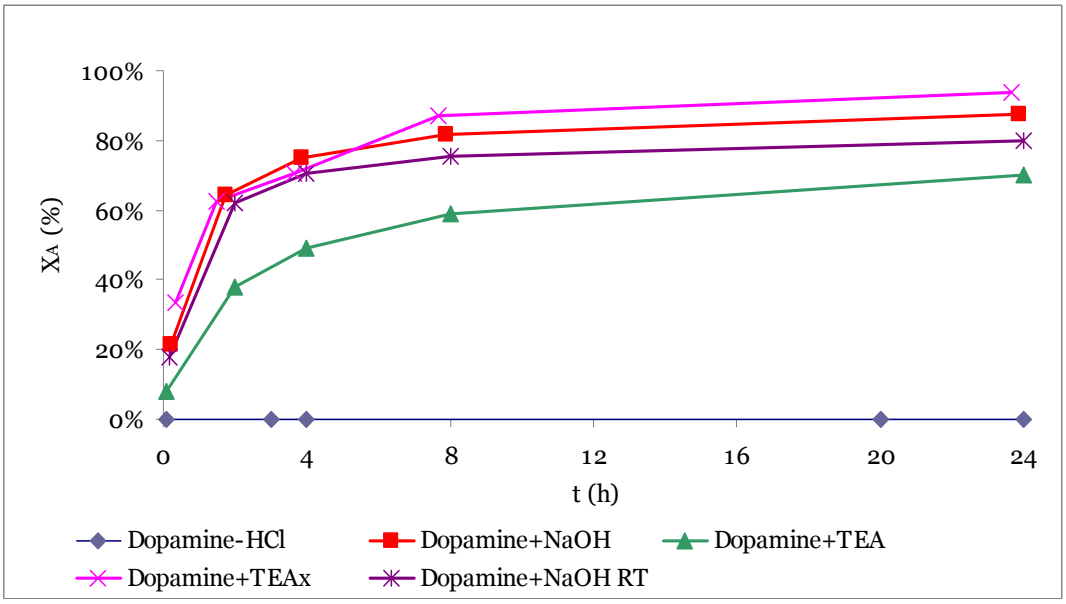

Figure 4.9: Effect of activation agent and reaction time on the conversion of dopamine in model Paal-Knorr reactions with 2,5-hexanedione in DMSO/water at 60 °C or room temperature (RT). TEAx denotes a three times molar excess of TEA.

The experiments carried out in this work were intended in the first place to provide quantitative data on the feasibility of the envisioned reaction and conversion levels attainable under the reaction conditions employed. It was also aimed to determine the kinetics of the reactions in more detail and to obtain specific kinetic expression. However, the experimental data obtained did not fit any simple kinetic model (first or second order in both reactants) as found for very similar systems [218], not even in the case of tyramine without any activating agents (derived data and graphs not shown). A more rigorous experimental set-up in terms of more measurements per sample (e.g. every 30 minutes), using triplicates for each run, testing at different temperatures and utilizing different initial ratios of reactants is recommended for obtaining quantitative kinetic data of higher quality.

4.3.2 Model compound synthesis

To investigate if the novel dopamine-pyrrole compounds could be made on a larger scale and what the properties of such a material would be, a reaction was conducted on a preparatory scale using the polyketone model compound 2,5-hexanedione. The product was obtained in reasonably high quantities (70% yield) and was found to be stable over at least 6 months. ^{1}H-NMR spectra of the reactants and the final purified product are shown in Figure 4.10. ^{13}C-NMR of the product showed two intact hydroxyl functionalities around 144 ppm, did not indicate any quinone-like oxidation products, nor did an insoluble fraction form when reattempting to dissolve the compound (in DMSO) after several months. Both proton and carbon NMR spectra were found to be comparable to an earlier reported Paal-Knorr reaction product made from 2-aminoethylbenzene and 2,5-hexanedione [253][253].

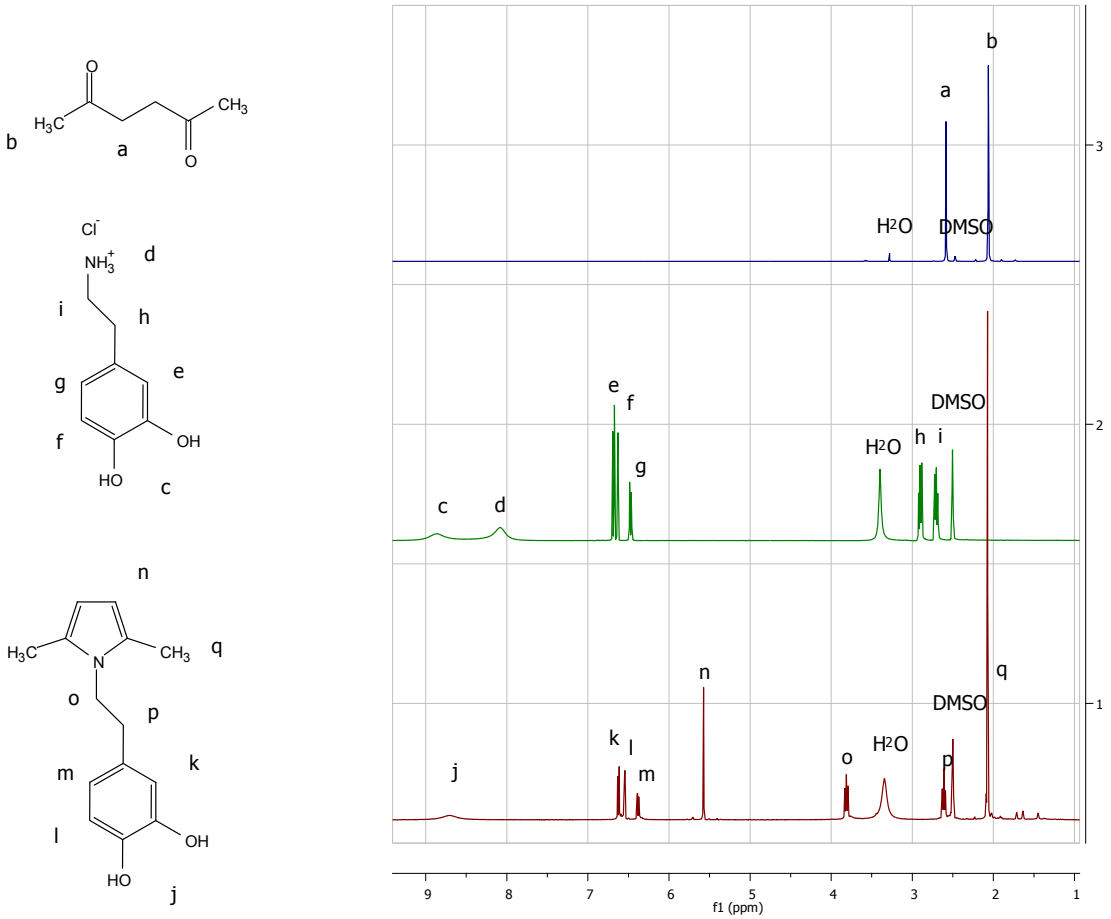

Figure 4.10: ^{1}H-NMR spectra of 2,5-hexanedione (top), dopamine-HCl (middle) and dopamine-pyrrole model compound (bottom).

The stability of the obtained compound is particularly surprising, given the fact that the synthesis and purification protocol included using the strong base NaOH, no protection/deprotection of the catechol-group was applied and no shielding from oxygen was implemented (see sections 3.2 and 4.1.2). Nevertheless: recrystallization has proven to be difficult and solutions of the product do darken over time, highlighting the reactive character of the catechol group. It may be relevant to point out that the physical appearance of the product (see Figure 4.11), best described as an amorphous dark purple (maroon coloured) powder, resembles a reported poly(dihydroxystyrene) [150]. However, the observed colour may also be related to partial oxidation triggered by the use of NaOH. Conclusive information on the true appearance of the compound is expected from using TEA during synthesis, working under oxygen free conditions and using decolourizing active carbon, e.g. when recrystallizing (if possible).

From a comparative point of view, the demonstrated Paal-Knorr reaction with dopamine also appears to be more effective than a previously reported route using 3-methoxytetrahydrofuran (purified with column chromatography, 8% yield) [254][254]. The reaction might thus find wider areas of application, for instance in opening an alternative pathway in the total synthesis of Ningalin D [255,256][255,256]. The

requirement of a suitable and sterically accessible dicarbonyl should be stressed however, given that this requirement is viewed upon as one of the main limitations of Paal-Knorr reactions [246].

Figure 4.11: Photograph of the purified dopamine-pyrrole model compound obtained

4.3.3 Polyketone modifications

Preparative reactions between pre-synthesized alternating aliphatic polyketones with 30% ethylene based on total olefin content (PK30, M_n = 2797 Da) and dopamine-HCl or tyramine were performed in methanol, using either NaOH or TEA as an activating agent and salicylic acid as a catalyst. The molar ratio between the polyketone dicarbonyl groups and the amine was varied between 1:0.05 and 1:0.5. The reaction time employed was 24 h to ensure enough time was given to reach near-maximum conversion. PK30 was selected as the polymeric backbone for its expected combination of good processability, proper resistance to crosslinking and suitable reactivity. Polyketones with lower amounts of ethylene content have been shown to be less reactive as they are more sterically hindered, whilst polyketones with higher ethylene content are less easily processed and more prone to crosslinking [96,218]. The experimental set-ups utilized were found to be more easily controlled when a metal U-shaped anchor impeller was used to stir the mixture. However, a magnetic stirring bar could also be used, because (i) high enough temperatures were employed to reduce the viscosity of the virgin PK30 and (ii) enough solvent was added to create a homogeneous low-viscosity reaction mixture.

Because the modified polymers could potentially be applied in a biomedical setting, purification of the modified polymers was first attempted without the use of an organic solvent. The desired protocol consisted of dispersing the crude modified polymers in water or acidified water (10 mM HCl), vortexing three times for 1 minute, centrifuging 2500 rpm for 5 minutes, removing the supernatant and repeating the procedure twice. However, the softer, viscous modified polymers were particularly difficult to handle, given that freezing with liquid nitrogen, crunching and washing with cooled water was required to increase the contact area between the liquid and the solid. Moreover, control experiments with non-activated dopamine-HCl showed that the protocol was not effective in removing water-soluble components such as the dopamine-salt from the polymeric matter. Therefore, the use of organic solvents appeared to be unavoidable.

The products purified using chlorinated solvents (and THF in case of 50% modified PK30) were initially characterized by ^{1}H-NMR, ^{13}C-NMR and FT-IR (ATR). Proton NMR spectra shown in Figure 4.12 show the broad pyrrole signals around 5.6 ppm, aromatic signals around 6.5 ppm and alcohol signals around 8.7 ppm. These signal increase in intensity at higher aimed conversion and correspond to the signals of the model compound reaction product, testifying the successful modification of the polyketones. Spectra from a control batch of non-activated dopamine-HCl (25% aimed modification) indicated that polyfurans were formed, which also darken over the course of the reaction and give rise to signals around 5.6 ppm. However, these polymers remained viscous and were effectively separated from unreacted dopamine through use of the established purification protocol (spectra not shown).

The spectra from Figure 4.12 also contain sharp signals assigned to residual DCM (5.7 ppm), chloroform (8.3 ppm), THF (3.6 and 1.7 ppm) or THF-stabilizer BHT (6.85, 2.15 and 1.32 ppm) which unfortunately could not be removed completely from the polymeric material through use of the developed protocol. Apparently, the use of a vacuum oven for 48 hours at 50 – 100 mbar and 50 °C was insufficiently effective in this regard. Use of a freeze-dryer that is also capable of handling organic solvents might be recommended to improve the purification efficiency, in addition to removing the BHT stabilizer prior to the use of THF.

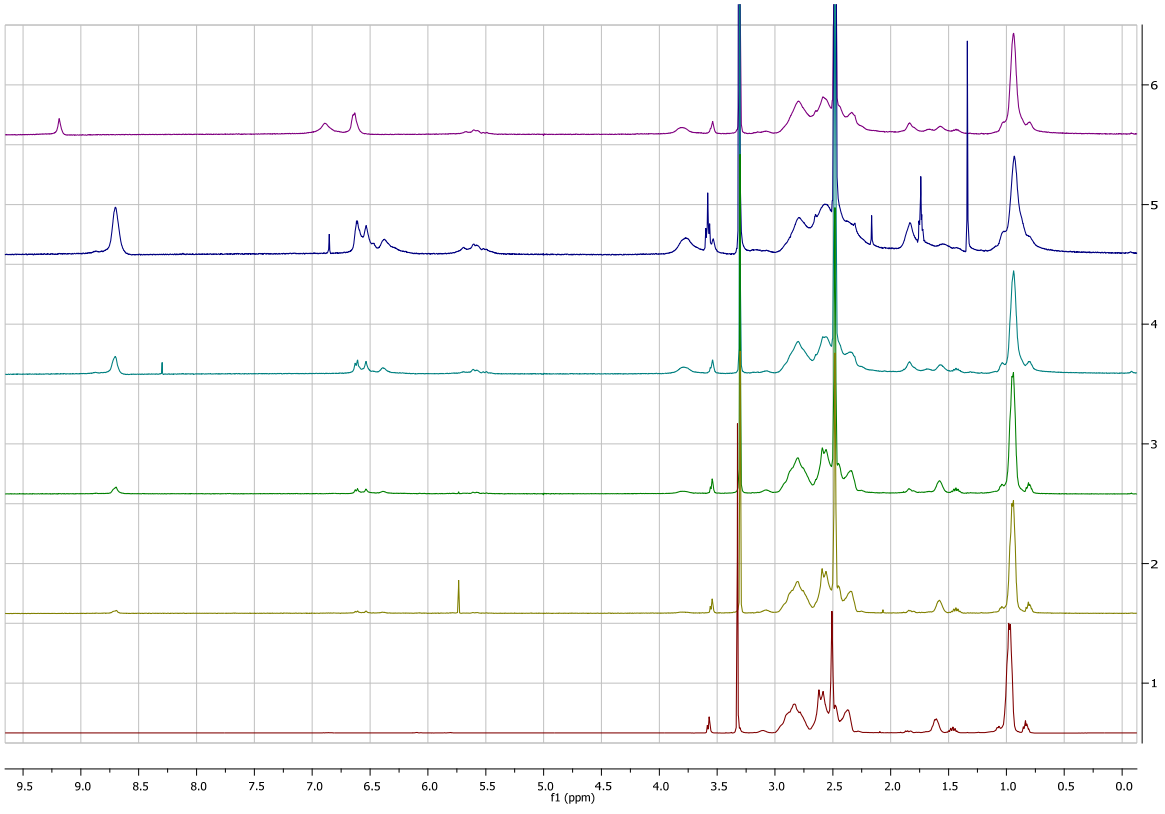

Figure 4.12: ^{1}H-NMR spectra of PK30 (bottom, 1), of dopamine-modified PK30 at 5% (2), 10% (3), 25 (4) and 50% (5) aimed conversion using TEA and of tyramine modified PK30 at 25% aimed conversion (6, top) in DMSO.

Carbon NMR spectra of dopamine-modified polyketones (25% aimed conversion, NaOH and TEA activated) corresponded to that of the model compound but failed to show clear pyrrole signals around 105 ppm, in contrast to that of the polyfurans obtained in the control batch. A possible explanation for it could be of experimental origin: samples of 25 mg of polymers were analysed with 4096 scans, resulting in a fairly low signal-to-noise ratio. FT-IR (ATR) was however able to provide some clarification on the matter.

Figure 4.13 shows the IR-ATR spectra of the model compound and of the 50% dopamine-modified PK30 in comparison with the starting materials dopamine-HCl and PK30. The spectra of the dopamine-modified polyketone and hexanedione show great similarities. Overlay of these product spectra (red and purple) with the dopamine salt (blue) mainly indicates increased absorption in the range of H-bonded alcohol and amine stretching frequencies (3506-3240 cm^{-1}), but where also the CH stretching frequency for pyrrole rings in amino-acid modified polyketones have been reported (at 3350 cm^{-1}) [218]. The characteristic absorption at 1695 cm^{-1} could correspond with carbonyl absorption of residual carbonyl groups in the polyketone or 2,5-hexanedione, although the latter is reported to show at 1715 cm^{-1} [257][257]. Alternatively, it may correspond with conjugated carbonyl groups of quinone-like structures, which would indicate (partial) oxidation of the catechol has occurred. The increased absorption at 1330-1440 cm^{-1} can be attributed to alkane bending frequencies, possibly of the product methyl groups attached at the pyrrole rings or of the starting compound 2,5-hexanedione [257]. Ring stretching of the pyrrole rings at ~1580 cm^{-1} mentioned in previous reports on amine-modified polyketones [96,218] could not be established here uncontroversially as dopamine-HCl also shows absorption at these wavenumbers.

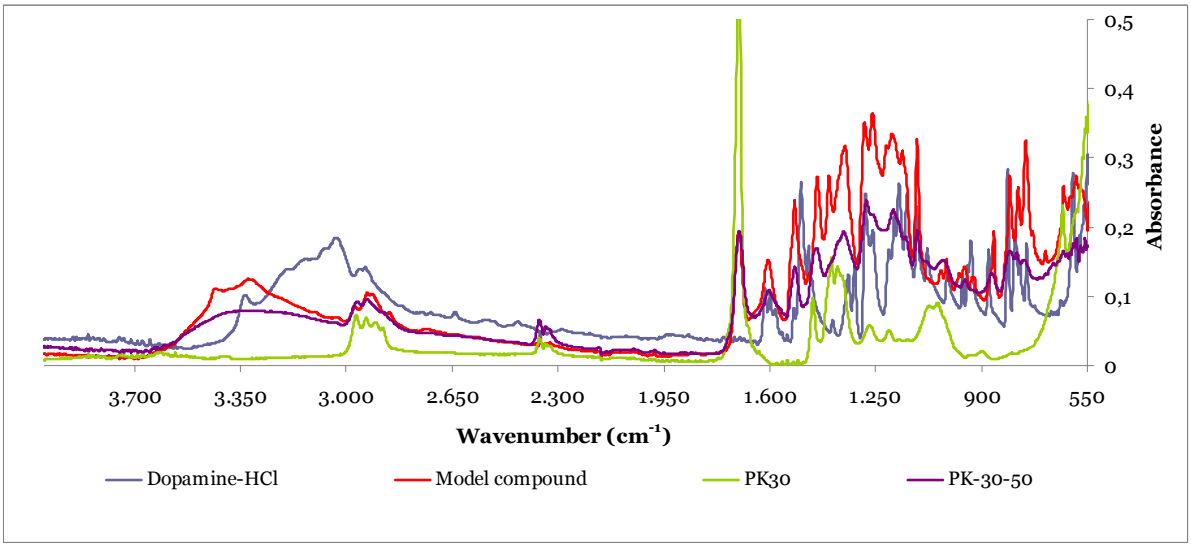

Figure 4.13: IR-ATR absorption spectra of dopamine-HCl, model compound, PK30 and 50% dopamine-modified PK30

The IR-ATR absorption spectra of dopamine-modified PK30s are shown in Figure 4.14. It is clear that the polyketone carbonyl absorption at 1695 cm^{-1} decreases with increasing modification degree, suggesting increased conversion through Paal-Knorr reactivity. Absorption at other wavelengths

generally show the opposite: these increase with a higher initial amine:carbonyl reactant ratio. A first attempt to illustrate this effect more clearly is shown in Figure 4.15. In this graph the absorption at 3300 cm^{-1} was chosen as a reference point for absorption originating from reacted groups and 1700 cm^{-1} was chosen as a reference point for absorption originating from unreacted dicarbonyl groups.

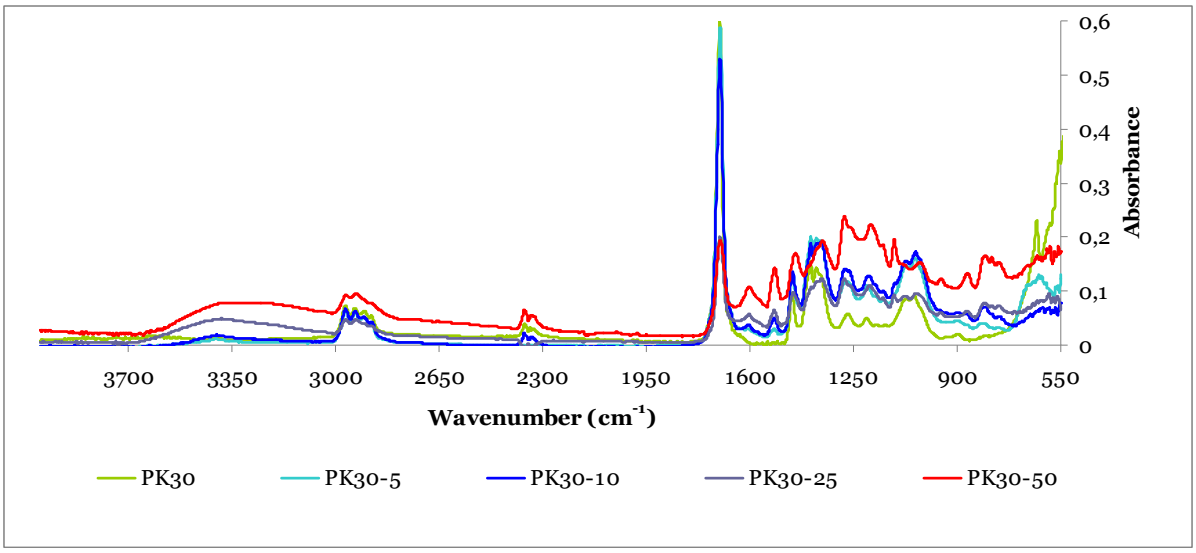

Figure 4.14: IR-ATR absorption spectra of dopamine-modified PK30s

Simultaneous TGA/DSC measurements conducted in Coimbra on the purified NaOH activated dopamine-modified polyketones proved to yield unreliable data due to hardware difficulties. DSC data obtained in Groningen on TEA activated dopamine-modified polyketones (see appendix III) did however show a clear correlation between the glass transition temperature (T_g) and the aimed modification degree (see Figure 4.16). The experimentally observed increasingly solid character of the modified polyketones at higher aimed modification degree is clearly illustrated by the increasing T_g. The plot also shows that the transition point from liquid-like to solid-like at room temperature can be expected above 25% (aimed) modification degree.

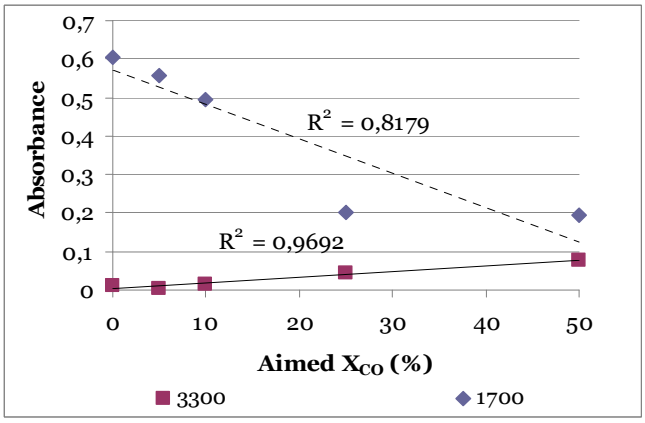

Figure 4.15: Trends in IR-ATR absorption of dopamine-modified PK30s at two wavelengths (3300 cm^{-1} and 1700 cm^{-1}).

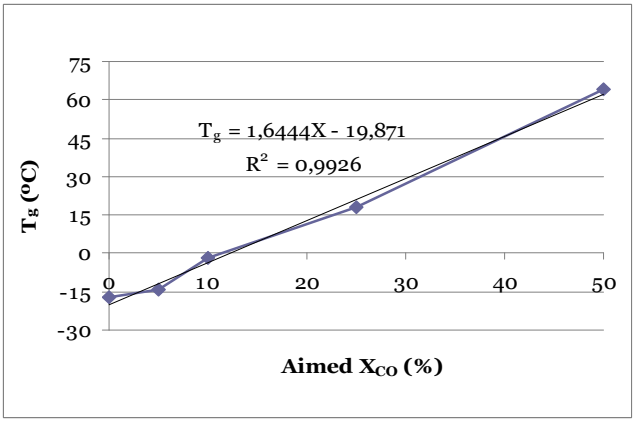

Figure 4.16: Relationship between T_g and aimed modification degree of dopamine-modified PK30s (TEA activated).

Established procedures with EA and UV-Vis were used independently to determine the actual modification degree of the polymers (see experimental section). The results of the elemental analysis data available at the time of writing are shown in Table 4.3. From these results it can be observed that amine conversions are close to quantitative for dopamine and quantitative for tyramine under the reaction conditions employed. This finding is in agreement with the high conversion attained in the kinetic experiments conducted on the model compound 2,5-hexanedione and with similar investigations [96,218]. The amine conversion does decrease relatively at higher aimed modification, which can be rationalized from increased steric hindrance of the available sites in the modified polyketones.

Table 4.3: Conversion of carbonyl groups and amine of modified PK30. Tyr denotes modification with tyramine instead of dopamine.

Sample	X_{CO} *(%)*	X_A *(%)*	*H Deviation** (%)*
PK30-05 NaOH*	9.7	193%	9.7%
PK30-10 NaOH*	16.5	165%	16.5%
PK30-25 NaOH	24.2	97%	-2.5%
PK30-50 NaOH	45.1	90%	-15.1%
PK30-25 Tyr	25.2	101%	-0.7%
PK30-25 TEA	24.0	96%	-2.0%
PK30-50 TEA	42.5%	85%	-0.4%

*: Viscous nature of the material makes accurate weighing difficult. Samples used of alternative purification procedure without use of organic solvents.

**: Difference between wt% of hydrogen found and wt% of hydrogen calculated.

Using equimolar amounts of TEA appears to be slightly less effective than using NaOH, but the use of NaOH results in larger deviations from the calculated amount of hydrogen (used as a control indicator), particularly for the 50% batches. The latter finding might be caused by the increased presence of oxidized components, but may also be caused by other impurities (e.g. BHT). Moreover, polymers with lower than 25% aimed conversion were too viscous to be weighed accurately and in a clean manner by the technicians responsible for the analysis in Groningen. Analysis of the 5% and 10% aimed conversion PK30 (NaOH activated) was only conducted thus far in Coimbra on batches that were not purified through use of organic solvents but through repeated dispersion in acidified water. As discussed earlier, this protocol appeared to be uneffective in removing unreacted products and the values obtained are indeed much higher than expected. Moreover, the above quantitative conversion suggests that the base N:C of the virgin polymer of PK30 (assumed 0) may contain a large absolute error, nitrogen-containing impurities were significantly present or that virgin polyketone material was lost somehow during synthesis. The latter is supported by the relatively low yield of these batches (typically <50%). More data will be incorporated in the near future to clarify these issues.

The UV-Vis spectra of dopamine-modified PK30s (0.125 mg/mL) in DMSO are shown in Figure 4.17. The spectra demonstrate increased absorbance at higher modification degrees. No significant

difference can be observed in the dopamine-absorption range of 260-300 nm between the TEA and NaOH activated batches. However, these spectra do show clearly that the NaOH activated samples have greater absorption at higher wavelengths, particularly at 380 nm and 480 nm. These wavelengths have been shown to correspond to oxidized moieties such as α,β-dehydro DOPA intermediates (320-380 nm), dopachrome (302, 473), DOPA quinone (395 nm) and dicatechol (420-510 nm) [197].

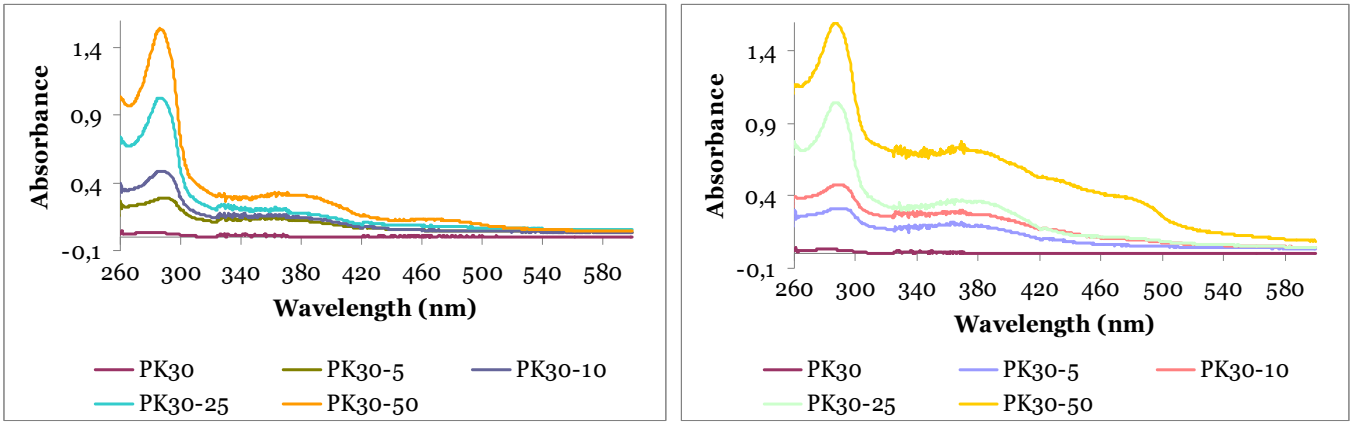

Figure 4.17: UV-Vis spectra of TEA activated dopamine-modified PK30s (left) and NaOH activated dopamine-modified PK30s (right) at concentrations of 0.125 mg/mL in DMSO.

Through use of a standard curve constructed from known concentrations of dopamine in DMSO (not shown) and by measuring the absorbance at 286 nm, the concentration of dopamine-groups in the modified polymers could be calculated [151]. Some iteration is needed in this calculation, as the degree of modification affects the molecular weight, which in turn affects the amount of polymer chains (molar concentration) calculated to be present in the samples. Moreover, the absorbance of (slightly oxidized) dopamine-pyrrole groups can be expected to differ from that of pure dopamine. A correction factor was used to attempt to compensate for this affect, by measuring the absorbance of the dopamine-pyrrole model compound product. The results of the assay are displayed in Table 4.4.

Table 4.4: Conversion of carbonyl groups and amine of modified PK30 as determined from UV-Vis assay.

Sample	A_{286}	*[Sample] (µmol/mL)*	*[Dopamine] (µmol/mL)*	*Ratio*	X_{CO} *(%)*	X_{CO} *Corrected (%)*	X_A *(%)*
MC	1.800	0.54	0.45	0.8	83.6	100	100
PK30	0.0271	0.045	0.01	0.1	0.6	0.5	-
PK30-05 TEA	0.2786	0.042	0.07	1.7	7.8	6.5	130
PK30-10 TEA	0.4817	0.040	0.12	3.0	14.3	12	119
PK30-25 TEA	1.027	0.034	0.26	7.6	35.7	30	120
PK30-50 TEA	1.536	0.029	0.39	13.5	63.6	53	106
PK30-05 NaOH	0.3075	0.042	0.08	1.8	8.7	7.3	145
PK30-10 NaOH	0.4713	0.040	0.12	3.0	13.9	12	116
PK30-25 NaOH	1.040	0.034	0.26	7.7	36.3	30	122
PK30-50 NaOH	1.590	0.028	0.40	14.2	67.2	56	112

The amine conversion calculated from the UV-Vis spectra are higher than was expected (conversions >100%), even though a correction factor of 0.836 from the model compound was applied to the calculated dicarbonyl conversion. It should be noted that a negative control in the form of virgin PK30 resulted in a calculated carbonyl conversion of 0.5% (corrected), which highlights the sensitivity to errors of this technique. Together with the elemental analysis data, is does appear that the modifications have indeed been successful within the experimental conditions applied. However, the quantitative extent remains uncertain, given de difference between the conversions calculated through both techniques. The methodology incorporated in the UV-Vis assay depends on various assumptions, critical ones being that (i) the number average degree of polymerization was 21.2 for the polymers and (ii) the absorption of the purified model compound is a justifiable correction factor for translating absorbance at 286 nm to dopamine concentration. In other words, this method is based on the assumption that no conflicting absorbance is present in the samples at 286 nm. The finding that the calculated amine conversions are more than quantitative suggests that this is not the case. The EA methodology is therefore deemed more reliable in determining the conversion.

4.3.4 Oxidation analysis

The expected reactivity of the synthesized dopamine-pyrrole products with oxidants was studied with ^{1}H-NMR, FT-IR (ATR) and UV-Vis spectroscopy. Prelimenary studies on the dopamine-pyrrole model compound with proton NMR unfortunately resulted in little information on structural changes when H_2O_2 or $NaIO_4$ were added. In the case of H_2O_2, no physical change could be observed and the spectra were mostly overwhelmed by the resonance of the non-deuterated hydrogen peroxide (data not shown). In case of addition of $NaIO_4$, flattening of the catechol resonance at 8.7 ppm and a slight increase in the water resonance at 3.4 ppm could be observed within 5 minutes, but rapid solidification of the material impeded further analysis. Analogous experiments with the dissolved model compound or dopamine-modified polyketones were conducted in acetone on a larger scale. These displayed a similar rapid solidification when $NaIO_4$ was added and no effect when H_2O_2 was added. The solidified material was studied with FT-IR ATR. The spectra of dopamine-HCl and dopamine-pyrrole model compound are shown before and after oxidation with $NaIO_4$ in Figure 4.18. The spectra of 25% dopamine-modified polyketones (aimed conversion) are shown in Figure 4.19.

Little detailed information could be obtained on the structure of the oxidized solid dopamine-pyrrole compounds from the FT-IR ATR spectra. However, clear features are the overall difference from the starting material and the similarity of the profiles from the oxidized dopamine-HCl and dopamine-pyrrole model in Figure 4.18. This is in contrast to the apparent preservation of the structural features in the polymeric material (Figure 4.19). This finding suggests that the low molecular weight material participates in many different polymerization reactions upon oxidation that lead to loss of its original structural identity, whilst the polymeric material undergoes these to far lesser extent. In order to attain a better understanding of the oxidation behaviour and possible chemical intermediates, UV-Vis analysis was conducted. The results of these experiments with dopamine-HCl and the dopamine-

pyrrole model compound with $NaIO_4$ are shown in Figure 4.20. Note: the addition of H_2O_2 to dopamine-HCl or the model compound in DMSO did not results in changes in the absorbance spectra over a period of four days.

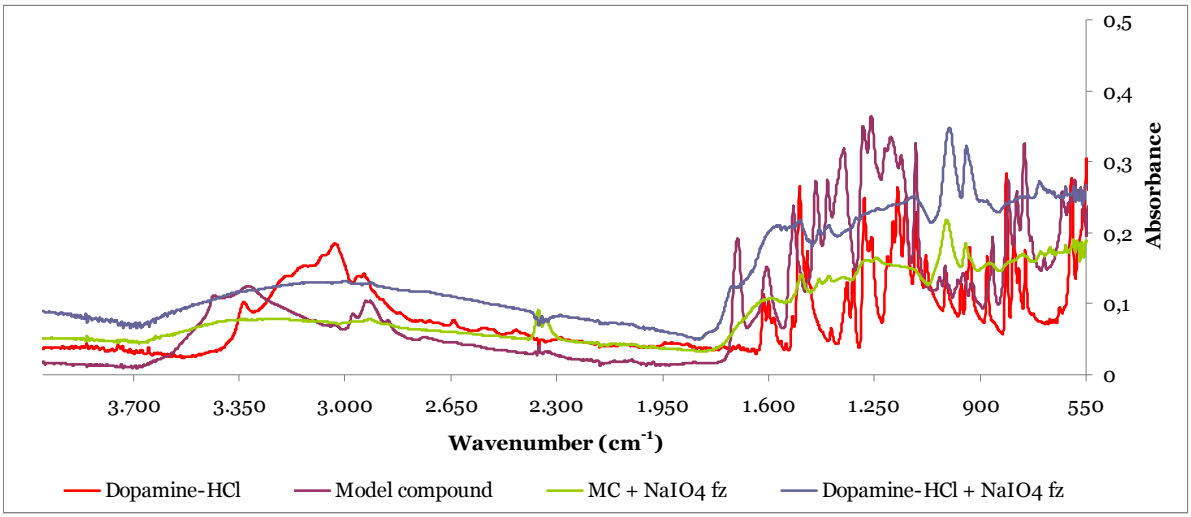

Figure 4.18: FT-IR ATR spectra of dopamine-HCl and dopamine-pyrrole model compound before and after oxidation with $NaIO_4$ in acetone/H_2O. Fz denotes samples were freeze-dried before analysis.

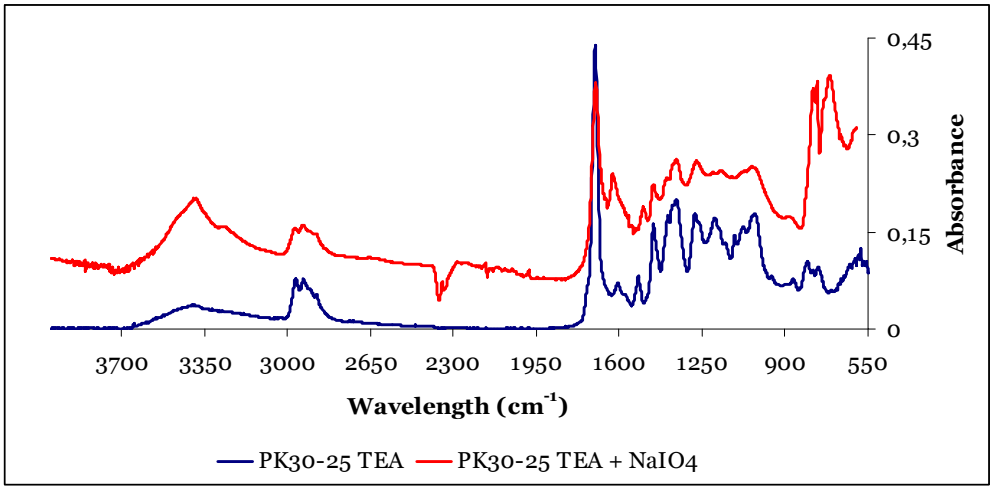

Figure 4.19: FT-IR ATR spectra of 25% dopamine-modified polyketone before and after oxidation with $NaIO_4$ in acetone/H_2O.

The spectra displayed in Figure 4.20 show comparable increases in absorption upon the addition of sodium periodate. A shoulder at 300-350 nm and a broad peak at 490-500 nm developed over the course of the reaction (24 h). Dopaminoquinone absorption (395 nm) is not observed, but this is probably caused by fast consumption of the species within the first minute [197,221,233]. The signals at 325 nm and close to 500 nm could be caused by aminochrome formation (302 nm and 473 nm) [146,233], but also compare favourably with the formation of dicatechol groups (270 nm and 490 nm) and α,β-dehydro intermediates (310-380 nm) [197]. The latter explanation seems more plausible for the model compound oxidation products, given that intramolecular cyclization is hindered by the

pyrrole unit. The formation of a sharp peak at 270 nm in the spectrum of the model compound between 6.5 h and 26h after mixing supports this hypothesis. It must be noted though that reference absorptions are given for water, whilst these experiment were carried out in DMSO. Although the λ_{max} of dopamine is 280 nm in both cases and the polarity of the solvents is comparable, other solvent effects (e.g. through hydrogen bonding) cannot be ruled out.

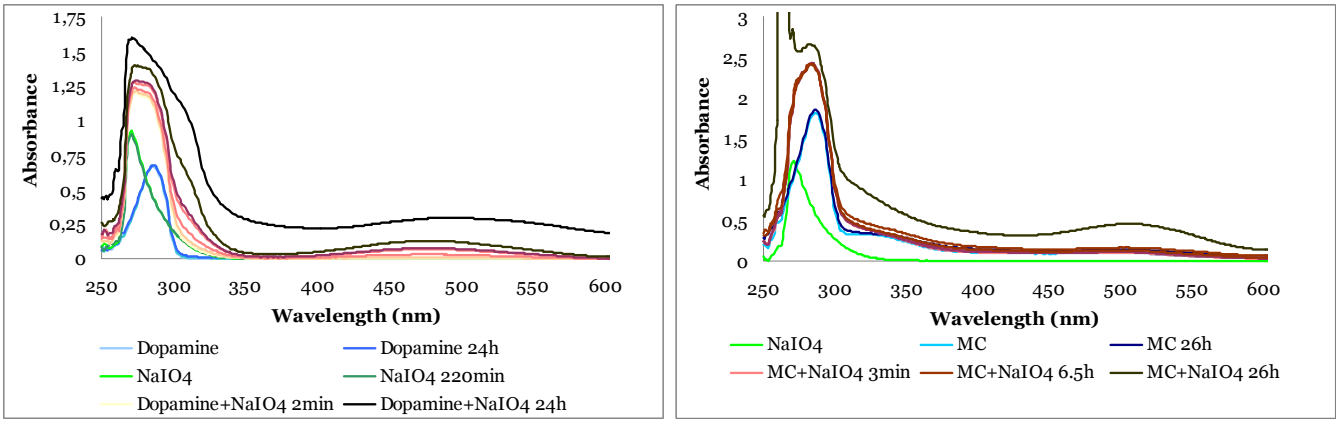

Figure 4.20: UV-Vis absorption spectra of dopamine-HCl (0.26 mM, left) and dopamine-pyrrole model compound (2 mM, right) oxidized by $NaIO_4$ (1.3 mM or 2 mM) in DMSO

The results of the experiments with $NaIO_4$ oxidized dopamine-modified polyketones (NaOH activated) are summarized in Figure 4.21. This graph has been constructed by subtracting the spectra from the oxidized samples at 26 h from that of the negative controls which did not contain $NaIO_4$. All samples displayed similar spectral changes, with those of higher dopamine-modification showing larger changes. The shoulder at 300 – 380 nm is again clearly present, suggesting the formation of α,β-dehydro intermediates [197]. No distinct absorption increases around 490 nm could be detected, but 25% and 50% dopamine-modified (aimed modification) did show the formation of a sharp peak at 270 nm in the spectrum between 6.5 h and 26h. This phenomenon was confirmed in duplo experiments, but it seems unjustified to unambiguously link it to dicatechol formation given the absence of a similar peak at 490 nm.

A photograph of the UV-Vis samples before and after oxidation is shown in Figure 4.22.

In summary, the dopamine-modified compounds have shown to be resistant to hydrogen peroxide oxidation but were easily oxidized by sodium periodate. Preliminary proton NMR and FT-IR ATR experiments have not been successful in identifying particular intermediates or oxidation mechanism, but UV-Vis spectroscopy has provided a strong case for the formation of α,β-dehydro intermediates. These intermediates have been shown to be instrumental in oxidative polymerization of *N*-Boc-protected PEG-DOPA polymers, similar to the cross-linking between *N*-acetyl-dopamine molecules [197].

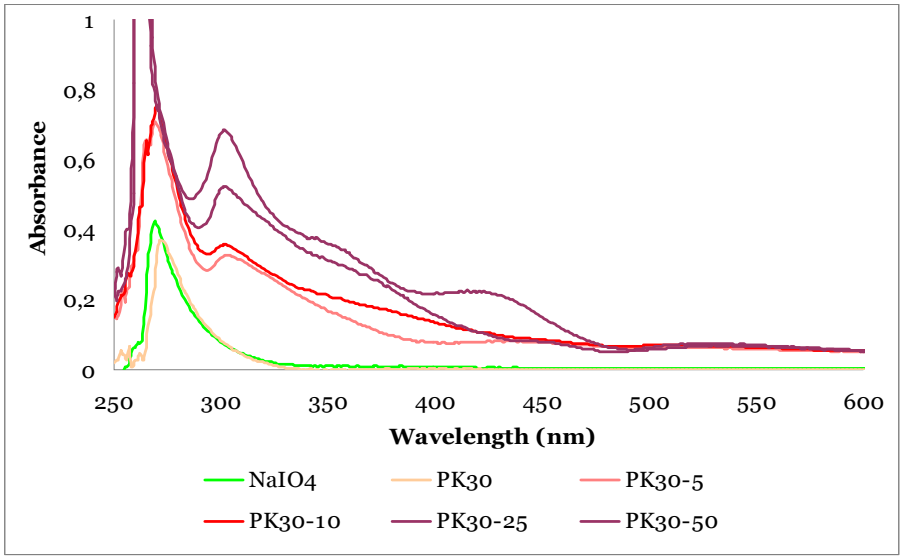

Figure 4.21: UV-Vis absorption spectra difference between $NaIO_4$ (1 mM) oxidized dopamine-modified polyketones (0.02 - 1 mM) and negative controls without oxidant in DMSO after 26h.

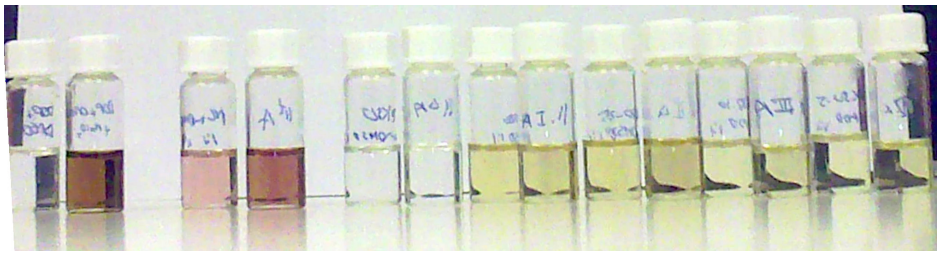

Figure 4.22: Photograph of UV-Vis samples before and after $NaIO_4$ oxidation. From left to right: dopamine-HCl, dopamine-pyrrolic model compound, PK30, PK30-5, PK30-10, PK30-25 and PK30-50

4.3.5 Biocompatibility analysis

The haemocompatibility of 25% dopamine-modified PK30 (aimed conversion, NaOH activated) was preliminary evaluated *in vitro* according to the ASTM F 756-00 protocol. A picture of one sample brought into contact with the blood, the positive control and the negative control is displayed in Figure 4.23. The haemoglobin released from the blood by haemolysis was measured by optical densities (OD) of the supernatants at 540 nm using a spectrophotometer UV-Vis. The percentage of haemolysis was determined from a triplicate and found to be 6.51 ± 0.12 through use of Equation 4.4.

According to ASTM F 756-00, haemolysis values (%) above negative controls of >5% are considered haemolytic (0 – 2 is non-haemolytic, 2 – 5 is slightly haemolytic) [250]. Although a blood-biocompatible material should be non-haemolytic by definition, values <7 are not very high and comparable to polyurethanes considered suitable for medical applications when subjected to additional purification (PBS incubation) [203]. Considering the fact that residual organic solvent (chloroform) could not be completely removed through use of the developed purification protocol (see section 4.3.3), it seems likely that a solvent-free dopamine-modified polymer could be considered

haemocompatible. It may therefore be worthwhile to further investigate if the developed materials can be used in a biomedical setting, such as proven for other polyketone-based materials [74,84].

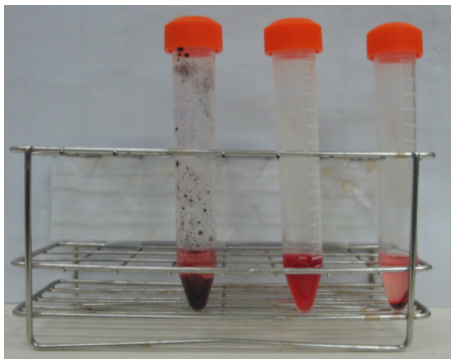

Figure 4.23: Photograph of haemocompatibility assay of 25% dopamine-modified PK30 (aimed conversion, NaOH activated) . From left to right: sample brought into contact with diluted rabbit blood, positive control from diluted blood and water and negative control from blood in PBS.

4.3.6 Adhesive bond strength measurements

Adhesive bond strength measurements were conducted according to a recently published procedure [251] by using aluminium adherends (5754) in a lap shear configuration (see Figure 4.24). Both dry and underwater bonding strengths were assessed of 25% dopamine-modified PK30 (NaOH and TEA activated) in the presence of either solvent alone, $Bu_4N(IO_4)$ or $Fe(acac)_3$ cross-linking solution. A negative control consisted of virgin PK30, which was tested in dry conditions. 25% tyramine-modified PK30 was tested with $Bu_4N(IO_4)$ under both wet and dry conditions. 25% dopamine-modified PK30 (TEA activated) was finally tested in the presence of either solvent alone, $Bu_4N(IO_4)$ or $Fe(acac)_3$ cross-linking solution underwater as well. The oxidant solutions delivered 0.3 equivalents of oxidant per catechol group present in the polymers and were partially chosen because of their solubility in the organic solvents tested [150,251]. The adhesive force for each assembly joint was obtained by dividing the maximum load (N) observed at bond failure by the area of the adhesive overlap (mm^2), resulting in the adhesive strength in Megapascals (MPa = N/mm^2). For each test, five samples were used and values are reported as an average with standard deviation.

The adhesive surface of dopamine-modified PK30s showed darkening discolouration upon the addition of cross-linker. This effect was absent when virgin PK30 or tyramine-modified PK30 was used. The results of the lap shear tests are displayed in Figure 4.25. All negative controls with PK30 failed before loading, as did all specimens tested under wet conditions. In the latter case, it was observed that the bubbles of chloroform containing the modified polymers were unable to spread the etched aluminium surface in artificial seawater. Most of the solution was subsequently displaced from the adherends upon the placement of the upper adherend. This may be the route cause for the lack of adhesive strength, given that the little material that remained on the surface did harden.

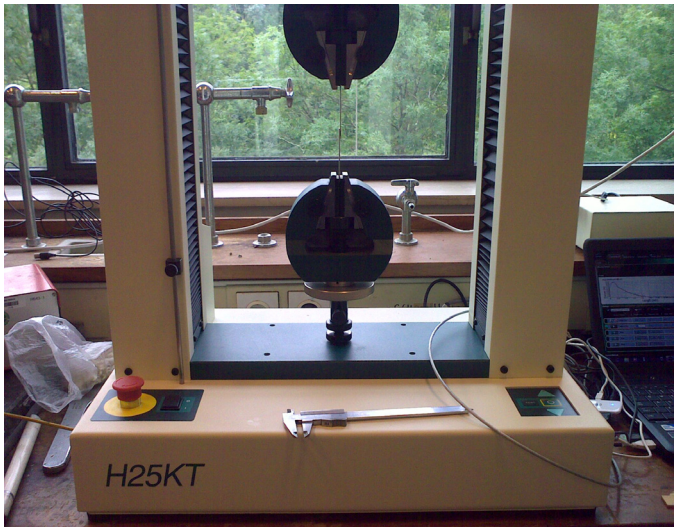

Figure 4.24: Adhesive testing set-up with aluminium adherends in lap shear configuration

Due to time constraints and the limited availability of the aluminium adherends, only one oxidant to catechol group ratio, one modification degree and only five samples were used per test. As clear from the results in Figure 4.25, the standard deviation in the lap shear experiments was very high for almost each sample set. Because lap shear sample sets are usually at least 10 specimens large (excluding the highest and lowest value for elimination from an original 12), it is highly recommended to expand the dataset in order to allow more specific conclusions. At this moment it can only be concluded that dopamine-and tyramine modified polyketones are able to build up significant adhesive bond strength on aluminium under dry conditions, whilst virgin PK30 cannot. Controls with only solvent instead of oxidant solution showed significantly lower adhesive strength in case of TEA activated dopamine-modified PK30, but that of the NaOH activated batch was unexpectedly high. Because the strong base had induced partial auto-oxidation of the material during synthesis (concluded from UV-Vis assay), the oxidized groups might have been able to cure by themselves to further extent under the curing conditions applied (dry, 55 °C).

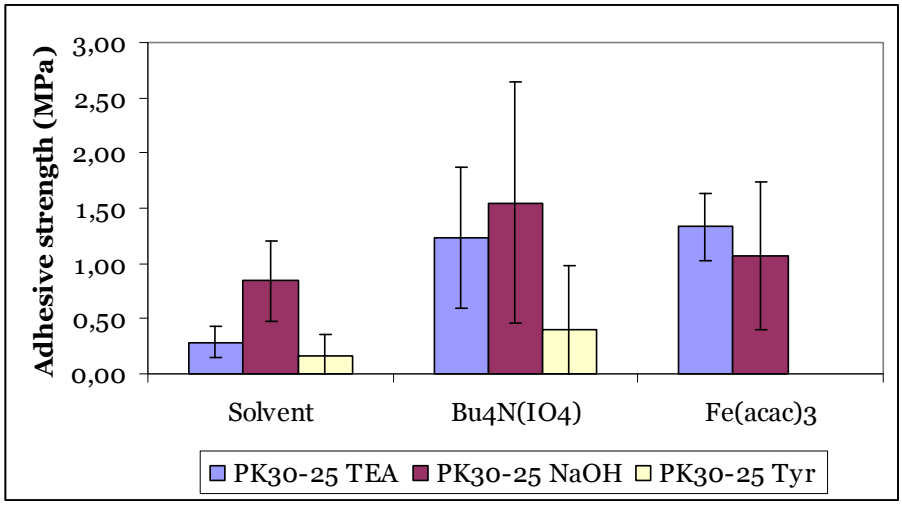

Figure 4.25: Adhesive bond strength data for dry testing of 25% dopamine- and tyramine-modified PK30 (NaOH and TEA activated).

Absolute adhesive strength values for 25% dopamine-modified PK30 lie between 0.5 and 3 MPa, which are comparable to the larger modified polystyrene molecules (10-16 kD vs 4 kD) tested earlier with the same protocol [150,251]. Detailed comparison with other types of adhesive (even on the same type of substrate) is not straightforward due to differences in formulation, cure, adherend preparation and measurement conditions. Moreover, such a comparison seems premature at this stage but will certainly follow in the near future when the dataset is expanded.

4.4 Conclusions

Can polyketone be used as a polymer backbone for acquiring a water-resistant adhesive which is inspired by aquatic organisms?

The most popular existing strategy applied to mimic the biochemistry of underwater adhesives from aquatic organisms has been to incorporate the multifunctional DOPA-catechol groups through use of dopamine. The experiments described in this chapter have shown that a particular type of alternating aliphatic polyketone could be successfully modified up to 45% conversion of the dicarbonyl units through Paal-Knorr chemistry with dopamine at reasonable yields (typically 50%). Activation of the dopamine-HCl salt was required by equimolar amounts of either triethylamine (TEA) or NaOH to successfully incorporate the salt in the presence of a weak protic acid catalyst from a methanol solution within 24h reaction time. UV-Vis analysis did indicate that partial oxidation occurred during synthesis when NaOH was applied.

The modified polymers were found to be non-water soluble, brown to black coloured and transitioned from viscous to solid at modification levels above 25%. The oxidants sodium periodate, tert-butylammonium periodate and iron(III) acetonyl acetone were found to be effective at cross-linking the dopamine-modified polyketones. UV-Vis analysis on modified PK30 suggested that α,β-dehydro intermediates played a key part in the curing mechanism. 25% Dopamine-modified polyketones obtained through both NaOH and TEA activation were effectively cured and use as an adhesive under dry conditions to yield adhesive bond strengths up to 3 MPa (lap shear). Unfortunately, all specimens tested under wet conditions failed to build up adhesive strength. This was most likely caused by failure of wetting the activated aluminium adherend surface from the chloroform delivery solution.

In summary, the results indicate that polyketones may indeed be used as a backbone material for acquiring the chemical catechol-functionalities known to be successful at attaining underwater adhesion in a relatively facile way. Although promising adhesive strengths have been attained under dry conditions, water-resistant adhesion has not yet been achieved successfully due to failure of adhesive spreading underwater.

5 General conclusion

Can alternating aliphatic polyketones be modified with dopamine and used subsequently as or in an effective water-resistant adhesive product that resembles the adhesion characteristics found in aquatic organisms and meets market requirements?

Overall, this report has described that the author has not yet been successful at achieving the ambitious goal of developing a novel polyketone-based adhesive that is inspired by aquatic organisms and attains water-resistant adhesive capabilities in such a way that it may be able to meet market requirements. The envisioned synthesis and cross-linking chemistry was successfully demonstrated and respectable dry adhesion strengths up to 3 MPa have been attained on aluminium adherends for the modified polymers. However, additional effort is required to push the concept further in order to be able to compete with existing commercial or proof-of-principle concepts. The next section details the author's recommendations for future research in this regard.

6 Recommendations for future research

Although [biomimetics] can strike a poetic cord in many, it is fraught with difficulty and controversy [54].

The general conclusion of the present work included the observation that the novel technology-push concept of modifying specific (patented) alternating aliphatic polyketones through Paal-Knorr chemistry with dopamine has been successful from a chemical point of view. However, the concept has not yet resulted in the development of a promising water-resistant adhesive product due to various reasons. Chemical, physical and engineering challenges remain to be addressed, as well as a reflection on how this work fits in with existing managerial literature on the development of chemical products within what is called chemical product engineering. Table 6.1 summarizes and prioritizes various recommendations for future research deemed necessary to advance at realizing the final goal put forward by the central research question in this work.

Table 6.1: Recommendations for future research

Domain	*Topic*	*Reference(s)*	*Priority level*
Chemistry	Additionally modify dopamine-modified polyketones with lysine, 1,2-diaminopropane or other diamines (simultaneous or sequential) to achieve polymer solubility in (acidic) water.	[96,144,218]	High
	Utilize different terpolymer polyketone types and of higher molecular weights to investigate reactivity and increase adhesion	[96,150]	Medium
	Incorporate p-serine and cysteine like molecules to mimic tubeworm coacervate adhesion	[114,115,119]	Low
	Implement protection-deprotection chemistry on dopamine-catechols during synthesis	[143,177,219]	Low
	Optimize tyramine-modification and assess adhesion capabilities upon enzymatic oxidation	[258][258]	Low
	Utilize laccase-mediated cross-linking chemistry for adhesive curing	[170, 186,214]	Low
	Assess the effect of the catechol-containing molecular compound structure on reactivity and adhesion (dopamine/DOPA/other)	[186]	Low
	Investigate oxidation chemistry of model compound and modified polyketones with advanced analytical techniques (e.g. Maldi-TOF, XPS, cyclic voltammetry)	[92,115,226]	Low
Biology	Assess biocompatibility (blood and/or cellular) of dopamine-modified polyketones at different modification degrees and purified to greater extent (freeze-dried, dialyzed, etc.)	[74,84,203]	High
	Assess biodegradability of modified polyketones	[72,84,138, 139,151,158]	Medium
Physics	Assess thermal stability (TGA) of modified polyketones		Medium
	Assess contact angles of various solvents on modified-polyketones to determine surface energies	[203]	Medium
	Assess contact angles of adhesive solutions on adherend substrates to determine surface wetting capabilities	[134,251]	Medium
	Assess oxidant effect on solution viscosities with brookfield viscometer or through storage and loss moduli with oscillatory rheometry	[91,186,196, 197]	Medium
Material science	Expand adhesive bond strength dataset to include 10 samples per test	[251]	Crucial
	Assess adhesive strength on different substrates, including biological.	[91,144]	Medium
	Assess fundamental adhesion of modified polymers through use of contact mechanics, membrane inflation, bulge/blister tests or other adhesive force testing methodology	[88,149,156, 182,183]	Low
	Assess other application areas for dopamine-modified polyketones such as multifunctional coatings and metal scavenger agents	[68,170,216, 259,260][259,260]	Low

(continued on next page)

(continued from previous page)

Formulation engineering	Test different concentration levels and different amounts of modified groups to maximize adhesion	[150]	High
	Test different ratios of catechol : oxidant to maximize adhesion	[91]	Medium
	Formulate dopamine-modified polyketones with surfactants (e.g. polymeric amines) to create water-based emulsions for adhesion delivery	[61,96]	Medium
	Replace virgin polyketones with different amounts of dopamine-modified polyketones and assess effect on water-resistant wood adhesion	[61]	Low
Chemical product engineering	Create a toolbox for developing aquatic-inspired adhesive products based on existing approaches and relevant parameters (chemical, structural, physical, biological and/or commercial)	[261][261]	High
	Expand on adhesive production processing implications based on chemical product development	[7,32,33]	Medium
	Establish chemical product pyramid for aquatic inspired adhesives by defining property, process and usage functions	[7]	Medium

Acknowledgements

A year of chemical engineering research at three different universities has been a rewarding experience in many aspects. The project has often resembled a roller-coaster ride of excitements and disappointments and has certainly never been dull. So much to do and to discover, but o so little time. Looking back, I have not made things easy for myself in terms of my experimental work and my stubbornness to try to understand everything from the literature which might be relevant. If all, I had to learn the importance of making choices, applying focus and not being too afraid of making mistakes. Many people are to thank and I hope the following list of people includes those who have been most instrumental.

First of all, I would like to thank professor *Ton Broekhuis* for the original research suggestion, the freedom to go abroad with the project and the patient supervision whilst I was working on it in Groningen. Next in line is *Raquel Costa*, from whom I owe so much for allowing me to visit Cambridge and Coimbra, keeping structure in the project and going through my drafts during it all. Likewise, I would like to thank *Geoff Moggridge* for his supervision whilst in Cambridge, it has truly been an inspiring time and place. For additional supervision and facilities when I needed them most, I would like to thank professors *Herminio Sousa* and *Francesco Picchioni*.

Doing a PhD and having to deal with ignorant master students now and then is probably a welcome break from doing a multi-year, headache-giving research project. Nevertheless, I still have to thank *Diego Wever, Claudio Toncelli, Arjan Kloekhorst, Jan-Willem Miel, Kyra Sedransk* and *Dina Marques* for their insightful assistance and cynicism. Especially *Diego* deserves many thanks for all the hours helping with NMR reservations, chemical ordering, deciphering obscure spectra, going through general product technology discussions and what not more.

From a financial point of view, I am very grateful for financial support from McKinsey, GUF and the University of Groningen (Marco Polo and Erasmus). *Geartsje Zondervan, Ali Nanning, Henk Hanson* and *Marijke Wiersema* are gratefully acknowledged for their administrative support in Groningen. *Linda Craft, Nigel Slater, Barrie Goddard, Vanessa Blake* and *Sarada Crowe* are thanked similarly for their support whilst in Cambridge.

From the labs I want to thank *Louis, Marcel, Piter,* and *Vincent* from Groningen*, Korakot*, *Stephen* and *James* from Cambridge, *Maria, Luisa, Pedro, Sofia* and *Patrícia* from Coimbra. For all the fun and social activities outside the labs I am especially grateful to *Victor*, *Adriano*, *Catherine*, *Will*, *Reinder*, *Vito*, *Jose*, *Carlos* and *Tiago*. An additional thank you to *Dina* and *Jose* for the Portuguese translation of my abstract; muito obrigado!

Last but not least I would like thank my parents deeply for their enthusiasm and support and *Marlies* for all her love, patience and personal support. I am forever in your debt.

References

[1] www.chemengworld.org, accessed 30 October 2010

[2] World Chemical Engineering Council (2004) *How Does Chemical Engineering Education Meet the Requirements of Employment?*, web source: www.chemengworld.org, accessed 30 October 2010

[3] Danckwerts, P.V. (1966) Science and chemical engineering, *Chem Eng*, 7, 155-159

[4] Mashelkar, R.A. (1995) Seamless chemical engineering science, C*hem Eng Sci*, 50, 1-22

[5] Wintermantel, K. (1999) Process and product engineering – achievements, present and future challenges, *Chem Eng Sci*, 54, 1601-1620

[6] Cussler, E.L., Moggridge, G.D. (2001) *Chemical Product Design*, Cambridge University Press

[7] Costa, R., Moggridge, G.D., Saraiva, P.M. (2006) Chemical Product Engineering: An Emerging Paradigm Within Chemical Engineering, *AIChE J*, 52, 1976-1986

[8] Moggridge, G.D., Cussler, E.L. (2000) An introduction to chemical product design, *Chem Eng Res Des*, 78, 5-11

[9] Saraiva, P.M., Costa, R. (2004) A chemical product design course with a quality focus, *Chem Eng Res Des*, 82, 1474–1484

[10] Wesselingh, J.A. (2001) Structuring of products and education of product engineers, *Powder Technol*, 119, 2-8

[11] Westerberg, A.W., Subrahmanian, E. (2000) Product design, *Comput Chem Eng*, 24, 959-966

[12] Cussler, E.L., Wei, J. (2003) Chemical product engineering, *AIChE J*, 49, 1072-1075

[13] Cobb, J.T., Burka, M., Cobb, C., Patterson, G., Schowalter, B., Self, F., Stephanopolous, G., Wechsler, A., Wei, J., Zagoria, A. (2008) *AIChE Centennial Chapter 24, How is the Marketplace Changing for Chemical Engineering?*

[14] Favre, E., Marchal-Heusler, L., Kind, M. (2002) Chemical product engineering: research and educational challenges, *Chem Eng Res Des*, 80, 65-74

[15] Kind, M. (1999) Product engineering, *Chem Eng Process*, 38, 405-410

[16] Voncken, R.M., Broekhuis, A.A., Heeres, H.J., Jonker, G.H. (2004) The many facets of product technology, *Chem Eng Res Des*, 82, 1411-1424

[17] Villadsen, J. (1997) Putting structure into chemical engineering: proceedings of an industry/university conference, *Chem Eng Sci*, 52, 2857-2864

[18] Charpentier, J.C., Trombouze, P. (1998) Process engineering and problems encountered by chemical and related industries in the near future. Revolution or continuity?, *Chem Eng Process*, 37, 559-565

[19] Villermaux, J. (1993) Future challenges of basic research in chemical engineering, *Chem Eng Sci*, 48, 2225-2235

[20] Villermaux, J. (1995) Future challenges in chemical engineering research, *Chem Eng Res Des*, 73, 105-109

[21] Grossmann, I.E. and Westerberg, A.W. (2000) Research challenges in process systems Engineering, *AIChE J*, 46, 1700-1703

[22] Charpentier, J. (2002) The triplet "molecular processes–product–process" engineering: the future of chemical engineering ?, *Chem Eng Sci,* 57, 4667-4690

[23] Kontogeorgis, G., Gani, R. (2004) *Computer aided property estimation for process and product design*, Elsevier

[24] Korevaar, G. (2004) *Sustainable chemical processes and products: new design methodologies and design tools*, Eburon

[25] Wei, J. (2006) *Product engineering: molecular structure and properties*, Oxford University Press

[26] Ng, K.M., Gani, R., Dam-Johansen, K. (2007) *Chemical product design: toward a perspective through case studies,* Elsevier

[27] Wesselingh, J.A., Kiil, S., Vigild, M.E (2007) *Design and development of biological, chemical, food and pharmaceutical product*, Wiley

[28] Bröckel, U., Meier, W., Wagner, G. (2007*) Product design and engineering*, Wiley

[29] Avramenko, Y., Kraslawski, A. (2008) *Case based design: applications in process engineering*, Springer

[30] Seider, W.D., Seader, J.D., Lewin, D.R (2010) *Product and process design principles: synthesis, analysis, and evaluation*, Wiley

[31] Churchill, S.W. (2007) Role of Universalities in Chemical Engineering, *Ind Chem Eng Res*, 46, 7851-7869

[32] Bernardo, F.P., Saraiva, P.M. (2005) Integrated process and product design optimization: a cosmetic emulsion application, *Comp Aid Chem Eng*, 20, 1507-1515

[33] Wibowo, C., Ng, K.M (2002) Product-centered processing: manufacture of chemical-based consumer products, *AIChE J*, 48, 1212-1230

[34] Rahse, W., Hoffmann S. (2003) Product Design - Interaction between chemistry, technology and marketing to meet customer needs, *Chem Eng Technol*, 26, 931-940

[35] (a) Hill, M. (2004) Product and process design for structured products, *AIChE J*, 50, 1656-1661 (b) Hill, M. (2009) Chemical product engineering – the third paradigm, *Comput Chem Eng*, 33, 947-953

[36] Gani, R. (2004) Chemical product design: challenges and opportunities, *Comput Chem Eng*, 28, 2441-2457

[37] (a) Bagajewicz, M.J. (2007) On the role of microeconomics, planning, and finances in product design, *AIChE J*, 53, 3155-3170 (b) Street, C., Woody, J., Ardilla, J., Bagajewicz, M. (2008) Product design: a case study of slow-release carpet deodorizers/desinfectants, *Ind Chem Eng Des*, 47, 1192-1200 (c) Whitnack, C., Heller, A., Frow, M.T., Kerr, S., Bagajewicz, M.J. (2009) Financial risk management in the design of products under uncertainty, *Comput Chem Eng*, 33, 1056-1066

[38] Seider, W.D., Widagdo, S., Seader, J.D., Lewin, D.R. (2009) Perspectives on chemical product and process design, *Comput Chem Eng*, 33, 930-935

[39] (a) Smith, B.V., Ierapetritou, M. (2009) Framework for consumer-integrated optimal product design, *Ind Chem Eng Res*, 48, 8566-8574 (b) Smith, B.V., Ierapepritou, M.G. (2010) Integrative chemical product design strategies: reflecting industry trends and challenges, *Comput Chem Eng*, 34, 857-865

[40] Pocius, A.V. (2008) Adhesive, *AccessScience*

[41] Pocius, A., Campbell, C. J. (2009) Adhesives, *Kirk-Othmer Encyclopedia of Chemical Technology*, 1–26

[42] www.prweb.com/releases/adhesives/sealants/prweb4652884.htm, accessed 4 November 2010

[43] Barash, M., Reshef, A., Brauner, P. (2010) The use of adhesive tape for the recovery of DNA from crime scene items, *J Forensic Sci*, 55, 1058-1064

[44] Sugita, Y., Winkelmann, C., La Saponara, V. (2010) Environmental and chemical degradation of carbon/epoxy lap joints for aerospace applications, and effects on their mechanical performance, *Compos Sci Technol*, 7, 829-839

[45] Boehm, R.D., Gittard, S.D., Byrne J.M.H., Doraiswamy, A ., Wilker J.J., Dunaway, T.M., Crombez, R., Shen, W.D., Lee, Y.S., Narayan, R.J. (2010) Piezoelectric inkjet printing of medical adhesives and sealants, *JOM*, 62, 56-60

[46] Kusumgar, M. (2011) *The global formulated adhesives market*, web source: http://www.adhesivesmag.com/Articles/Feature_Article/BNP_GUID_9-5-2006_A_1000000000000964465, accessed 14 February 2011

[47] Packham, D.E. (2009) Adhesive technology and sustainability, *Int J Adhes Adhes*, 29, 248-252

[48] Global Industry Analysts Inc. (2010) *Adhesives and sealants – a global strategic business report,* web source: www.strategyr.com/Adhesives_and_Sealants_Market_Report.asp, accessed 4 November 2010

[49] Graham, L.D. (2008) Biological adhesives from nature, *Encyclopedia of Biomaterials and Biomedical Engineering*, 1, 236-253

[50] Silverman, H.G., Roberto, F.F. (2007) Understanding marine mussel adhesion, *Mar Biotechnol*, 9, 661-681

[51] http://en.wikipedia.org/wiki/Bioadhesive, accessed 06 November 2010

[52] Smart, J.D. (2008) Bioadhesion, *Encyclopedia of Biomaterials and Biomedical Engineering*, 1, 152-161

[53] Wiegemann, M. (2005) Adhesion in blue mussels (Mytilus edulis) and barnacles (genus Balanus): Mechanisms and technical applications, *Aquat Sci*, 67, 166–176

[54] Waite, J.H., Andersen, N.H., Jewhurst, S., Sun, C. (2005) Mussel adhesion: finding the tricks worth mimicking, *J Adhesion*, 81, 297-317

[55] Liu, K., Yao, X., Jiang, L. (2010) Recent developments in bio-inspired special wettability, *Chem Soc Rev*, 39, 3240–3255

[56] Gebeshuber, I.C., Drack, M. (2008) An attempt to reveal synergies between biology and mechanical engineering, *J Mech Eng Sci*, 222, 1281-1287

[57] Jung, Y.C., Bhushan, B. (2010) Biomimetic structures for fluid drag reduction in laminar and turbulent flows, *J Phys-Condens Mat*, 22, 1-9

[58] Stewart, R. J. (2011) Protein-based underwater adhesives and the prospects for their biotechnological production, *Appl Microbiol Biotechnol*, 89, 27-33

[59] Smith, A.M., Callow, J.A. (2006) *Biological adhesives*, Springer

[60] Von Byern, J., Grunwald, I. (2010) *Biological Adhesive Systems*, Springer

[61] Zhang, Y., Broekhuis, A.A., Picchioni, F. (2007) Aqueous polymer emulsions by chemical modifications of thermosetting alternating polyketones, *J Appl Polym Sci*, 106, 3237-3247

[62] Hamarneh, A.I., Heeres, H.J., Broekhuis, A.A., Sjollema, K.A., Zhang, Y., Picchioni, F. (2010) Use of soy proteins in polyketone-based wood adhesives, *Int J Adhes Adhes*, 30, 626-635

[63] Dintses, D.I. (1939) Title unknown, *Byull Vses Khim O-va im D.I. Mendeleeva*, 10, 31

[64] Ballauf, F., Bayer, O., Leichmann, L. (1941) Verfahren zur Herstellung von hohermolekularen Additionsprodukten aus niederen Olefinen und Kohlenoxyd, DE 863711

[65] Reppe, W., Magin, A. (1951) Production of ketonic bodies, US 2577208

[66] Drent, E., Budzelaar, P.H.M (1996) Palladium-catalyzed alternating copolymerization of alkenes and carbon monoxide, *Chem Rev*, 96, 663-681

[67] Sommazzi, A., Garbassi, F. (1997) Olefin-carbon Monoxide Copolymers, *Prog Polym Sci*, 11, 1547-1605

[68] Bianchini, C., Meli, A. (2002) Alternating copolymerization of carbon monoxide and olefins by single-site metal catalysis, *Coord Chem Rev*, 225, 35-66

[69] (a) Foullerat, D.P. (2005) *Further developments on polymers from olefins and carbon monoxide. Studies on the synthesis and material properties of novel 1,4-polyketone structures*, PhD Thesis, University Ulm (b) Malinova, V. (2006) *Synthesis of novel functional poly(1,4-ketone)s bearing pendant bioactive moieties: An approach to design biocompatible materials*, PhD Thesis, University Ulm (c) Zhang, Y. (2008) *Chemical modifications and applications of alternating aliphatic polyketones*, PhD Thesis, University of Groningen

[70] Sen, A. (1993) Mechanistic aspects of metal-catalyzed alternating copolymerization of olefins with carbon monoxide, *Acc Chem Res*, 26, 303-310

[71] Guillet, J. (1985) *Polymer Photophysics* and *photochemistry*, Cambridge University Press, 261

[72] Sen, A. (1986) The copolymerization of carbon-monoxide with olefins, *Adv Polym Sci*, 73-74, 125-144

[73] Müller, G., Rieger, B. (2002) Propene based thermoplastic elastomer by early and late transition metal catalysis, Prog Polym Sci, 27, 815-851

[74] (a) Reuter, P., Fuhrmann, R., Mucke, A., Voegele, J., Rieger, B., Franke, R.P. (2003) CO/alkene copolymers as a promising class of biocompatible materials, 1 - Examination of the in vitro toxicity, *Macromol Biosci*, 3, 123-130 (b) Röhlke, W., Fuhrmann, R., Franke, R.P., Mucke, A., Voegel, J., Rieger, B. (2003) CO/alkene copolymers as a promising class of biocompatible materials, 2 - Bone growth directed performance of bone marrow cell spreading, *Macromol Biosci*, 3, 131-135

[75] Sen, A., Jiang, Z.Z., Chen, J.T. (1989) Novel nitrogen-containing heterocyclic polymers derived from the alternating ethylene-carbon monoxide copolymer, *Macromolecules*, 22, 2012-2014

[76] Kinneberg, P.A., Armer, T.A., Van Breen, A.W., Barton, R.E.C., Klei, E. (1989) Polyketone-based structural adhesive, US 4880904

[77] Krutzel, L. (1995) Hot melt adhesive compositions comprising low molecular weight ethylene copolymers, US 5391434

[78] Hefner, J.G., Robeson, L.M. (2001) Hot melt adhesives produced from linear alternating polyketones, US 6239250 B1

[79] Patil, A.O., Schulz, D.N., Matturro, M.G., Schlosberg, R.H. (2004) Use of carbon monoxide containing polymers as, adhesives additives, and fluids, US 6677279 B2

[80] Wang, P.C., Wong, P.K., Pace, A.R., Weber, R.C. (1999) Water soluble polyketones, US 5955563

[81] Broekhuis, A.A., Freriks, F. (1999) Polymeric amines, US 5952459

[82] Drent, E., Broekhove, J.A.M., Doyle, M.J. (1991) Efficient palladium catalysts for the copolymerization of carbon monoxide with olefins to produce perfectly alternating polyketones, *J Organom Chem*, 417, 235-251

[83] Mul, W.P., Dirkzwager, H. Broekhuis, A.A., Heeres, H.J., Van der Linden, A.J., Orpen, A.G. (2002) Highly active, recyclable catalyst for the manufacture of viscous, low molecular weight, CO–ethene–propene-based polyketone, base component for a new class of resins, *Inorg Chim Acta*, 147-159

[84] Bartsch, G.C., Malinova, V., Volkmer, B.E., Hautmann, R.E., Rieger, B. (2006) CO-alkene polymers are biocompatible scaffolds for primary urothelial cells in vitro and in vivo, *BJU Int*, 99, 447-453

[85] Malinova, V., Rieger, B. (2005) A catalytic approach to functional poly(1,4-ketone)s bearing pendant monosaccharide fragments, *Macromol Rapid Commun*, 26, 945-949

[86] Malinova, V., Rieger, B. (2006) Synthesis of functional poly(1,4-ketone)s bearing bioactive moieties by Pd-catalyzed insertion polymerization, *Biomacromolecules*, 7, 2931-2936

[87] Tatehata, H., Mochizuki, A., Kawashima, T., Yamashita, S., Yamamoto, H. (2000) Model polypeptide of mussel adhesive protein. I. Synthesis and adhesive studies of sequential polypeptides (X-Tyr-Lys)n and (Y-Lys)n, *J Appl Polym Sci*, 76, 929–937

[88] Shull, K.R., Guvendiren, M., Messersmith, P.B., Lee, B.P. (2010) Modified acrylic block copolymers for hydrogels and pressure sensitive wet adhesives, US 7732539 B2

[89] Brubaker, C.E., Kissler, H., Wang, L.J., Kaufman, D.B., Messersmith, P.B. (2010) Biological performance of mussel-inspired adhesive in extrahepatic islet transplantation, Biomaterials, 31, 420-427

[90] Burzio, L.O., Burzio, V.A., Silva, T., Burzio, L.A., Pardo, J. (1997) Environmental bioadhesion: themes and applications, *Curr Opin Biotech*, 8, 309-312

[91] Yu, M., Deming, T.J. (1998) Synthetic polypeptide mimics of marine adhesives, *Macromolecules*, 31, 4739-4745

[92] Yu, M., Hwang, J., Deming, T.J. (1999) Role of L-3,4-dihydroxyphenylalanine in mussel adhesive proteins, *J Am Chem Soc*, 121, 5825-5826

[93] Sun, C.J., Waite, J.H. (2005) Mapping chemical gradients within and along a fibrous structural tissue, mussel byssal threads, *J Biol Chem*, 280, 39332-39336

[94] Brooksby, P.A., Schiel, D.R., Abell, A.D. (2008) Electrochemistry of catechol terminated monolayers with Cu(II), Ni(II) and Fe(III) cations: a model for the marine adhesive interface, *Langmuir*, 24, 9074-9081

[95] Kostyanovsky, R.G., Kadorkina, G.K., Mkhitaryan, A.G., Chervin, I.I., Aliev, A.E. (1993) New scope and limitations in the Knorr-Paal synthesis of pyrroles, *Mendeleev Commun*, 3, 22-24

[96] Zhang, Y., Broekhuis, A.A., Stuart, M.C.A., Picchioni, F. (2008) Polymeric amines by chemical modifications of alternating aliphatic polyketones, *J Appl Polym Sci*, 107, 262-271

[97] Pocius, A.V., (2002) Adhesion. *Kirk-Othmer Encyclopedia of Chemical Technology*, 501-524

[98] Waite, J.H. (1987) Nature's underwater adhesive specialist, *International Journal of Adhesion and Adhesives*, 7, 9-14

[99] Smith, D.C. (1996) Adhesives and sealants, *Biomaterials Science: An Introduction to Materials in Medicine*, Academic Press, 319-328

[100] Peppas, N.A., Sahlin, J.J. (1996) Hydrogels as mucoadhesive and bioadhesive materials: a review, *Biomaterials*, 17, 1553-1561

[101] Aldred, N., Ista, L.K., Callow, M.E., Callow, J.A., Lopez, G.P., Clare, A.S. (2006) Mussel (*Mytilus edulis*) byssus deposition in response to variations in surface wettability, *J R Soc Interface*, 3, 37-43

[102] Grunwald, I., Rischka, K., Kast, S.M., Scheibel, T., Bargel, H. (2009) Mimicking biopolymers on a molecular scale: nano(bio)technology based on engineered proteins, *Phil. Trans. R. Soc. A*, 367, 1727-1747

[103] Kamino, K. (2008) Underwater adhesive of marine organisms as the vital link between biological science and material science, *Mat Biotechnol*, 10, 111-121

[104] Wilker, J.J. (2010) Marine bioinorganic materials: mussels pumping iron, *Curr Opin Chem Biol*, 14, 276-283

[105] Burkett, J.R., Wojtas, J.L. , Cloud, J.L., Wilker, J.J. (2009) A method for measuring the adhesion strength of marine mussels, *The Journal of Adhesion*, 85, 601-615

[106] Bitton, R., Bianco-Peled, H. (2008) Novel biomimetic adhesives based on algae glue, *Macromol Biosci*, 8, 393-400

[107] Bitton, R., Josef, E., Shimshelashvili, I., Shapira, K., Seliktar, D., Bianco-Peled, H. (2009) Phloroglucinol-based biomimetic adhesives for medical applications, *Acta Biomaterialia*, 5, 1582-1587

[108] Burkett, J.R., Hight, L.M., Kenny, P., Wilker, J.J. (2010) Oysters produce an organic-inorganic adhesive for intertidal reef construction, *J Am Chem Soc*, 132, 12531-12533

[109] Flammang, P., Michel, A., Van Cauwenberge, A., Alexandre, H., Jangoux, M. (1998) A study of the temporary adhesion of the podia in the sea star *Asterias rubens* (Echinodermata, Asteroidea) through their footprints, *J Exp Biol*, 201, 2383-2395

[110] Hennebert, E., Haesaerts, D., Dubois, P., Flammang, P. (2010) Evaluation of the different forces brought into play during tube foot activities in sea stars, *J Exp Biol*, 213, 1162-1174

[111] Hennebert, E., Viville, P., Lazzaroni, R., Flammang, P. (2008) Micro- and nanostructure of the adhesive material secreted by the tube feet of the sea star *Asterias rubens*, *J Struct Biol*, 164, 108-118

[112] Kamino, K. (2010) Molecular design of barnacle cement in comparison with those of mussel and tubeworm, *J Adhes*, 86, 96-110

[113] Jensen, R.A., Morse, D.E. (1988) The bioadhesive of *Phragmatopoma californica* tubes: a silk-like cement containing L-DOPA, *J Comp Physiol B*, 158, 317-324

[114] Stewart, R.J., Weaver, J.C., Morse, D.E., Waite, J.H. (2004) The tube cement of *Phragmatopoma californica*: a solid foam, *J Exp Biol*, 207, 4727-4734

[115] Zhao, H., Sun, C., Stewart, R.J., Waite, J.H. (2005) Cement Proteins of the Tube-building Polychaete *Phragmatopoma californica*, *J Biol Chem*, 280, 42938-42944,

[116] Sun, C.J., Srivastava, A., Reifert, J.R., Waite, J.H. (2009) Halogenated DOPA in a marine adhesive protein, *J Adhes*, 85, 126-138

[117] Fournier, J., Etienne, S., Le Cam, J-B. (2010) Inter- and intraspecific variability in the chemical composition of the mineral phase of cements from several tube-building polychaetes, *Geobios*, 43, 191-200

[118] Endrizzi, B.J., Stewart, R.J. Glueomics: an expression survey of the adhesive gland of the sandcastle worm, *J Adhes*, 85, 546-559

[119] Stevens, M.J., Steren, R.E., Hlady, V., Stewart, R.J. (2007) Multiscale structure of the underwater adhesive of *Phragmatopoma californica*: a nanostructured latex with a steep microporosity gradient, *Langmuir*, 23, 5045-5049

[120] Le Cam, J-B., Fournier, J., Etienne, S., Couden, J. (2011) The strength of biogenic sand reefs: Visco-elastic behaviour of cement secreted by the tube building polychaete *Sabellaria alveolata*, Linnaeus, 1767, *Estuar Coast Shelf S*, 91, 333-339

[121] Waite, J.H. (2002) *Adhesion à la Moule*, *Integr Comp Biol*, 42, 1172-1180

[122] Holten-Andersen, N., Waite, J.H. (2008) Mussel-designed protective coatings for compliant substrates, *J Dent Res*, 87, 701

[123] Urushida, Y., Nakano, M., Matsuda, S., Inoue, N., Kanai, S., Kitamura, N., Nishino, T., Kamino, K. (2007) Identification and functional characterization of a novel barnacle cement protein, *FEBS J*, 274, 4336-4346

[124] Walker, G. (1971) A study of the cement apparatus of the cypris larva of the barnacle *Balanus balanoides*, *Mar Biol*, 9, 205-212

[125] Waite, J.H., Jensen, R., Morse, D.E. (1992) Cement precursor proteins of the reef-building polychaete *Phragmatopoma californica* (Fewkes), *Biochemistry*, 31, 5733-5738

[126] Lee, H., Schrer, N.F., Messersmith, P.B. (2006) Single-molecule mechanics of mussel adhesion, *PNAS*, 103, 12999-13003

[127] Flammang, P., Lambert, A., Bailly, P., Hennebert, E. (2009) Polyphosphoprotein-containing marine adhesives, *J Adhes*, 85, 447-464

[128] Xu, W., Faisal, M. (2009) Development of a cDNA microarray of zebra mussel (*Dreissena polymorpha*) foot and its use in understanding the early stage of underwater adhesion, *Gene*, 436, 71-80

[129] Brazee, S.L., Carrington, E. (2006) Interspecific comparison of the mechanical properties of mussel byssus, *Biol Bull*, 211, 263-274

[130] Waite, J.H., Tanzer, M.L., Polyphenolic substance of *Mytilus edulis*: novel adhesive containing L-DOPA and hydroxyproline, *Science*, 212, 1038-1040

[131] Sever, M.J., Weisser, J.T., Monahan, J., Srinivasan, S., Wilker, J.J. (2004) Metal-mediated cross-linking in the generation of a marine-mussel adhesive, *Angew Chem Int Ed*, 43, 447-450

[132] Harrington, M.J., Masic, A., Holten-Anderson, N., Waite, J.H., Fratzl, P. (2010) Iron-clad fibers: a metal-based biological strategy for hard flexible coating, *Science*, 328, 216-220

[133] Zeng, H., Hwang, D.S., Israelachvili, J.N., Waite, J.H. (2010) Strong reversible Fe^{3+}-mediated bridging between dopa-containing protein films in water, *PNAS*, 107, 12850-12853

[134] Callow, J.A., Callow, M.E., Ista, L.K., Lopez, G., Chaudhury, M.K. (2005) The influence of surface energy on the wetting behaviour of the spore adhesive of the marine alga *Ulva linza* (synonym Enteromorpha linza), *J R Soc Interface*, 2, 319-325

[135] Carrington, E. (2002) The ecomechanics of mussel attachment: from molecules to ecosystems, *Integrative and Comparative Biology*, 42, 846-852

[136] Carrington, E., Gosline, J.M. (2004) Mechanical design of mussel byssus: load cycle and strain rate dependence, *American Malacological Bulletin*, 18, 135-142

[137] Dodou, D., Breedveld, P., de Winter, J.C.F., Dankelman, J., van Leeuwen, J.L. (2011) Mechanisms of temporary adhesion in benthic animals, *Biol Rev*, 86, 15-32

[138] Hoffmann, B., Volkmer, E., Kokott, A., Augat, P., Ohnmacht, M., Sedlmayr, N., Schieker, M., Claes, L., Mutschler, W., Ziegler, G. (2009) Characterisation of a new bioadhesive system based on polysaccharides with the potential to be used as bone glue, *J Mater Sci: Mater Med*, 20, 2001-2009

[139] Ninan, L., Monahan, J., Stroshine, R.L., Wilker, J.J., Shi, R. (2003) Adhesive strength of marine mussel extracts on porcine skin, *Biomaterials*, 24, 4091-4099

[140] Ninan, L., Stroshine, R.L., Wilker, J.J., Shi, R. (2007) Adhesive strength and curing rate of marine mussel protein extracts on porcine small intestinal submucosa, *Acta Biomaterialia*, 3, 687-694

[141] Liu, Y., Li, K. (2002) Chemical modification of soy protein for wood adhesives, *Macromol Rapid Commun*, 23, 739-742

[142] Liu, Y., Li, K. (2004) Modification of soy proteins for wood adhesives using mussel protein as a model: the influence of a mercapto group, *Macromol Rapid Commun*, 1835-1838

[143] Li, K., Liu, Y. (2008) Modified protein adhesives and lignocellulosic composites made from the adhesives, US 7393930 B2

[144] Wang, J., Liu, C., Lu, X., Yin, M. (2007) Co-polypeptides of 3,4-dihydroxyphenylalanine and L-lysine to mimic marine adhesive protein, *Biomaterials*, 28, 3456-3468

[145] Yamamoto, H., Sakai, Y., Ohkawa, K. (2000) Synthesis and wettability characteristics of model adhesive protein sequences inspired by a marine mussel, *Biomacromolecules*, 1, 543-551

[146] Yamada, K., Chen, T., Kumar, G., Vesnovsky, O., Topoleski, L.D.T., Payne, G.F. (2000) Chitosan based water-resistant adhesive. Analogy to mussel glue, *Biomacromolecules*, 1, 252-258

[147] Noto, K., Matsumoto, S., Takahasi, Y., Hirati, M., Yamada, K. (2009) Adhesion of surface-grafted low-density polyethylene plates with enzymatically modified chitosan solutions, *J Appl Polym Sci*, 113, 3963-3971

[148] Lee, B.P., Huang, K., Nunalee, F.N., Shull, K.R., Messersmith, P.B. (2004) Synthesis of 3,4-dihydroxyphenylalanine (DOPA) containing monomers and their co-polymerization with PEG-diacrylate to form hydrogels, *J Biomater Sci Polymer Edn*, 15, 449-464

[149] Lee, B.P., Chao, C.Y., Nunalee, F.N., Motan, E., Shull, K.R., Messersmith, P.B. (2006) Rapid gel formation and adhesion in photocurable and biodegredable block copolymers with high DOPA content, *Macromolecules* 39, 1740-1748

[150] Westwood, G., Horton, T.N., Wilker, J.J. (2007) Simplified polymer mimics of cross-linking adhesive proteins, *Macromolecules*, 40, 3960-3964

[151] Murphy, J.L., Vollenweider, L., Xu, F., Lee, B.P. (2010) Adhesive performance of biomimetic adhesive-coated biologic scaffolds, *Biomacromolecules*, 11, 2976-2984

[152] Suzuku, S., Ikada, Y. (2010) Adhesion of cells and tissues to bioabsorbable polymeric materials: scaffolds, surgical tissue adhesives and anti-adhesive materials, *J Adhes Sci Technol*, 24, 2059-2077

[153] (a) Spotnitz, W.D., Burks, S. (2010) State-of-the-art review: hemostats, sealants, and adhesives II: update as well as how and when to use the components of the surgical toolbox, *Clin Appl Thromb Hemost*, 16, 497-514 (b) Spotnitz, W.D., Burks, S. (2010) State-of-the-art review: hemostats, sealants, and adhesives II: update as well as

how and when to use the components of the surgical toolbox (vol 16, pg 497, 2010), *Clin Appl Thromb Hemost*, 17, 713

[154] Shao, H., Bachus, K.N., Stewart, R.J. (2009) A water-borne adhesive modeled after the sandcastle glue of *P. californica*, *Macromol Biosci,* 9, 464-471

[155] Coulthard, P., Esposito, M., Worthington, H.V., Van der Elst, M., Van Waes, O.J.F., Darcey, J. (2010) Tissue adhesives for closure of surgical incisions (Review), *Cochrane Db Syst Rev*, 5, 1-47

[156] Perrin, B.R.M., Dupeux, M., Tozzi, P., Delay, D., Gersbach, P., Von Segesser, L.K. (2009) Surgical glues: are they really adhesive?, *Eur J Cardiothorac Surg*, 36, 967-972

[157] Perrin, B.R.M., Braccini, M., Dupeux, M., Von Segesser, L.K. (2010) Reply to Dragu et al., *Eur J Cardiothorac Surg*, 37, 985-986

[158] Hsu, S.-h., Lin, C.-H. (2007) The properties of gelatin–poly (γ-glutamic acid) hydrogels as biological glues, *Biorheology*, 44, 17-28

[159] Hwang, D.S., Gim, Y., Yoo, H.J., Cha, H.J. (2007) Practical recombinant hybrid mussel bioadhesive fp-151, *Biomaterials*, 28, 3560-3568

[160] Deming, T.J. (2007) Synthetic polypeptides for biomedical applications, *Prog Polym Sci*, 32, 858-875

[161] Cha, H.J., Hwang, D.S., Lim, S. (2008) Development of bioadhesives from marine mussels, *Biotechnol J*, 3, 631-638

[162] Mori, Y., Urushida, Y., Nakano, M., Uchiyama, S., Kamino, K. (2007) Calcite-specific coupling protein in barnacle underwater cement, *FEBS J*, 274, 6436-6446

[163] Kaplan, D.L. Gatenholm, P., Berglin, M., Platko, J.D., Pepper, L.R., Ngangan, A.V. (2003) Barnacle adhesion proteins, WO 03/093413 A2

[164] Qvist, M. (2004) Use of an acidic aqueous solution of a bioadhesive polyphenolic protein as an adhesive or coating, WO 2004/005421

[165] Qvist, M. (2007) Method and kit providing bioadhesive binding or coating with polyphenolic mussel proteins, US 7303646 B2

[166] Qvist, M. (2008) Method for attaching two surfaces to each other using a bioadhesive polyphenolic protein and periodate ions, US 7393926 B2

[167] Qvist, M., Hansson, H.A. (2007) New bioadhesive composition comprising a bioadhesive polyphenolic protein, a polymer comprising carbohydrate groups, pharmaceutically acceptable fine filaments and uses thereof, EP 1589088 B1

[168] Cha H.J., Hwang, D.S., Lim, S., White, J.D., Matos-Perez, C.R., Wilker, J.J. (2009) Bulk adhesive strength of recombinant hybrid mussel adhesive protein, *Biofouling*, 25, 99-107

[169] Lim, S., Choi, Y.S., Kang, D. G., Song, Y.H., Cha, H. J. (2010) The adhesive properties of coacervated recombinant hybrid mussel adhesive proteins, *Biomaterials*, 31, 3715-3722

[170] Mikolasch, A., Hahn, V., Manda, K., Pump, J., Illas, N., Gördes, D., Lalk, M., Salazar, M.G., Hammer, E., Jülich, W.-D., Rawer, S., Thurow, K., Lindequist, U., Schauer, F. (2010) Laccase-catalyzed cross-linking of amino acids and peptides with dihydroxylated aromatic compounds, *Amino Acids*, 39, 671-683

[171] Burzio, L.A., Waite, J.H. (2000) Cross-linking in adhesive quinoproteins: studies with model decapeptides, *Biochemistry-US*, 39, 11147-11153

[172] Anderson, T.H., Yu, J., Estrada, A., Hammer, M.U., Waite, J.H., Israelachvili, J.N. (2010) The contribution of DOPA to subtrate-peptide adhesion and internal cohesion of mussel-inspired synthetic peptide films, *Adv Funct Mater*, 20, 4196-4205

[173] Deming, T.J., Yu, M. (2003) Synthesis and crosslinking of catechol containing copolypeptides, US 6506577 B1

[174] Ohkawa, K., Nagai, T., Nishida, A., Yamamoto, H. (2009) Purification of DOPA-containing foot proteins from green mussel, Perna viridian, and adhesive properties of synthetic model copolypeptides, *J Adhes*, 85, 770-791

[175] Glass, P., Chung, H., Washburn, N.R., Sitti, M. (2009) Enhanced reversible adhesion of dopamine methacrylamide-coated elastomer microfibrillar structures under wet conditions, *Langmuir*, 25, 6607-6612

[176] Glass, P., Chung, H., Washburn, N.R., Sitti, M. (2010) Enhanced wet adhesion and shear of elastomeric micro-fiber arrays with mushroom tip geometry and a photopolymerized p(DMA-co-MEA) tip coating, *Langmuir*, 26, 17357-17362

[177] Chung, H., Glass, P., Pothen, J.M., Sitti, M., Washburn, N.R. (2011) Enhanched adhesion of dopamine methacrylamide elastomers via viscoelasticity tuning, *Biomacromolecules*, 12, 342-347

[178] Lee, H., Lee, B.P., Messersmith, P.B. (2007) A reversible wet/dry adhesive inspired by mussels and geckos, *Nature*, 448, 338-342

[179] Messersmith, P.B., Dalsin, J.L., Lee, B.P., Burke, S.A. (2008) DOPA-functionalized, branched, poly(alkylene oxide) adhesives, US 2008/0247984 A1

[180] Shazly, T.M., Baker, A.B., Naber, J.R., Bon, A., Van Vliet, K.J., Edelman, E.R. (2010) Augmentation of postswelling surgical sealant potential of adhesive hydrogels, *J Biomed Mater Res A*, 95, 1159-1169

[181] Lee, Y., Chung, H.J., Yeo, S., Ahn, C.-H., Lee, H., Messersmith, B.P., Park, T.G. (2010) Thermo-sensitive, injectable, and tissue adhesive sol-gel transition hyaluronic acid/pluronic composite hydrogels prepared from bio-inspired catechol-thiol reaction, *Soft Matter*, 6, 977-983

[182] Guvendiren, M., Messersmith, P.B., Shull, K.R. (2008) Self-assembly and adhesion of DOPA-modified methacrylic triblock hydrogels, *Biomacromolecules*, 9, 122-128

[183] Guvendirent, M., Brass, D.A., Messersmith, P.B., Shull, K.R. (2009) Adhesion of DOPA-functionalized model membranes to hard and soft surfaces, *J Adhes*, 85, 631-645

[184] Yamada, K., Aoki, T., Ikeda, N., Hirata, M. (2007) Application of enzymatically gelled chitosan solutions to water-resistant adhesives, *J App Polym Sci*, 104, 1818-1827

[185] Yamada, K., Aoki, T., Ikeda, N., Hirata, M., Hata, Y., Higashida, K., Nakamura, Y. (2008) Application of chitosan solutions gelled by *melB* tyrosinase to water-resistant adhesives, *J App Polym Sci*, 107, 2723-2731

[186] Peshkova, S., Li, K. (2003) Investigation of chitosan-phenolics systems as wood adhesives, *J Biotechnol*, 102, 199-207

[187] Peshkova, S., Li, K., (2003) Investigation of poly(4-vinylphenol) as a wood adhesive, *Wood Fiber Sci*, 35, 41-48

[188] Zhang, C., Li, K., Simonsen, J. (2003) A novel wood-binding domain of a wood-plastic coupling agent: development and characterization, *J App Polym Sci*, 89, 1078–1084

[189] Li, K., Geng, X., Simonsen, J., Karchesy, J. (2004) Novel wood adhesives from condensed tannins and polyethylenimine, *Int J Adhes Adhes*, 24, 327-333

[190] Li, K., Geng, X. (2005) Formaldehyde-free wood adhesives from decayed wood, *Macromol Rapid Comm*, 26, 529-532

[191] Geng, X., Li, K. (2006) Investigations of wood adhesives from kraft lignin and polyethylenimine, *J Adhesion Sci Technol*, 20, 847-858

[192] Li, K., Geng, X. (2007) Adhesive compositions and methods of using and making the same, US 7265169 B2

[193] Sun, P.Y., Tian, L.Y., Zheng, Z., Wang, X.L. (2009) Dopamine-containing mussel mimetic polyurethane, *Acta Polym Sin,* 8, 803-808

[194] Samyn, P., Rühe, J., Biesalski, M. (2010) Polymerizable biomimetic vesicles with controlled local presentation of adhesive functional DOPA groups, *Langmuir*, 26, 8573-8581

[195] Shao, H., Stewart, R.J. (2010) Biomimetic underwater adhesives with environmentally triggered setting mechanisms, *Adv Mater*, 22, 729-733

[196] Shao, H., Weerasekare, G.M., Stewart, R.J. (2011) Controlled curing of adhesives complex coacervates with reversible periodate carbohydrate complexes, *J Biomed Mater Res A*, 97, 46-51

[197] Lee, B.P., Dalsin, J.L., Messersmith, P.B. (2002) Synthesis and gelation of DOPA-modified poly(ethylene glycol) hydrogels, *Biomacromolecules*, 3, 1038-1047

[198] Huang, S.-Y., Lipp, D.W., Farinato, R.S. (2001) Acrylamide polymers, *Kirk-Othmer Encyclopedia of Chemical Technology,* 1, 304-342

[199] Wang, J., Tahir, M.N., Kappl, M., Tremel, W., Metz, N., Barz, M., Theato, P., Butt, H.-J. (2008) Influence of binding-site density in wet bioadhesion, *Adv Mater*, 20, 3872-3876

[200] Monahan, J., Wilker, J.J. (2004) Cross-linking the protein precursor of marine mussel adhesives: bulk measurements and reagents for curing, *Langmuir*, 20, 3724-3729

[201] Wilson, M.A., Filzen, G., Welmaker, G.S. (2009) A microwave-assisted, green procedure for the synthesis of *N*-aryl sylfonyl and *N*-aryl pyrroles, *Tetrahedron Lett*, 50, 4807-4809

[202] Mahdavi, A., Ferreira, L., Sundback, C., Nichol, J.W., Chan, E.P., Carter, D.J.D., Bettinger, C.J., Patanavanich, S., Chignozha, L., Ben-Jospeh, E., Galakatos, A., Pryor, H., Pomerantseva, I., Masiakos, P.T., Faquin, W., Zumbuehl, A., Hong, S., Borenstein, J., Vacanti, J., Langer, R., Karp, J.M. (2008) A biodegradable and biocompatible gecko-inspired tissue adhesive, *PNAS*, 105, 2307-2312

[203] Ferreira, P., Silva, A.F.M., Pinto, M.I., Gil, M.H. (2008) Development of a biodegradable bioadhesive containing urethane groups, *J Mater Sci: Mater Med*, 19, 111-120

[204] Bilic, G., Brubaker, C., Messersmith, P.B., Mallik, A.S., Quinn, T.M., Haller, C., Done, E., Gucciardo, L., Zeisberger, S.M., Zimmermann, R., Deprest, J., Zisch, A.H. (2010) Injectable candidate sealants for fetal membrane repair: bonding and toxicity in vitro, *Am J Obstet Gynecol*, 202, 1-9

[205] Winslow, B.D., Shao, H., Stewart, R.J., Tresco, P.A. (2010) Biocompatibility of adhesive complex coacervates modeled after the sandcastle glue of *Phragmatopoma californica* for craniofacial reconstruction, *Biomaterials*, 31, 9373-9381

[206] Tatehata, H., Mochizuki, A., Ohkawa, K., Yamada, M., Yamamoto, H. (2001) Tissue adhesive using synthetic model adhesive proteins inspired by the marine mussel, *J Adhes Sci Technol*, 15, 1003-1013

[207] Huang, K., Lee, B.P., Ingram, D.R., Messersmith, P.B. (2002) Synthesis and characterization of self-assembling block copolymers containing bioadhesive end groups, *Biomacromolecules*, 3, 397-406

[208] Berchane, N.S., Andrews, M.J., Kerr, S., Slater, N.K.H., Jebrail, F.F. (2008) On the mechanical properties of bovine serum albumin (BSA) adhesives, *J Mater Sci: Mater Med*, 19, 1831-1838

[209] Wilson, D.J., Chenery, D.H., Bowring, H.K., Wilson, K., Turner, R., Maughan, J., West, P.J., Ansell, C.W.G. (2005) Physical and biological properties of a novel siloxane adhesive for soft tissue applications, *J Biomater Sci Polym Edn*, 16, 449-472

[210] Cha, H.J., Hwang, D.S. (2009) Mussel bioadhesive, US 7622550 B2

[211] www.bdbiosciences.com, retrieved 29-05-2011

[212] www.kollodis.com, retrieved 29-05-2011

[213] Sherman, L. (2007) Nature's Glue. Kaichang Li teaches soybeans to act like shellfish, *Terra*, 2, 1-4, web source: http://www.cof.orst.edu/cof/wse/faculty/li/NatureGlue_reprint-Terra-4-2-07.pdf

[214] Speitling, A.W., Procter, P., Schomburg, J., Schultz, C., Jülich, W.D., Lindequist, U., Schauer, F., Mikolasch, A., Manda, K. (2011) Adhesive for medical applications and means for haemostasis, U2 7923003 B2

[215] Messersmith, B.P., Brubaker, C., Zisch, A.H., Zisch, C. (2011) Sealants for fetal membrane repair, US 2011/0027250 A1

[216] http://www.kenseynash.com/kensey-nash-technologies/Adhesive-and-Coating-Technology, retrieved 29-05-2011

[217] Zhang, Y., Broekhuis, A.A., Picchioni, F (2009) Thermally self-healing polymeric materials: The next step to recycling thermoset polymers?, *Macromolecules,* 42, 1906-1912

[218] Hamarneh, A.I. (2010) *Novel Wood Adhesives from Bio-based Materials and Polyketones*, PhD Thesis, University of Groningen, 21-28

[219] Liu, Z., Hu, B.H., Messersmith, P.B. (2010) Acetonide protection of dopamine for the synthesis of highly pure N-docosahexaenoyldopamine, *Tetrahedron Letters*, 51, 2403-2405

[220] Li, G., Zhang, H., Sader, F., Vadhavkar, N., Njus, D. (2007) Oxidation of 4-methylcatechol: implications for the oxidation of catecholamines, *Biochemistry*, 46, 6978-6983

[221] Graham, D.G. (1978) Oxidative pathways for catecholamines in the genesis of neuromelanin and cytotoxic quinones, *Molecular Pharmacology*, 14, 633-643

[222] Bindoli, A., Rigobello, M.P., Deeble, D.J. (1992) Biochemical and toxicological properties of the oxidation products of catecholamines, *Free Radical Biology & Medicine*, 13, 391-405

[223] Mattammal, M.B., Strong, R., V, White, E., Shu, F.F. (1994) Characterization of peroxidate oxidation products of dopamine by mass spectroscopy, *Journal of Chromatography B*, 658, 21-30

[224] Hawley, M.D., Tatawawadi, S.V., Piekarski, S., Adams, R.N. (1967) Electrochemical studies of the oxidation pathways of catecholamines, *Journal of the American Chemical Society*, 89, 447-450

[225] Tse, D.C.S., McCreery, R.L., Adams, R.N. (1976) Potential oxidative pathways of brain catecholamines, *Journal of Medicinal Chemistry*, 19, 37-40

[226] Zhang, F., Dryhurst, G. (1993) Oxidation chemistry of dopamine: possible insights into age-dependant loss of dopaminergic nigrostriatal neurons, *Bioorganic chemistry*, 21, 392-410

[227] Heacock, R.A. (1959) *The chemistry of adrenochrome and related compounds*, Chemical Reviews, 59, 181–237

[228] Kerr, S. (2003) Unpublished work, University of Cambridge

[229] Berfield, J.L., Wang, L.C., Reith, M.E.A. (1999) Which form of dopamine is the substrate for the human dopamine transporter: the cationic or the uncharged species?, *The Journal of Biological Chemistry*, 274, 4876-4882

[230] Po, H.N., Senozan, N.M. (2001) The Henderson-Hasselbalch equation: its history and limitations, *Journal of Chemical Education*, 78, 1499-1503

[231] Bu'Lock, J.D. Harley-Mason, J. (1951) The chemistry of adrenochrome. Part II. Some analogues and derivatives, *Journal of the Chemical Society*, 712-716

[232] Harrison, W.H., Whisler, W.W., Hill, B.J. (1968) Catecholamine oxidation and ionization properties indicated from the H+ release, tritium exchange and spectral changes which occur during ferricyanide oxidation, *Biochemistry*, 7, 3089-3094

[233] Garcia-Moreno, M. Rodriguez-Lopez, J.N., Martinez-Ortiz, F., Tudela, J., Varon, R., Garcia-Canovas, F. (1991) Effect of pH on the oxidation pathway of dopamine catalyzed by tyrosinase, *Archives of Biochemistry and Biophysics*, 288, 427-434

[234] Tono, T. (1971) A tetrahydroisoquinoline derivative isolated from the acetone extract of *Dioscorea batatas*, *Agr Biol Chem Tokyo*, 35, 619-621

[235] Morita, S., Ito, T., Tono, T. (1975) Syntheses of isoquinolines by condensation of dopamine with carbonyl compounds, Agricultural and Biological Chemistry, 39, 547-549

[236] Li, J.J. (2005) *Name reactions in heterocyclic chemistry*, Wiley

[237] Felder-Flesch, D., Steibel, J., Bertin, A. (2010) Dendritic chelated compounds, methods for making the same and pharmaceutical compositions containing the same, US 2010/0104512 A1

[238] Cai, W., Kwok, S.W., Taulane, J.P., Goodman, M. (2004) Metal-assisted assembly and stabilization of collagen-like triple helices, *JACS*, 126, 15030-15031

[239] Amarnath, V., Anthony, D.C., Amarnath, K., Valentine, W.M., Wetterau, L.A., Graham, D.G. (1991) Intermediates in the Paal-Knorr synthesis of pyrroles, *Journal of Organic Chemistry*, 56, 6924-6931

[240] Sen, A., Jiang, Z., Chen, J.T. (1989) Novel nitrogen-containing heterocyclic polymers derived from the alternating ethylene-carbon monoxide copolymer, *Macromolecules*, 22, 2012-2014

[241] Kostyanovsky, R.G., Kadorkina, G.K., Mkhitaryan, A.G., Chervin, I.I., Aliev, A.E. (1993) New scope and limitations in the Knorr-Paal synthesis of pyrroles, *Mendeleev Communications*, 3, 22-24

[242] Artico, M., Corelli, F., Massa, S., Stefancich, G. (1983) A facile and convenient synthesis of the unknown 1-aroylmethyl-1H-pyrroles, *Synthesis-Stuttgart*, 931

[243] Werner, S., Iyer, P.S., Twining, L.A., Fodor, M.D., Mitasev, B., Coleman, C.M., Brummond, K.M. (2006) Solution-phase synthesis of a tricyclic pyrrole-2-carboxamide discovery library applying a Stetter-Paal-Knorr reaction sequence, *Journal of Combinatorial Chemistry*, 8, 368-380

[244] Solomons, G., Fryhle, C. (2000) *Organic Chemistry*, Wiley

[245] Sinai-Zingde, G.D. (1993) Polymer formed by reaction of a polyketone and an amino acid, WO 93/19114

[246] Kürti, L., Czakó, B. (2005) *Strategic applications of named reactions in organic synthesis: background and detailed mechanisms*, Elsevier

[247] http://www.organic-chemistry.org/namedreactions/paal-knorr-pyrrole-synthesis.shtm, accessed 22 February 2011

[248] Ohlsson, J., Somfai, P., Åberg, P.M. (1999) Conjugation of amines and α-amino acid derivatives as pyrroles using tethered 1,4-diketones, *Acta Chemica Scandinavica*, 53, 480-486

[249] Drent, E., Keijsper, J. (1993) Polyketone polymer preparation with tetra alkyl bis phosphine ligand and hydrogen, 5225523

[250] American Society for Testing and Materials (2000) ASTM F 756-00 – Standard practices for assessment of haemolytic properties of materials

[251] White, J.D., Wilker, J.J. (2011) Underwater bonding with charged polymer mimics of marine mussel adhesive proteins, *Macromolecules*, 44, 5058-5088

[252] American Society for Testing and Materials (2005) ASTM International D1002-05 – Standard Test Method for Apparent Shear Strength of Single-Lap-Joint Adhesively Bonded Metal Specimens by Tension Loading (Metal-to-Metal)

[253] Chen, J.X., Liu, M.C., Yang, X.L., Ding, J.C., Wu, H.Y. (2008) Indium(III)-catalyzed synthesis of *N*-substituted pyrroles under solvent-free conditions, *J Braz Chem Soc*, 19, 877-883

[254] Ion, A., Ion, I., Popescu, A., Ungureanu, M., Moutet, J.C., SaintAman, E. (1997) A ferrocene crown ether functionalized polypyrrole film electrode for the electrochemical recognition of barium and calcium cations, *Adv Mater*, 9, 711-713

[255] Kang, H., Fenical, W. (1997) Ningalins A-D: Novel aromatic alkaloids from a Western Australian ascidian of the genus *Didemnum*, *J Org Chem*, 62, 3254-3262

[256] Hamasaki, A., Zimpleman, J.M., Hwang, I., Boger, D.L. (2005) Total synthesis of Ningalin D, *J Am Chem Soc*, 127, 10767-10770

[257] National Institute of Advanced Industrial Science and Technology (AIST), Spectral Database for Organic Compounds SDBS, No.: 4729, accessed 26-05-2011

[258] (a) Jin, R., Hiemstra, C., Zhong, Z., Feijen, J. (2007) Enzyme-mediated fast in situ formation of hydrogels from dextran-tyramine conjugates, *Biomaterials*, 2791-2800 (b) Lee, F., Chung, J.E., Kurisawa, M. (2008) An injectable enzymatically crosslinked hyaluronic acid-tyramine hydrogel system with independent tuning of mechanical strength and gelation rate, *Soft Matter*, 4, 880-887.

[259] Lee, H., Dellatore, S.M., Miller, W.M., Messersmith, P.B. (2007) Mussel-inspired surface chemistry for multifunctional coatings, *Science*, 318, 426-430

[260] An, J.H., Huynh, N.T., Jeon, Y.S., Kim, J.-H. (2011) Surface modification using bio-inspired adhesive polymers based on polyaspartamide derivatives, *Polym Int*, online publication

[261] Wever, D.A.Z., Picchioni, F., Broekhuis, A.A. (2011) Polymers for enhanced oil recovery: A paradigm for structure-property relationship in aqeous solution, *Prog Polym Sci*, 36, 1158-1628

Appendix

I Amino acids

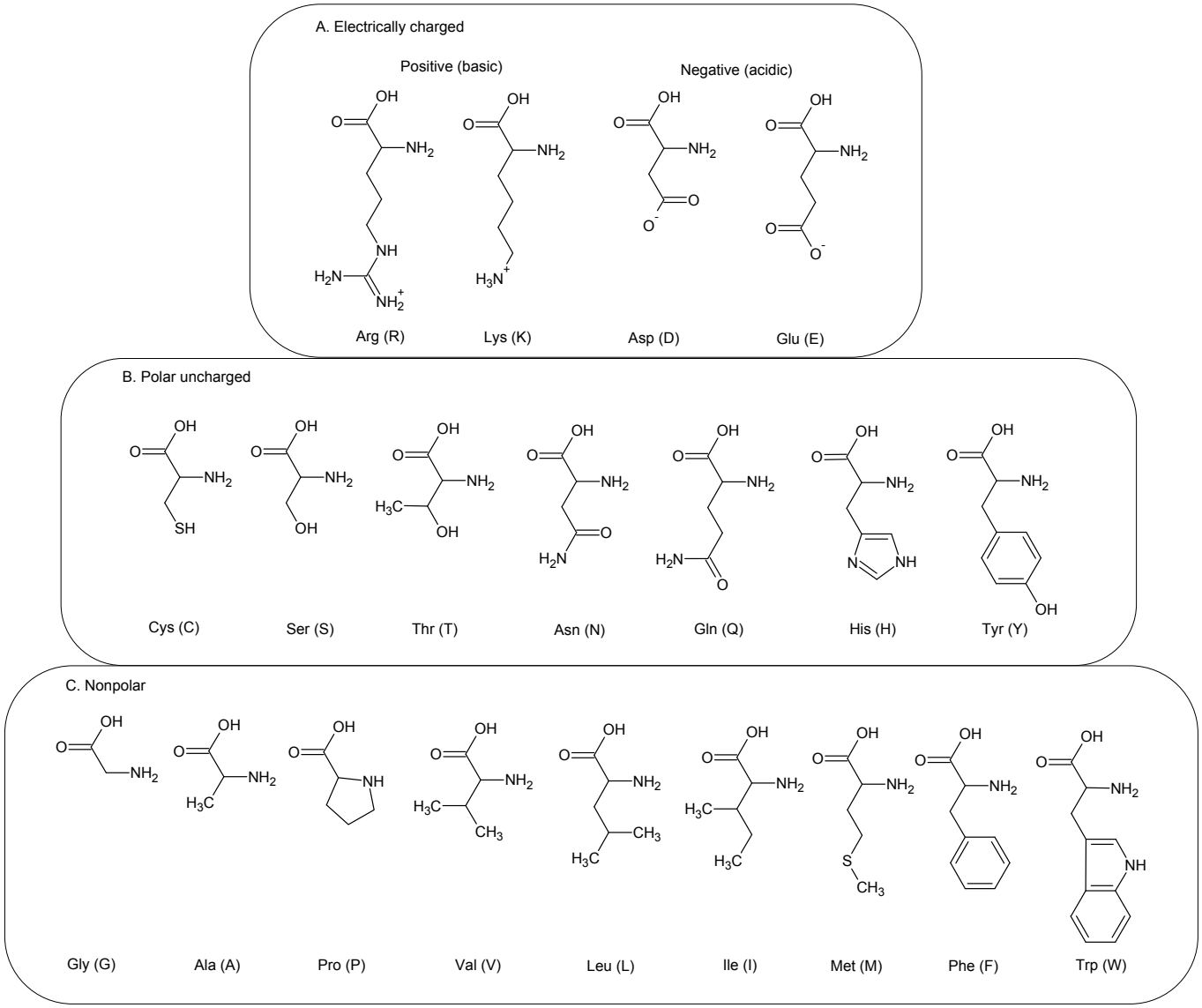

Figure I.1: 20 common amino acids with their main structure at physiological pH (7.4). Selenocysteine (U), stereospecificity and resonance forms not shown.

II Elemental analysis calculations for conversion determination

The following alternating terpolymer (CO-ethylene-propylene) has been used as a backbone:

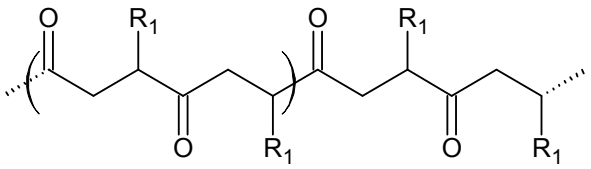

Figure II.1 Polyketone used with repeating dicarbonyl unit marked with brackets, R_1 = H, CH_3

Polyketone type	*Ethylene fraction (x)*	*Molecular weight of repeating di-carbonyl unit*
PK-0	0	140.18
PK-30	0.3	131.76
PK-50	0.5	126.15

Element (atomic weight)	Number of atoms in repeating di-carbonyl unit
C (12.0107)	$6\ (backbone) + x \cdot 0 + (1-x) \cdot 2 = 8 - 2 \cdot x$
H (1.0079)	$6\ (backbone) + x \cdot 2 + (1-x) \cdot 6 = 12 - 4 \cdot x$
N (14.0067)	0
O (15.9994)	2 (*backbone*)

The following reactants have been used:

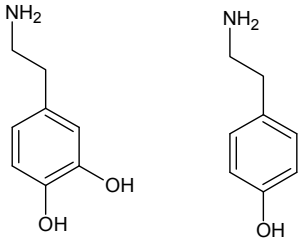

Figure II.2 Dopamine (left) and tyramine (right). Elemental composition: C = 8, H = 11, N = 1, O = 2 (dopamine) or O = 1 (tyramine)

Resulting in the following structure:

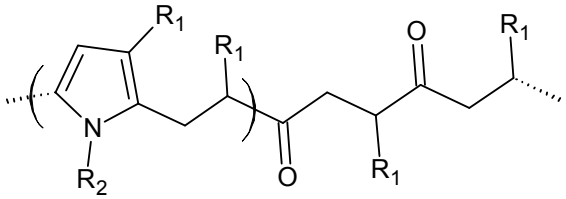

Figure II.3 Modified polyketone, reacted di-carbonyl unit marked with brackets, R_1 = H or CH_3, R_2 = dopamine or tyramine fragment

	Number of atoms in reacted di-carbonyl unit	
Element (atomic weight)	Dopamine reacted	Tyramine reacted
C (12.0107)	$6 + (1 - x) \cdot 2 + 8 = 16 - 2 \cdot x$	
H (1.0079)	$4 + x \cdot 2 + (1 - x) \cdot 6 + 9 = 19 - 4 \cdot x$	
N (14.0067)	1	
O (15.9994)	2	1

Define:

Unit	Description	Calculation
N(wt%)	mass percentage of nitrogen (as outcome of elemental analysis)	
C(wt%)	mass percentage of carbon (”)	
H(wt%)	mass percentage of hydrogen (”)	
$M_W(R)$	molecular weight of reacted di-carbonyl unit	
$M_W(U)$	molecular weight of unreacted di-carbonyl unit	
ΔM_W	difference in molecular weight of reacted and unreacted di-carbonyl unit	$M_W(R) - M_W(U)$
α	fraction of reacted (di-)carbonyl units (between 0 and 1)	
M_W	Average molecular weight of repeating unit in polymer	$\alpha \cdot M_W(R) + (1 - \alpha) \cdot M_W(U) = \alpha \cdot \Delta M_W + M_W(U)$

Now, the weight percentage of an element in the polymer is related to the conversion. It can be calculated straightforward from taking the ratio between (i) the elemental weight in an average repeating unit and (ii) the total average molecular weight of a repeating unit. In formulas per element:

$$N(wt\%) = \frac{14.0067 \cdot (\alpha \cdot 1 + (1-\alpha) \cdot 0)}{M_W} \cdot 100 = \frac{1400.67 \cdot \alpha}{M_W} \quad (1)$$

$$C(wt\%) = \frac{12.0107 \cdot (\alpha \cdot (16 - 2 \cdot x) + (1-\alpha) \cdot (8 - 2 \cdot x))}{M_W} \cdot 100 = \frac{1201.07 \cdot (16\alpha - 2x\alpha + 8 - 8\alpha + 2x\alpha - 2x)}{M_W} = \frac{1201.07 \cdot (8\alpha - 2x + 8)}{M_W} \quad (2)$$

$$H(wt\%) = \frac{1.0079 \cdot (\alpha \cdot (19 - 4 \cdot x) + (1-\alpha) \cdot (12 - 4 \cdot x))}{M_W} \cdot 100 = \frac{100.79 \cdot (19\alpha - 4x\alpha + 12 - 12\alpha + 4x\alpha - 4x)}{M_W} = \frac{100.79 \cdot (7\alpha - 4x + 12)}{M_W} \quad (3)$$

Because samples can easily be contaminated with water (H_2O) from the air, the use of (3) is not very reliable in itself, but can be used as a control. The ratio between the nitrogen (eq. 1) and carbon (eq. 2) content would be the most reliable as this uses all other data available, thus minimizing the error (assuming purity of the sample in nitrogen and carbon content, e.g. no organic solvent or by-product contamination). Algebraically, making α explicit through this ratio results in:

$$\frac{N(wt\%)}{C(wt\%)} = \frac{\frac{1400.67 \cdot \alpha}{M_W}}{\frac{1201.07 \cdot (8\alpha - 2x + 8)}{M_W}} = \frac{1400.67 \cdot \alpha}{1201.07 \cdot (8\alpha - 2x + 8)}$$

$$\rightarrow \; N(wt\%) \cdot 1201.07 \cdot (8\alpha - 2x + 8) = C(wt\%) \cdot 1400.67 \cdot \alpha$$

$$N(wt\%) \cdot 1201.07 \cdot 8\alpha + N(wt\%) \cdot 1201.07 \cdot (-2x + 8) = C(wt\%) \cdot 1400.67 \cdot \alpha$$

$$N(wt\%) \cdot 1201.07 \cdot 8\alpha - C(wt\%) \cdot 1400.67 \cdot \alpha = N(wt\%) \cdot 1201.07 \cdot (2x - 8)$$

$$\alpha \cdot (N(wt\%) \cdot 1201.07 \cdot 8 - C(wt\%) \cdot 1400.67) = N(wt\%) \cdot 1201.07 \cdot (2x - 8)$$

$$\alpha = \frac{N(wt\%) \cdot 1201.07 \cdot (2x-8)}{N(wt\%) \cdot 1201.07 \cdot 8 - C(wt\%) \cdot 1400.67} = \frac{N(wt\%) \cdot (8 - 2 \cdot x)}{C(wt\%) \cdot 1.1662 - N(wt\%) \cdot 8} \quad (4)$$

The reactant amine conversion is directly linked to the initial molar ratio between the amine reactant and the carbonyl groups (r) and to carbonyl conversion (α). For the latter it needs to be corrected by the factor ½ as each amine group reacts with two carbonyl groups in the Paal-Knorr reaction. In order to apply a more common abbreviation for conversion (X) and make a clearer distinction between the conversion of polymer groups (X_{CO}) and the conversion of the amine reactant (X_A), the following final equations are obtained:

$$X_{CO} = \frac{N(wt\%)\cdot(8-2\cdot x)}{C(wt\%)\cdot 1.1662 - N(wt\%)\cdot 8} \tag{5}$$

$$X_A = \frac{X_{CO}}{2\cdot r} \tag{6}$$

III DSC thermograms

PK30, TEA activated PK30-5, PK30-10, PK30-25, PK30-50 (from first to last).

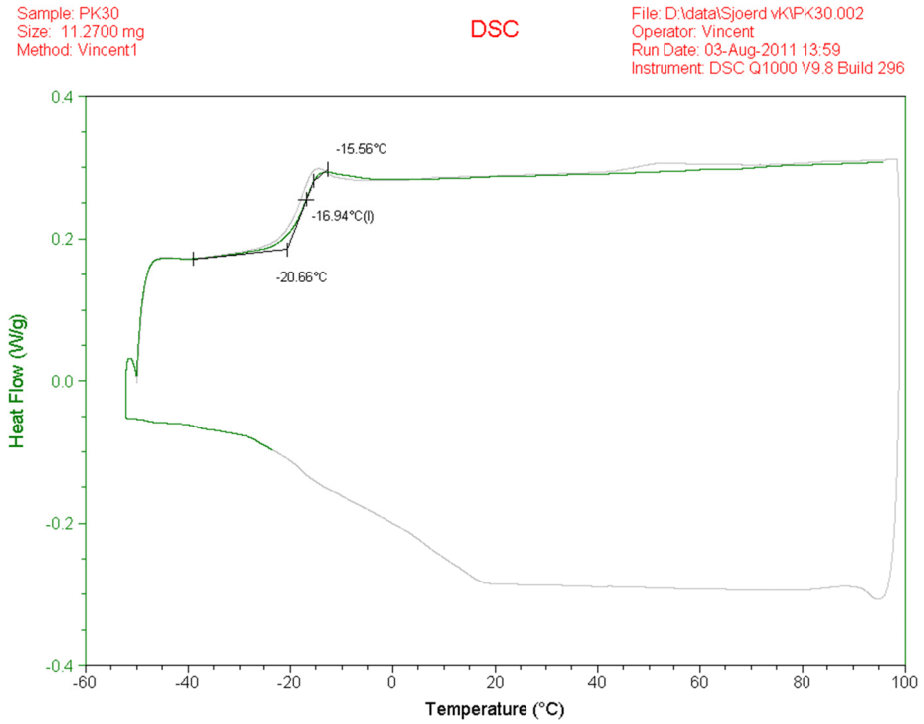

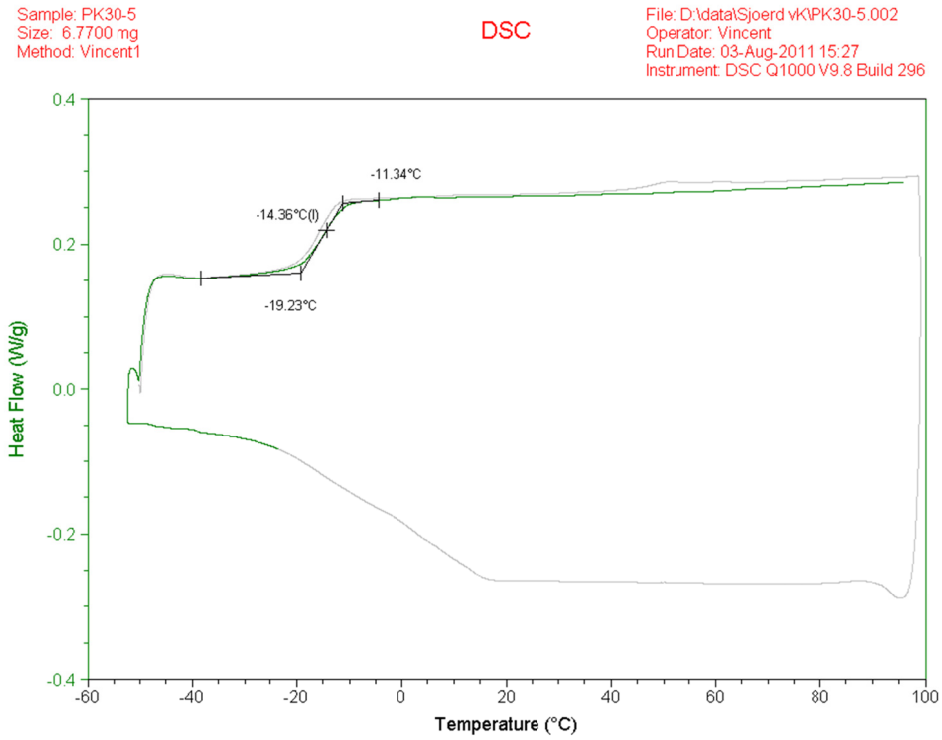
Sample: PK30-5
Size: 6.7700 mg
Method: Vincent1
DSC
File: D:\data\Sjoerd vK\PK30-5.002
Operator: Vincent
Run Date: 03-Aug-2011 15:27
Instrument: DSC Q1000 V9.8 Build 296
-11.34°C
-14.36°C(I)
-19.23°C
Heat Flow (W/g)
Temperature (°C)

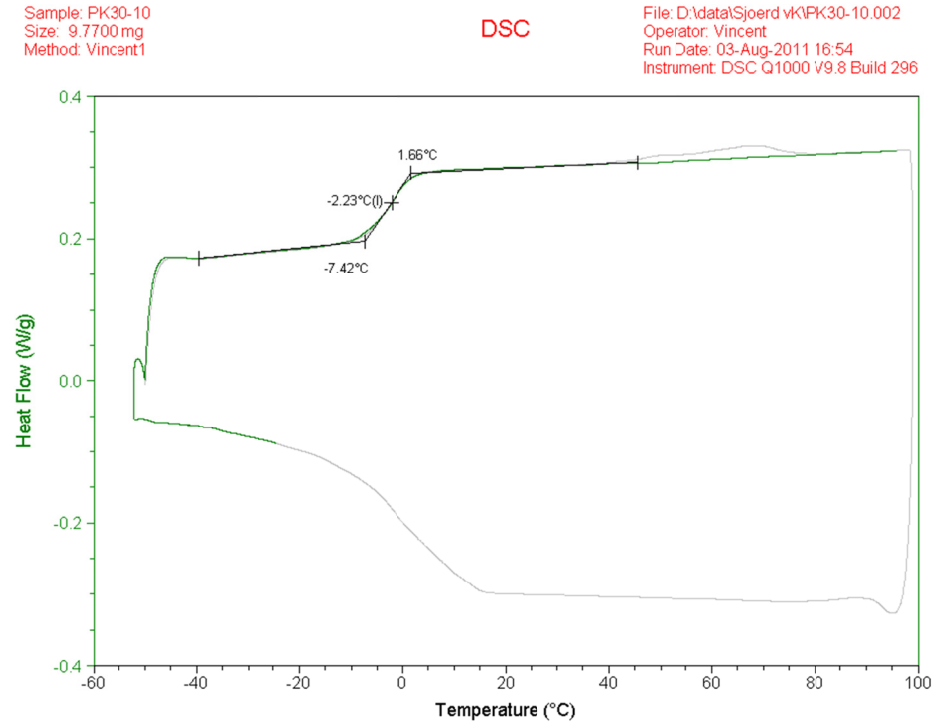
Sample: PK30-10
Size: 9.7700 mg
Method: Vincent1
DSC
File: D:\data\Sjoerd vK\PK30-10.002
Operator: Vincent
Run Date: 03-Aug-2011 16:54
Instrument: DSC Q1000 V9.8 Build 296
1.66°C
-2.23°C(I)
-7.42°C
Heat Flow (W/g)
Temperature (°C)

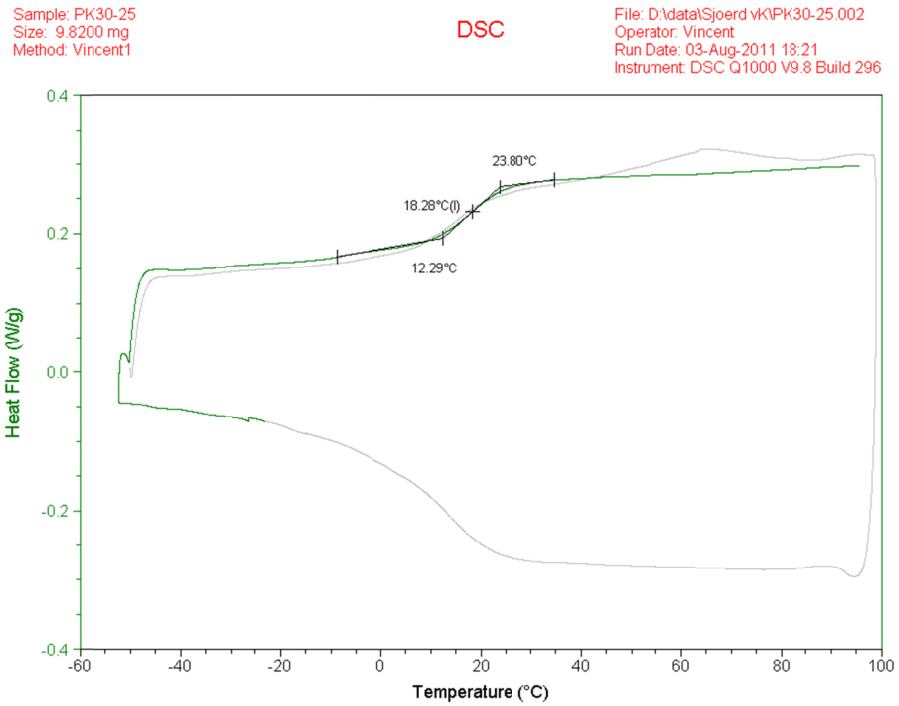
Sample: PK30-25
Size: 9.8200 mg
Method: Vincent1
DSC
File: D:\data\Sjoerd vK\PK30-25.002
Operator: Vincent
Run Date: 03-Aug-2011 13:21
Instrument: DSC Q1000 V9.8 Build 296
23.80°C
18.28°C(I)
12.29°C
Heat Flow (W/g)
Temperature (°C)

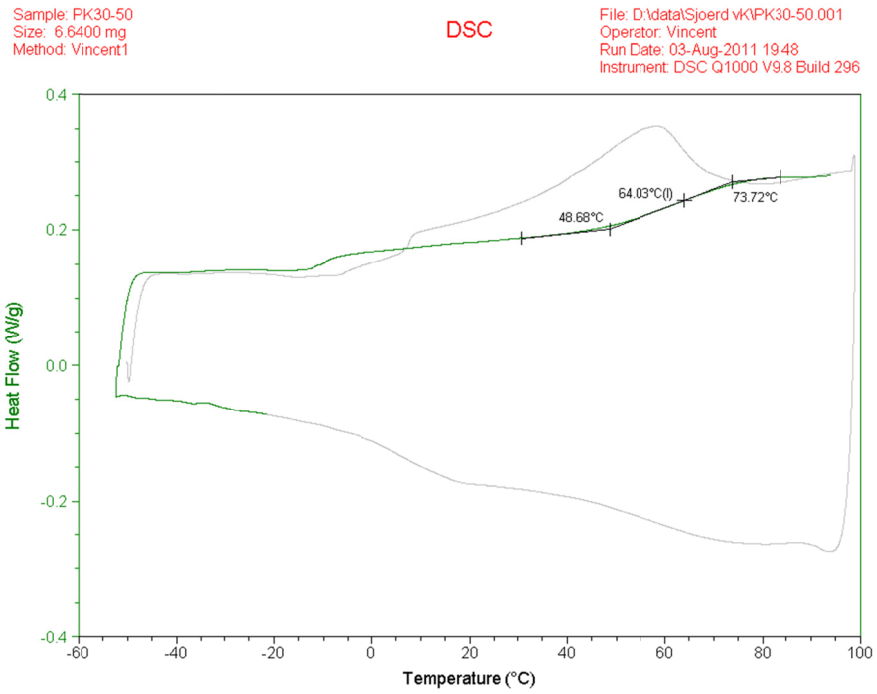
Sample: PK30-50
Size: 6.6400 mg
Method: Vincent1
DSC
File: D:\data\Sjoerd vK\PK30-50.001
Operator: Vincent
Run Date: 03-Aug-2011 19:48
Instrument: DSC Q1000 V9.8 Build 296
64.03°C(I)
48.68°C
73.72°C
Heat Flow (W/g)
Temperature (°C)